UNIVERSITÉ DU QUÉBEC

VARIATIONS SPATIALES DE LA PRODUCTION PRIMAIRE ET DE L'EXPORTATION DU MATÉRIEL ORGANIQUE PARTICULAIRE SOUS LA ZONE EUPHOTIQUE DANS LE SYSTÈME DE LA BAIE D'HUDSON, CANADA

THÈSE

PRÉSENTÉE À

L'UNIVERSITÉ DU QUÉBEC À RIMOUSKI

comme exigence partielle

du programme de doctorat en océanographie

PAR

AMANDINE LAPOUSSIÈRE

JUILLET 2010

« La science excelle à décrire et nous savons si peu de chose que les scientifiques font des découvertes là où se pose leur regard. Mais chaque découverte révèle tout bonnement l'étendue de notre ignorance. Loin d'achever le portrait, les découvertes nous indiquent simplement tout ce qu'il reste encore à apprendre »

David Suzuki

« L'équilibre sacré »

« La mer est tout ! C'est l'immense désert où l'homme n'est jamais seul, car il sent frémir la vie à ses côtés. La mer est le vaste réservoir de la nature. C'est par la mer que le globe a pour ainsi dire commencé, et qui sait s'il ne finira pas par elle »

Jules Verne

« 20 000 lieues sous les mers »

AVANT-PROPOS

Cette thèse présente les premiers travaux de recherche menés parallèlement sur les processus de production et d'exportation du matériel organique particulaire dans le système de la baie d'Hudson en période libre de glace. Au cours de ce doctorat, je me suis plus particulièrement intéressée à quantifier et caractériser la production et la biomasse phytoplanctoniques en fonction des conditions du milieu ; ainsi qu'à déterminer l'influence de la production primaire et de la structure des communautés planctoniques sur l'exportation verticale du matériel organique en termes de quantité et de qualité du matériel exporté.

Cette thèse se compose d'une introduction générale rédigée en français, suivie de trois chapitres rédigés sous forme d'articles scientifiques en anglais, d'une conclusion générale en français résumant et discutant de l'ensemble des résultats puis de la liste des références. Le premier chapitre traite de l'étude de la variabilité spatiale de la sédimentation du phytoplancton et du matériel particulaire sous la zone euphotique dans le système de la baie d'Hudson en période automnale. Ce chapitre a fait l'objet d'un article publié dans la revue Continental Shelf Research (Lapoussière A, Michel C, Gosselin M, Poulin M, 2009. Spatial variability in organic material sinking export in the Hudson Bay system, Canada, during fall. Cont Shelf Res 29:1276–1288).

Le second chapitre caractérise la relation entre la production primaire et son exportation hors de la zone euphotique dans le système de la baie d'Hudson en période automnale. Ce second chapitre a été soumis pour publication dans la revue Marine Ecology

Progress Series (Lapoussière A, Michel C, Gosselin M, Poulin M, Martin J, Tremblay J-É. Primary production and sinking export during fall in the Hudson Bay system, Canada).

Le troisième chapitre détermine le rôle des bactéries attachées aux particules en termes de dégradation *versus* contribution à l'exportation verticale du matériel organique. Ce dernier chapitre a aussi été soumis pour publication dans un numéro spécial de la revue Journal of Marine Systems sur la baie d'Hudson (Lapoussière A, Michel C, Starr M, Poulin M, Gosselin M. Abundance of free-living *versus* particle-attached bacteria and their role in the recycling and export of organic material in the Hudson Bay system).

Les résultats de ce doctorat ont fait l'objet de plusieurs présentations orales et affiches lors de congrès nationaux tels que la réunion scientifique annuelle d'ArcticNet en 2005, 2006 et 2007, l'assemblée générale annuelle de Québec-Océan en 2007 et 2008, le 43^{e} congrès de la Société canadienne de météorologie et d'océanographie à Halifax en 2009 ; ou internationaux tels que la Gordon Research Conference on Polar Marine Science à Ventura en 2007, Arctic Change à Québec en 2008, Aquatic Sciences Meeting de l'American Society of Limnology and Oceanography à Nice en 2009 et la 4^{e} école d'été internationale du programme Surface Ocean-Lower Atmosphere Study à Cargèse en 2009.

Ce projet de recherche a été financé par le Réseau des Centres d'excellence du Canada ArcticNet, le Conseil de recherches en sciences naturelles et en génie (CRSNG) du Canada, le ministère des Pêches et Océans Canada (MPO), l'Institut des sciences de la mer de Rimouski (ISMER) et le Musée canadien de la nature. Je tiens à remercier la Fondation de l'Université du Québec à Rimouski, ArcticNet, Québec-Océan, la Société canadienne de météorologie et océanographie, l'American Society of Limnology and Oceanography et la Gordon Research Conference pour leur contribution financière qui m'a permis de participer à de nombreux congrès au cours de mon doctorat. Les travaux de recherche menés au cours

de cette thèse sont une contribution aux programmes de recherches du Réseau des Centres d'excellence du Canada ArcticNet, de l'Institut des eaux douces de Winnipeg (MPO), de l'ISMER et de Québec-Océan.

REMERCIEMENTS

Je tiens tout d'abord à remercier Christine Michel, Michel Gosselin et Michel Poulin, mes directeurs, et principaux acteurs de ce projet, pour m'avoir fait confiance et m'avoir permis d'intégrer votre équipe. Vous m'avez ainsi offert l'inestimable opportunité de pérenniser ma passion pour le milieu marin et de découvrir la magie du monde polaire. Au cours des missions en mer dans ce royaume où l'eau et la glace règnent en maîtres, je n'ai pu qu'admirer cet immense univers à la fois hostile et captivant et éprouver un profond respect de la nature. Je vous suis également reconnaissante pour vos précieux conseils avisés, le temps que vous m'avez consacré et votre patience tout au long de mon doctorat et tout particulièrement au cours de la rédaction de ce manuscrit.

Je tiens également à remercier Christian Nozais et Richard Rivkin pour avoir accepté de juger ma thèse et d'être intervenus en tant que président du jury et examinateur externe lors de ma soutenance.

Un remerciement tout particulier à Michel Starr pour être intervenu en qualité de membre externe au cours de mon doctorat et pour m'avoir accueillie dans ton laboratoire pour mon cours en nouveaux développements. Je te suis enfin reconnaissante pour ta contribution et ton aide précieuse pour mon troisième chapitre. Je tiens également à remercier Lilianne Saint-Amand pour ta bonne humeur, tes conseils, ton soutient et tes mots d'encouragements.

Merci à toutes les personnes qui sont intervenues de près ou de loin dans ce projet de par leur contribution scientifique et technique : Joannie Ferland, Yves Gratton, Bernard LeBlanc, Mélanie Simard, Jean-Éric Tremblay, et beaucoup d'autres... Tout le travail de

terrain n'aurait jamais été possible et a été grandement facilité par l'aide et la collaboration des équipages des navires de la garde côtière canadienne.

La réalisation d'une thèse est un savant mélange de travail et de réflexion mais également de force mentale. C'est pourquoi ce manuscrit ne serait pas sans le soutien que ma famille m'a apporté malgré la distance tout au long de cette aventure avec son lot de joies, de doutes et de pleurs. Je n'y serais également jamais arrivée sans le soutient des amis du Québec et tout particulièrement Adeline et Nicolas, qui ont toujours été là pour moi au cours de ces cinq dernières années et qui ont fait preuve d'une incroyable patience et écoute face à mes « ralages » perpétuels. Je n'oublie pas non plus Johannie Martin, nous avons fait nos débuts ensembles et nous avons ensuite suivi le même chemin. Pourvu que la route soit encore longue.

Enfin je tiens à dédier cette thèse à toutes les personnes qui n'ont pas cru en moi et qui m'ont permis d'avoir cette rage essentielle à la poursuite de mon cheminement. Il y a quatre ans j'ai quitté ma « Douce France » sans aucune hésitation pour partir à la découverte de la « Nouvelle France ». À présent, si le vent me porte ailleurs, je me souviendrais…

RÉSUMÉ

Pour la première fois, la production primaire et l'exportation de matériel organique particulaire hors de la zone euphotique ont été étudiées dans le système de la baie d'Hudson (SBH) en période libre de glace. Cette étude s'est principalement intéressée aux variations spatiales des conditions du milieu et à leur influence sur la répartition spatiale des processus biologiques. Le rôle des bactéries dans l'exportation du matériel organique particulaire a également été évalué en termes de reminéralisation du matériel au cours sa sédimentation et de contribution de la biomasse bactérienne au matériel qui sédimente.

Cette étude montre qu'en période automnale le SBH est peu productif (70–435 mg C m^{-2} j^{-1}) et présente de faibles flux verticaux de carbone organique particulaire (COP) (50–77 mg C m^{-2} j^{-1}) à 50 m, comparativement à d'autres mers arctiques ou sub-arctiques (e.g. mer de Chukchi ou baie de Baffin). La répartition spatiale de la production et de la biomasse phytoplanctoniques était influencée par les facteurs du milieu conditionnés par les différents apports d'eau douce ou salée dans le SBH. Malgré les importantes variations spatiales observées pour la production primaire et la biomasse chlorophyllienne, les flux verticaux de COP à 50 m étaient relativement homogènes sur l'ensemble du SBH. Toutefois d'importantes variations spatiales de la composition du matériel exporté à 50 m ont été mises en évidence. Le COP exporté à 50 m était principalement composé de matériel dégradé non identifiable (i.e. détritus amorphes) (4–78%). La contribution des bactéries au flux de COP à 50 m était relativement importante sur l'ensemble du SBH (6–21%) et même parfois supérieure à la contribution des protistes intacts (5–28%) et à celle des pelotes fécales de brouteurs zooplanctoniques (3–97%).

L'étude du couplage entre la production primaire et son exportation sous la zone euphotique a montré que les rapports d'exportation (i.e. rapport entre le flux de COP à 50 m et la production primaire) les plus élevés ont été observés aux stations où la production primaire était faible et où la biomasse des hétérotrophes était importante ; alors que les rapports d'exportation les plus faibles ont été observés aux stations où la production primaire était plus élevée et associée à une forte contribution des diatomées.

L'étude plus approfondie des bactéries attachées aux particules qui sédimentent a mis en évidence qu'au sein du SBH à la fin de l'été, les bactéries attachées contribuaient

peu à l'abondance bactérienne totale dans le matériel en suspension (i.e. < 3%). Les résultats de cette étude ont montré que l'attachement des bactéries aux particules leur permet de sédimenter à la même vitesse que les particules qu'elles colonisent et donc de potentiellement contribuer aux flux verticaux de matériel organique particulaire. Cependant, les pertes estimées de COP liées à la respiration des bactéries attachées sont plus importantes que leur contribution au COP.

Les résultats obtenus au cours de cette thèse de doctorat ont permis d'approfondir les connaissances sur le fonctionnement des processus de production et d'exportation verticale du matériel organique particulaire dans le SBH jusqu'alors jamais étudié en période libre de glace. Ces données uniques sont indispensables à l'élaboration et la calibration de modèles climatiques afin d'envisager le devenir des écosystèmes arctiques et sub-arctiques face aux changements climatiques.

TABLE DES MATIÈRES

CHAPITRE I

SPATIAL VARIABILITY IN ORGANIC MATERIAL SINKING EXPORT IN THE HUDSON BAY SYSTEM, CANADA, DURING FALL

CHAPITRE II

PRIMARY PRODUCTION AND SINKING EXPORT DURING FALL IN THE HUDSON BAY SYSTEM, CANADA

CHAPITRE III

ABUNDANCE OF FREE-LIVING *VERSUS* PARTICLE-ATTACHED BACTERIA AND THEIR ROLE IN THE RECYCLING AND EXPORT OF ORGANIC MATERIAL IN THE HUDSON BAY SYSTEM

LISTE DES TABLEAUX

INTRODUCTION GÉNÉRALE

CHAPITRE I

SPATIAL VARIABILITY IN ORGANIC MATERIAL SINKING EXPORT IN THE HUDSON BAY SYSTEM, CANADA, DURING FALL

CHAPITRE II

PRIMARY PRODUCTION AND SINKING EXPORT DURING FALL IN THE HUDSON BAY SYSTEM, CANADA

CHAPITRE III

ABUNDANCE OF FREE-LIVING *VERSUS* PARTICLE-ATTACHED BACTERIA AND THEIR ROLE IN THE RECYCLING AND EXPORT OF ORGANIC MATERIAL IN THE HUDSON BAY SYSTEM

LISTE DES FIGURES

INTRODUCTION GÉNÉRALE

CHAPITRE I

SPATIAL VARIABILITY IN ORGANIC MATERIAL SINKING EXPORT IN THE HUDSON BAY SYSTEM, CANADA, DURING FALL

CHAPITRE III

ABUNDANCE OF FREE-LIVING *VERSUS* PARTICLE-ATTACHED BACTERIA AND THEIR ROLE IN THE RECYCLING AND EXPORT OF ORGANIC MATERIAL IN THE HUDSON BAY SYSTEM

LISTE DES SYMBOLES

BioSi = biogenic silica

B_L = biomass of large phytoplankton cells (≥ 5 μm)

B_S = biomass of small phytoplankton cells (0.7–5 μm)

B_T = total phytoplankton biomass

Chl *a* = chlorophyll *a*

CID = carbone inorganique dissous

CO_2 = dioxyde de carbone

COP = carbone organique particulaire

EHB = eastern Hudson Bay

EPS = exopolymeric substances

FB = Foxe Basin

FL1 = green fluorescence

FPC = fecal pellet carbon

FWC = freshwater content

HB = Hudson Bay

HNA = high nucleic acid

HS = Hudson Strait

LNA = low nucleic acid

N_2 = Brunt-Väisälä frequency

NH_4^+ = ammonium

NO_2^- = nitrite

NO_3^- = nitrate

Pheo = pheopigments

PIC = particulate inorganic carbon

P_L = production of large phytoplankton cells (≥ 5 μm)

PO_4^{3-} = phosphate

POC = particulate organic carbon

POM = particulate organic matter

P_S = production of small phytoplankton cell (0.7–5 μm)

P_T = total particulate primary production

SBH = système de la baie d'Hudson

SD = standard deviation

SEM = scanning electron microscopy

$Si(OH)_4$ = silicic acid

SSC = side angle light scatter

TPC = total particulate carbon

WHB = western Hudson Bay

$Z_{50\%}$ = depth of 50% of surface irradiance

Z_{CFM} = depth of chlorophyll fluorescence maximum

Z_{eu} = euphotic zone depth

Z_{mix} = surface mixed layer depth

INTRODUCTION GÉNÉRALE

Le rôle prépondérant de l'océan dans le cycle global du carbone

Le cycle global du carbone comprend quatre réservoirs principaux : l'atmosphère, les océans, les écosystèmes terrestres et les réserves de combustibles fossiles. La vitesse des échanges entre ces réservoirs varie grandement, de quelques secondes (e.g. fixation du carbone inorganique dissous (CID) par photosynthèse) à plusieurs millénaires (e.g. accumulation du carbone fossile après dépôt et diagénèse de la matière organique) (Houghton 2003, Emerson & Hedges 2008). L'océan actuel contient 39 000 Gt de carbone, dont 700 Gt dans l'océan de surface, ce qui représente 50 fois le contenu en carbone de l'atmosphère (Takahashi 1989, Fasham 2003, Houghton 2003, Emerson & Hedges 2008). Les principaux échanges du réservoir océanique ont lieu avec l'atmosphère. Le transfert du dioxyde de carbone (CO_2) de l'atmosphère vers l'océan se fait par dissolution liée à la différence des pressions partielles de ce gaz dans l'air et dans l'eau (Mann & Lazier 1996, Sarmiento & Gruber 2006). Pour qu'il y ait transfert du CO_2 atmosphérique vers l'océan, il faut une différence de pression partielle entre les eaux de surface océaniques et l'atmosphère. Ce gradient de pression partielle peut être créé par l'exportation du carbone présent dans les couches de surface océaniques suivi de sa séquestration en profondeur sous forme organique ou inorganique, empêchant ainsi sa réémission vers l'atmosphère pour

plusieurs centaines voire milliers d'années. L'exportation du carbone vers l'océan profond peut avoir lieu par l'intermédiaire de différents mécanismes physiques ou biologiques qui constituent les trois pompes océaniques : la pompe à solubilité, la pompe à carbonates et la pompe biologique à CO_2 (Volk & Hoffert 1985) et interviennent ainsi dans les échanges de carbone entre l'océan et l'atmosphère.

La pompe à solubilité

La solubilité du CO_2 étant inversement proportionnelle à la température (Mann & Lazier 1996, Sarmiento & Gruber 2006), plus les eaux sont froides plus elles peuvent contenir de CID (Takahashi 1989, Emerson & Hedges 2008). Dans l'océan Arctique, les eaux froides de surface favorisent donc le transfert du CO_2 atmosphérique vers les couches de surface océaniques (Murata & Takizawa 2003). Les eaux froides sont généralement plus denses et plongent en profondeur dans les zones de formation d'eau profonde (e.g. mers de Norvège, du Groenland et du Labrador). Le CID est alors entraîné avec les masses d'eau plus denses en profondeur créant ainsi un déficit de CID dans les couches de surface et, par conséquent, un pompage du CO_2 de l'atmosphère vers l'océan. Ce mécanisme est appelé la pompe à solubilité (Volk & Hoffert 1985, Fasham 2003, Houghton 2003). Selon Sarmiento et al. (1995), les pompes biologiques contribuent très faiblement à l'exportation et à la séquestration du carbone comparativement à la pompe à solubilité ; excepté aux hautes latitudes où les pompes biologiques seraient responsables de 20% du gradient vertical de CID.

La pompe à carbonates

Dans les couches de surface, le CID peut être incorporé dans la fabrication d'exosquelettes calcaires par des organismes photosynthétiques comme les coccolithophoridés (Riebesell et al. 2000, de la Rocha et al. 2008, Fischer et al. 2009) ou des organismes hétérotrophes comme les foraminifères (Field et al. 2006, Stoll et al. 2007) et les ptéropodes (Orr et al. 2005). Dans l'eau, le CO_2 s'hydrate pour former de l'acide carbonique (H_2CO_3) puis se dissocie et forme l'ion bicarbonate (HCO_3^-). Cet ion est ensuite associé à un ion calcium (Ca^{2+}) pour former du carbonate de calcium ($CaCO_3$) selon l'équation suivante (Riebesell 2004, Sarmiento & Gruber 2006) :

$$Ca^{2+} + 2HCO_3^- \rightarrow CaCO_3 + CO_2 + H_2O$$

Les exosquelettes calcaires ainsi formés sont efficacement exportés en profondeur car ils jouent un rôle de ballast pour les organismes qu'ils recouvrent (de la Rocha et al. 2008, Fischer et al. 2009). Environ 50% du carbonate de calcium incorporé aux exosquelettes de l'océan de surface atteignent le fond océanique et 13% du carbonate de calcium exporté de la surface sont enfouis dans les sédiments chaque année (Sarmiento & Gruber 2006). La pompe à carbonates joue donc un rôle important dans la capacité de séquestration du carbone. Toutefois, cette pompe agit sur une longue période de temps de l'ordre de 10^5 années (Sarmiento & Gruber 2006) et à court terme ne contribue pas au pompage actif de CO_2 de l'atmosphère vers l'océan car la formation du carbonate de calcium libère du CO_2 dans les eaux de surface.

La pompe biologique à CO_2

La pompe biologique à CO_2 inclut l'ensemble des processus de fixation du CID par le phytoplancton sous forme de carbone organique en surface et d'exportation de la matière organique ainsi produite de la surface vers l'océan profond (Volk & Hoffert 1985, Legendre & Le Fèvre 1995, Fasham 2003, Houghton 2003). Dans la couche de surface, le CID est fixé sous forme de carbone organique par le phytoplancton via le processus de photosynthèse (Falkowski & Raven 2007). La photosynthèse combine du carbone, de l'azote et du phosphore sous forme inorganique avec de l'eau pour former, en présence de lumière, de la matière organique et de l'oxygène selon l'équation suivante (Sarmiento & Gruber 2006) :

$$106CO_2 + 16HNO_3 + H_3PO_4 + 78H_2O \rightarrow C_{106}H_{175}O_{42}N_{16}P + 150O_2$$

où si l'on ne considère que le carbone (Falkowski & Raven 2007) :

$$CO_2 + H_2O \rightarrow HCHO + O_2$$

la molécule HCHO correspond aux carbohydrates à la base des glucides et est, par conséquent, à la base de la production de la matière organique susceptible d'alimenter plusieurs voies de transfert vers les milieux pélagiques et benthiques. La photosynthèse utilise donc du CO_2 pour former de l'O_2 alors que la reminéralisation ou respiration (relation inverse) utilise de l'O_2 et produit du CO_2.

La matière organique ainsi formée peut être exportée de la surface vers les couches plus profondes sous différentes formes (Boyd & Trull 2007). Les cellules phytoplanctoniques peuvent sédimenter intactes ou fragmentées ou être consommées par des herbivores principalement le zooplancton (Wassmann 1998, Caron et al. 2004, Buesseler et al. 2008). Le zooplancton produit ensuite des pelotes fécales qui peuvent, dans certains cas, sédimenter rapidement vers le fond (Pilskaln & Honjo 1987, Wexel Riser et al. 2007, Buesseler & Boyd 2009). Enfin, les cellules phytoplanctoniques et les détritus liés à la dégradation de la matière organique peuvent s'agglomérer et former des agrégats, aussi appelés « neige marine » (Alldredge & Silver 1988, Kiørboe & Hansen 1993, Turner 2002), qui peuvent sédimenter rapidement (Alldredge & Jackson 1995, Passow & de la Rocha 2006). L'exportation verticale du carbone organique et sa séquestration dans les couches profondes entraînent un déficit en CO_2 dans les couches de surface, ce qui favorise sa diffusion de l'atmosphère vers l'océan.

La fixation du carbone par le phytoplancton marin représente environ 45 Gt de carbone par an (Falkowski et al. 1998, Field et al. 1998, Houghton 2003, Emerson & Hedges 2008) soit plus de 100 millions de tonnes de carbone par jour. Il a été estimé qu'environ 35% de ce carbone organique synthétisé dans la zone euphotique sont exportés vers le fond de l'océan par an (i.e. 16 Gt C a^{-1} ; Falkowski et al. 1998, Feely et al. 2001, Boyd & Trull 2007), le reste est respiré ou recyclé dans les eaux de surface (Rivkin & Legendre 2001, Fasham 2003). Le carbone organique en voie de sédimentation est lui aussi oxydé ou recyclé au cours de sa descente vers les couches profondes et seuls < 0,5% de la

production primaire de surface seront vraisemblablement séquestrés dans les sédiments marins (Feely et al. 2001, Fasham 2003, Middelburg & Meysman 2007). La fixation nette annuelle de carbone par le phytoplancton est estimée à 2 Gt par an (Dyrssen 2001, Feely et al. 2001, Houghton 2003, Gruber et al. 2009) soit un tiers du carbone émis dans l'atmosphère chaque année par les activités anthropiques (i.e. > 6 Gt C ; Feely et al. 2001, Houghton 2003, Emerson & Hedges 2008). Ainsi, le fonctionnement et l'intensité de ces trois pompes influencent directement la concentration de CO_2 dans l'atmosphère et ont, par conséquent, une action directe sur les changements climatiques globaux.

Les changements climatiques

Au cours des dernières décennies, l'augmentation rapide des concentrations des gaz à effet de serre dans l'atmosphère, et principalement du CO_2, a entraîné une augmentation de la température atmosphérique globale (Takahashi 1989, Watterson 2003, IPCC 2007, Serreze 2010). L'émission de ces gaz à effet de serre majoritairement liée aux activités anthropiques est en constante augmentation (IPCC 2007, Serreze 2010). Par exemple, les émissions de CO_2 dans l'atmosphère mondiale ont augmenté d'environ 80% entre 1970 et 2004, et représentent 77% des émissions anthropiques totales de gaz à effet de serre en 2004 (IPCC 2007). Les modèles globaux sur la circulation atmosphérique et océanique prévoient que le réchauffement planétaire déjà constaté, à l'échelle du globe, se poursuivra au cours des prochaines décennies et sera amplifié aux hautes latitudes à cause de la réduction des couverts de glace de mer et de neige terrestre (Singarayer et al. 2006, IPPC 2007, Stroeve et al. 2007, Holland et al. 2010). La température atmosphérique moyenne

globale a augmenté d'environ 0,7°C au cours du siècle dernier (IPCC 2007, Serreze 2010), avec un réchauffement deux fois plus rapide en Arctique (IPCC 2007). En effet, Overpeck et al. (1997) ont estimé qu'en Arctique, la température moyenne globale avait augmenté de 1,5°C depuis le début de la révolution industrielle.

Les effets du réchauffement climatique sur l'environnement

Les effets du réchauffement climatique déjà constatés se traduisent, par exemple en Arctique, par la diminution du volume de la calotte glaciaire au Groenland (Köberle & Gerdes 2003), le recul des marges de la banquise multi-annuelle (Johannessen et al. 1999, Vinnikov et al. 1999, Comiso 2006a, Howell et al. 2009), l'allongement de la période libre de glace de mer annuelle (Overpeck et al. 1997, Comiso 2006a, Howell et al. 2009) et un changement du régime de précipitations (Peterson et al. 2002, 2006, Callaghan et al. 2004, Higgins & Cassano 2009). Un suivi satellitaire du couvert de glace de mer dans l'océan Arctique entre 1979 et 2007 a révélé une nette diminution de l'étendue minimale du couvert de glace de mer au cours de la période étudiée (Serreze et al. 2007) avec une accélération du déclin de son étendue ces dernières années (Comiso et al. 2008). Ces cinq dernières années ont vu les plus faibles valeurs de l'étendue minimale du couvert de glace des trente dernières années (Comiso 2006b, Kwok 2007, Comiso et al. 2008, NSIDC 2010). L'étendue minimale du couvert de glace de mer arctique a diminué de 2,2% par décennie entre 1979 et 1996 et de 10,1% par décennie entre 1997 et 2007 (Comiso 2006a, Comiso et al. 2008). Le déclin de l'étendue du couvert de glace de mer entre 1979 et 2008 a été estimé à 8,7% par décennie pour l'archipel arctique canadien (Howell et al. 2009).

Les changements climatiques et les pompes océaniques à carbone

Le réchauffement climatique diminue la solubilité du CO_2 dans les couches de surface océaniques et ralentit ainsi la pompe à solubilité (Maier-Reimer et al. 1996, Archer 2005). L'altération de la pompe à solubilité par le réchauffement global est souvent anticipée mais l'impact du réchauffement sur les pompes biologiques est souvent considéré comme mineur (Sarmiento & Le Quéré 1996). Toutefois, de nombreuses études ont montré que les pompes biologiques pouvaient également être profondément altérées par l'augmentation des concentrations en CO_2 et les changements environnementaux qui en découlent.

Dans les régions polaires, il est prévu que le réchauffement climatique et l'augmentation des apports d'eau douce contribueront à réduire le mélange vertical, à modifier la disponibilité de la lumière et à prolonger la saison productive (Richardson & Schoeman 2004, Doney 2006). Certaines études proposent que la prolongation de la période libre de glace permettra à la lumière de pénétrer dans la colonne d'eau plus longtemps et, par conséquent, entraînera une augmentation de la production primaire annuelle aux hautes latitudes et une activation de la pompe biologique (e.g. Rysgaard et al. 1999, Sarmiento et al. 2004, Ellingsen et al. 2008, Pabi et al. 2008). Par exemple, selon Arrigo et al. (2008), la production primaire annuelle de l'océan Arctique a augmenté en moyenne de 28 Tg C a^{-1} entre 2003 et 2007 et, plus particulièrement, de 35 Tg C a^{-1} entre 2006 et 2007. De plus, 30% de cette augmentation seraient associés à la diminution de l'étendue du couvert de glace en été et 70% à l'augmentation de la durée de la saison productive. Au contraire, d'autres études envisagent que l'augmentation de la production

primaire dans les régions arctiques sera limitée par la disponibilité des éléments nutritifs (Behrenfeld et al. 2006, Tremblay et al. 2006). Selon ce scénario, l'augmentation de la stratification limitera les apports en sels nutritifs et donc influencera la composition des producteurs primaires en favorisant la croissance des petites cellules phytoplanctoniques au détriment des diatomées réduisant ainsi l'intensité de la pompe biologique à CO_2 (Bopp et al. 2001, 2005).

Bates et al. (2006) ont montré que le flux de CO_2 de l'atmosphère vers l'océan Arctique avait triplé au cours des 30 dernières années passant de 24 à 66 Tg C a^{-1}. Ces auteurs attribuent cette augmentation à l'influence de la diminution du couvert de glace qui favorise les échanges océan-atmosphère et la production primaire. Il a par ailleurs été démontré qu'une augmentation de la concentration en CID dans l'eau de mer influence la composition taxonomique du phytoplancton par l'intermédiaire d'une compétition inter-espèces pour l'utilisation du CID (Tortell et al. 2002). Il a également été démontré que cette augmentation de la concentration en CID provoque l'acidification du milieu et entraîne la dissolution des exosquelettes calcaires de certaines espèces phytoplanctoniques (Riebesell et al. 2000, Feely et al. 2004, Orr et al. 2005, Yamamoto-Kawai et al. 2009). Ces deux mécanismes altèrent ainsi l'intensité des pompes biologiques. Selon Wohlers et al. (2009), l'augmentation de la température de surface accentuera également la respiration du carbone organique par rapport à sa production par les autotrophes et ainsi diminuera l'exportation verticale de carbone organique vers le fond. L'allongement de la période productive pourrait aussi conduire à un pic d'exportation précoce, avec de nombreuses implications

trophiques pour les communautés pélagiques mais surtout benthiques (Ducklow et al. 2008). Il apparaît donc que les effets des changements climatiques sur l'intensité de la production primaire et la composition taxonomique du phytoplancton se traduiront par des changements dans les processus d'exportation verticale du matériel organique et, par conséquent, auront de profondes implications pour l'apport de nourriture pour les communautés benthiques ainsi que la séquestration du carbone dans l'océan profond.

Le couplage entre la production primaire de surface et son exportation verticale

Au cours des dernières décennies, de nombreux algorithmes ont été développés afin de modéliser la relation existant entre la production primaire et l'exportation verticale du matériel organique particulaire (Tableau 1). Les premières études ont d'abord supposé que l'exportation verticale était directement liée à la production primaire par l'intermédiaire d'une fonction non-linéaire (e.g. Eppley & Peterson 1979, Suess 1980, Betzer et al. 1984, Wassmann 1990). En 1967, Dugdale & Goering ont défini la production nouvelle comme étant la portion de la production primaire dérivée d'un apport de nouveaux sels nutritifs provenant de l'extérieur de la zone euphotique (i.e. couche de la surface à la profondeur du 0,1—1% de lumière incidente). Sur cette base, Eppley & Peterson (1979) ont proposé que l'exportation du matériel organique hors de la zone euphotique soit égale à la production nouvelle sur une échelle de temps et d'espace adéquate. Ces auteurs ont ainsi développé le concept du *f*-ratio (i.e. rapport entre la production nouvelle et la production totale, la production totale étant la somme de la production nouvelle et de la production régénérée) afin d'estimer la proportion de la production primaire qui sédimente hors de la zone

euphotique. Une fois testés sur des données réelles, ces algorithmes n'ont pas toujours donné de bonnes estimations (e.g. Boyd & Newton 1995, Olesen & Lundsgaard 1995, Karl et al. 1996) suggérant que la production primaire n'était pas le seul facteur conditionnant l'exportation verticale du matériel organique hors de la zone euphotique.

Par la suite, différents auteurs ont proposé que la structure des communautés phytoplanctonique et zooplanctonique était le principal facteur contrôlant l'intensité et la composition des flux verticaux de matériel organique (e.g. Michaels & Silver 1988, Boyd & Newton 1995, 1999, Boyd et al. 2008). Le raisonnement de ces auteurs était basé sur le fait que les cellules phytoplanctoniques de plus grande taille sédimentent plus rapidement que les cellules plus petites (Legendre & Le Fèvre 1991, Buesseler 1998, 2008) ; tout particulièrement les diatomées pour lesquelles les frustules siliceux (Brzezinski 1985, Armstrong et al. 2009, Fischer et al. 2009, Lee et al. 2009) et la formation d'agrégats (Passow & de la Rocha 2006, de la Rocha et al. 2008) augmentent la vitesse de chute. Les cellules de grande taille peuvent également être intégrées dans le réseau trophique herbivore par broutage par le mésozooplancton et être rapidement exportées vers le fond sous forme de pelotes fécales (Legendre & Le Fèvre 1991, Aksnes & Wassmann 1993, Buesseler 1998, 2008). Sur la base de ce raisonnement, Tremblay et al. (1997) ont recalculé le *f*-ratio à partir de la structure de taille de la communauté phytoplanctonique et plus particulièrement à partir de la contribution des grandes cellules à la production primaire totale (Tableau 1). Cependant, Richardson & Jackson (2007) ont récemment mis en évidence que la contribution des petites cellules à l'exportation verticale du carbone

organique était proportionnelle à leur contribution à la production totale. En effet, les petites cellules peuvent être exportées rapidement lorsqu'elles forment des colonies ou agrégats, être incorporées dans le mucus de filtreurs (e.g. salpes, ptéropodes) ou broutées par le mésozooplancton et incorporées dans des pelotes fécales qui sédimentent.

Une autre approche pour établir la relation entre production et exportation consiste à calculer le rapport d'exportation (i.e. rapport entre le flux de carbone organique particulaire (COP) sous la zone euphotique et la production primaire totale) (Wexels Riser et al. 2002). Olesen & Lundsgaard (1995) et Karl et al. (1996) ont calculé les rapports d'exportation en milieu côtier et dans l'océan ouvert, respectivement. Ils n'ont pas observé de contrôle évident de l'exportation ni par la production primaire ni par la structure de taille des communautés planctoniques. Plus récemment, il a été mis en évidence que le couplage entre la production primaire et son exportation verticale était influencé par des facteurs du milieu tels que la température (Laws et al. 2000), le mélange vertical (Tian et al. 2001) et la profondeur de la zone euphotique (Dunne et al. 2005) (Tableau 1) mais également par des facteurs biologiques comme la présence d'exosquelettes siliceux ou calcaires à la surface des cellules de certains groupes phytoplanctoniques (Armstrong et al. 2002, 2009, François et al. 2002, Fischer et al. 2009) ou l'état physiologique des cellules (Waite & Nodder 2001, Kahl et al. 2008). Toutefois, tous ces paramètres ne permettent pas toujours d'estimer de façon précise l'exportation du matériel organique vers le fond.

Tableau 1. Algorithmes proposés pour modéliser la relation entre la production primaire et l'exportation verticale du matériel organique particulaire et équations proposées pour le calcul du *f*-ratio.

Référence	Équation	Milieu
Relations entre la production primaire et le flux vertical		
Eppley & Peterson 1979	$F = 0.0025 \times P_T^2$ pour $P_T \leq 200$ g C m^{-2} a^{-1}	Océan mondial
	$F = 0.5\ P_T$ pour $P_T > 200$ g C m^{-2} a^{-1}	
Suess 1980	$F = P_T / (0.0238 \times Z + 0.212)$	Océan mondial
Betzer et al. 1984	$F = (-0.388 \times Z)^{-0.628} \times P_T^{1.41}$	Océan Pacifique équatorial
Wassmann 1990	$F = 0.049 \times P_T^{1.41}$	Atlantique Nord boréal
Laws et al. 2000	$F = f(P_T ; 1/T)$	Océan mondial
Tian et al. 2001	$F = f(P_T ; 1/Z ; \Phi_L ; K_z)$	Écosystèmes polaires côtiers
Dunne et al. 2005	$F = f(P_T ; 1/T ; 1/Z_{eu} ; \Phi_L)$	Océan mondial
Calculs du *f*-ratio		
Eppley & Peterson 1979	$f\text{-ratio} = P_{new} / P_T$	Océan mondial
Tremblay et al. 1997	$f\text{-ratio} = 0.04 + 0.74\ (P_L / P_T)$	Océan mondial
	$f\text{-ratio} = 0.08 + 0.53\ (B_L / B_T)$	

F = flux vertical (mg C m^{-2} j^{-1}) ; P_T = production primaire totale (mg C m^{-2} j^{-1}) ; P_{new} = production primaire nouvelle (mg C m^{-2} j^{-1}) ; P_L = production des grandes cellules (mg C m^{-2} j^{-1}) ; B_T = biomasse phytoplanctonique totale (mg chl *a* m^{-3}) ; B_L = biomasse des grandes cellules phytoplanctoniques (mg chl *a* m^{-3}) ; Z = profondeur où le flux est mesuré (m) ; Z_{eu} = profondeur de la zone euphotique (m) ; T = température (°C) ; Φ_L = contribution des grandes cellules ; K_z = mélange vertical (m^2 j^{-1}) ; *f* = fonction des variables entre parenthèses.

Ce découplage potentiel entre la production de surface et l'exportation sous la zone euphotique peut être en partie lié à la dégradation du matériel au cours de sa sédimentation (Legendre & Le Fèvre 1995, Buesseler et al. 2008, Reigstad et al. 2008, Steinberg et al. 2008, Buesseler & Boyd 2009). Cette dégradation est principalement due à la reminéralisation bactérienne (Azam et al. 1983, Azam 1998, Aristegui et al. 2009, Buesseler & Boyd 2009) ainsi qu'au broutage des cellules phytoplanctoniques intactes et des pelotes fécales (Steinberg et al. 2008, Buesseler & Boyd 2009). Les bactéries atténuent

le flux vertical de matériel organique principalement par hydrolyse enzymatique mais également en fragmentant et désagrégeant les particules (Cho & Azam 1988, Simon et al. 2002, Gasol et al. 2008). La reminéralisation du matériel organique a lieu tout au long de sa sédimentation et certaines bactéries restent accrochées à la surface des particules (e.g. Alldredge et al. 1986, Grossart et al. 2003a, b, Garneau et al. 2009). En s'attachant les bactéries peuvent non seulement reminéraliser mais également contribuer au flux vertical de matériel organique (e.g. Ducklow et al. 1982, Pedrós-Alió & Mas 1993, Turley & Mackie 1994). Au cours de leur sédimentation, les pelotes fécales peuvent être non seulement reminéralisées par les bactéries mais également recyclées par le zooplancton lui-même. En effet, des phénomènes tels que la coprophagie, la coprohéxie et la coprochalie des pelotes fécales réduisent le flux vertical de pelotes fécales dans la colonne d'eau (Noji et al. 1991, Poulsen & Kiørboe 2005, Wilson et al. 2008). Seule une faible proportion du matériel organique exporté sous la zone euphotique sédimente en profondeur. De façon typique, on observe une diminution exponentielle du flux de COP liée aux processus de reminéralisation pendant la descente (Martin et al. 1987). Par ailleurs, certains auteurs ont mis en évidence que l'atténuation des flux et donc l'intensité de la reminéralisation pouvaient varier en fonction de la quantité de matériel organique exporté sous la zone euphotique (e.g. Berelson 2001, Pommier et al. 2008).

Il apparaît donc évident que le couplage entre la production primaire et son exportation vers l'océan profond dépend d'un ensemble complexe de facteurs biologiques et environnementaux (Wassmann 1998, Boyd & Trull 2007). Au cours des dernières

décennies, plusieurs études utilisant des pièges à particules à long terme (e.g. Hargrave et al. 2002, Forest et al. 2007, Lalande et al. 2009) ou à court terme (e.g. Atkinson & Wacasey 1987, Andreassen & Wassmann 1998, Michel et al. 2002, Caron et al. 2004, Juul-Pedersen et al. 2006, 2008, Lalande et al. 2007a) ainsi que le thorium-234 (e.g. Moran et al. 2005, Lalande et al. 2007b, Lepore & Moran 2007) ont porté sur l'exportation du matériel organique hors de la zone euphotique dans les régions arctiques. Toutefois, aucune étude n'a été publiée sur l'exportation du matériel organique particulaire dans la baie d'Hudson pendant la période d'eau libre de glace.

Le système de la baie d'Hudson

Le système de la baie d'Hudson (SBH) constitue la plus grande mer intérieure au monde ($1{,}23 \times 10^6$ km^2 ; Jones & Anderson 1994, Granskog et al. 2007) et comprend : la baie d'Hudson, le détroit d'Hudson et le bassin de Foxe (Fig. 1). Le SBH se situe dans la région subarctique du Canada et connaît un cycle cryogénique complet chaque année. Dans la baie d'Hudson, la glace commence à se former à la fin octobre et la baie est libre de glace début août (Markham 1986, Wang et al. 1994, Gagnon & Gough 2005a, 2006). Dans le détroit d'Hudson, la formation de la glace débute plus tardivement en novembre et le dégel est plus précoce en juin (Houser & Gough 2003). Dans le bassin de Foxe, la durée du couvert de glace est plus longue et s'étend du début octobre à la fin septembre (Markham 1986).

Le SBH est soumis à l'influence de différents apports d'eau salée provenant de la baie de Baffin et de l'océan Arctique, et d'eau douce liés aux rivières, aux précipitations et à la fonte de la glace de mer. Les eaux de l'océan Arctique entrent dans le SBH par le détroit de Fury et Hecla puis traversent le bassin de Foxe vers le sud (Sadler 1982, Prinsenberg 1986a) (Fig. 1). Une partie de ces eaux s'associe aux eaux sortant de la baie d'Hudson et sort du SBH le long de la rive sud du détroit d'Hudson (Straneo & Saucier 2008a), le reste entre dans la baie d'Hudson par les détroits de Roes Welcome et d'Evans situés de part et d'autre de l'île Southampton (Prinsenberg 1986b, Ingram & Prinsenberg 1998, Straneo & Saucier 2008b). Les eaux de la baie de Baffin, quant à elles, entrent dans le SBH par le nord du détroit d'Hudson et rejoignent les eaux sortant du bassin de Foxe pour entrer dans la baie d'Hudson (Prinsenberg 1986b, Jones & Anderson 1994, Straneo & Saucier 2008a). La baie d'Hudson reçoit également d'importants apports d'eau douce (environ $592\ km^3\ a^{-1}$) provenant du large bassin versant qui l'entoure (i.e. environ $3{,}1 \times 10^6\ km^2$; Déry et al. 2005). Les apports fluviaux et les entrées d'eau plus salée provenant du détroit d'Hudson et du bassin de Foxe génèrent une circulation cyclonique au sein de la baie d'Hudson (Prinsenberg 1986c, Saucier et al. 2004).

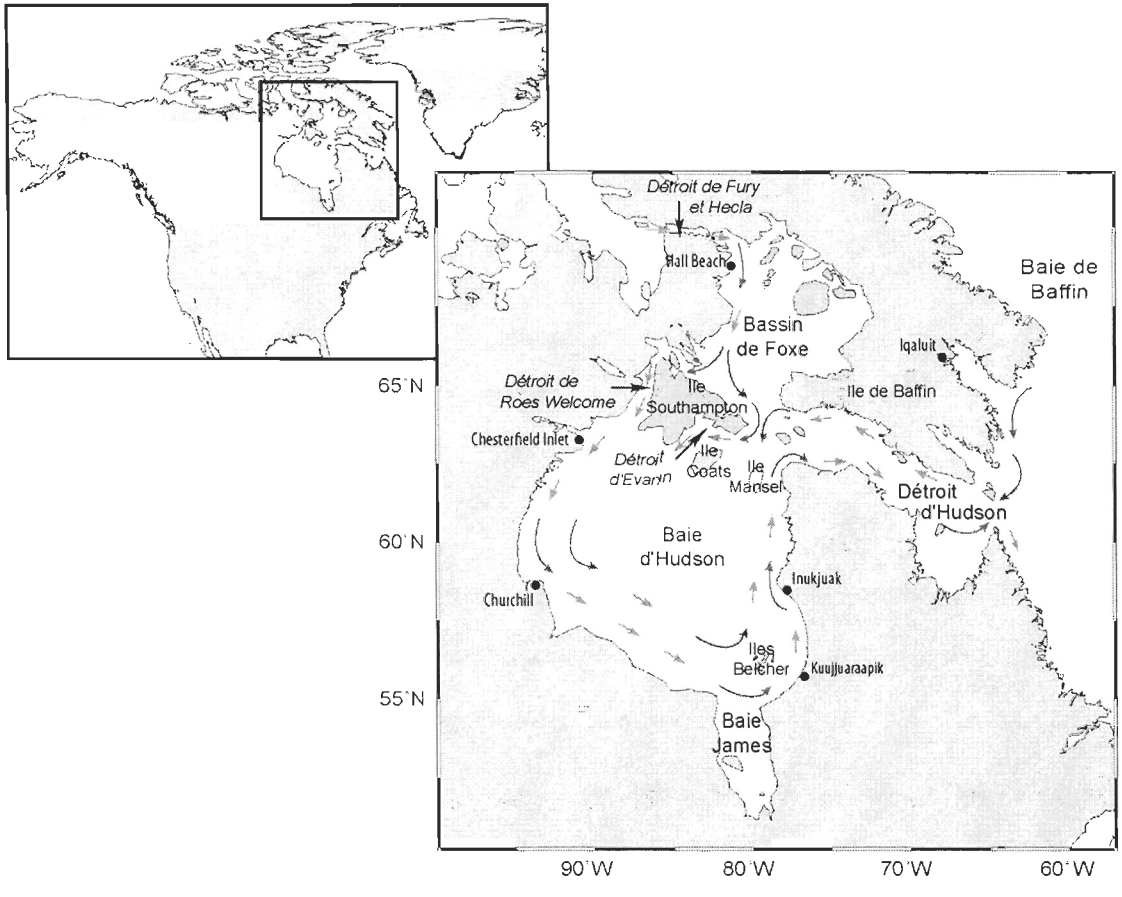

Fig. 1. Carte du système de la baie d'Hudson avec la circulation des eaux de surface (d'après Prinsenberg 1986a, b).

Les importants apports d'eau douce contribuent à fortement stratifier la colonne d'eau de cette mer peu profonde qu'est la baie d'Hudson (profondeur moyenne 120 m, Prinsenberg 1984). Le bassin de Foxe est caractérisé par une profondeur moyenne inférieure à 100 m avec des profondeurs plus élevées (i.e. environ 200 m) au niveau du chenal de Foxe qui relie le bassin au détroit et à la baie d'Hudson (Jones & Anderson 1994). Les apports d'eau douce y sont vingt fois plus faibles que dans la baie d'Hudson. Cependant, le cycle plus long de la glace de mer entraîne des gradients de température et de salinité importants qui contribuent, comme pour la baie d'Hudson, à stratifier fortement la colonne d'eau (Prinsenberg 1986b). Comparativement aux bassins précédents, le détroit d'Hudson qui relie la baie d'Hudson et le bassin de Foxe à la mer du Labrador, est plus profond (profondeur moyenne 400 m) et on y observe de forts courants de marée (i.e. > 2–3 m s^{-1}) et une grande amplitude de marée (i.e. > 4 m) qui génèrent un fort mélange vertical (Drinkwater & Jones 1987, Drinkwater 1988, Arbic et al. 2007).

Sa localisation géographique et son couvert de glace saisonnier rendent le SBH particulièrement vulnérable aux changements climatiques (Rouse 1991). Plusieurs études ont déjà démontré une diminution de l'étendue du couvert de glace dans la région de la baie d'Hudson (Stirling et al. 1999, Gough et al. 2004, Gagnon & Gough 2006). Par exemple, une diminution de l'étendue du couvert de glace de 2000 ± 900 km^2 a^{-1} a été observée entre 1978 et 1996 (Parkinson et al. 1999). Une augmentation de la température annuelle de surface, un dégel précoce et un regel tardif ont également été observés entre 1971 et 2003 (Gagnon & Gough 2005a). Markus et al. (2009) ont estimé la précocité du dégel de la glace

de mer dans la baie d'Hudson à 10 jours par décennie pendant la période de 1979 à 2009. Des tendances similaires ont été rapportées pour le détroit d'Hudson (Houser & Gough 2003). Selon les modèles climatiques, la température projetée pour 2070–2099 sera de 4,8 à 8,0°C plus élevées que les températures moyennes relevées entre 1961 et 1990 (Gagnon & Gough 2005b) et la saison pendant laquelle la baie d'Hudson est couverte de glace sera réduite de 7 à 9 semaines pour la période de 2041 à 2070 (Joly et al. 2010). Cela laisse entrevoir une plus longue période de productivité et possiblement une augmentation de la production primaire dans le SBH. Toutefois, contrairement à la plupart des mers arctiques et sub-arctiques, la baie d'Hudson est actuellement, pour l'ensemble de la saison libre de glace, une source de CO_2 avec un flux de l'océan vers l'atmosphère estimé à 1,60 Tg C (Else et al. 2008). Il apparaît donc difficile de prévoir l'effet des changements climatiques attendus sur la capacité de captage *versus* libération du carbone au sein du SBH.

Études antérieures de la production primaire et de sa sédimentation dans la zone d'étude

Les premiers travaux océanographiques dans le SBH ont débuté en 1930 avec la mission sur le chalutier « Loubyrne », lors de laquelle plusieurs stations ont été échantillonnées à l'aide d'un filet à plancton. À partir de ces échantillons, Davidson (1931) a observé un gradient géographique de l'abondance des grandes formes phytoplanctoniques croissant de l'ouest de la baie d'Hudson vers l'embouchure du détroit d'Hudson. Par la suite, Bursa (1961, 1968) a constaté que les abondances phytoplanctoniques estivales étaient moins élevées dans la baie que dans le détroit d'Hudson. Legendre & Simard (1979)

ont obtenu les premières données de production primaire entre les îles Belcher et la côte au sud-est de la baie avec des taux horaires mesurés à la fin de l'été entre 1,3 et 2,5 mg C m^{-3}. À partir de ces taux horaires, Roff & Legendre (1986) ont estimé une production primaire annuelle dans la région du détroit de Manitounuk (sud-est de la baie d'Hudson) de 35 g C m^{-2}. Grainger (1982) a, par la suite, mesuré un taux moyen de production primaire horaire de 3 mg C m^{-3} autour des îles Belcher et estimé la production primaire annuelle dans ce secteur à 26 g C m^{-2}.

La première étude sur le phytoplancton couvrant l'ensemble de la baie d'Hudson a été réalisée par Anderson & Roff (1980) en période estivale. Au cours de cette étude, ces auteurs ont observé un gradient de la côte vers le large : au large, la salinité était plus élevée (i.e. < 28 *versus* ≥ 28, respectivement), et la biomasse chlorophyllienne (i.e. 0,28 mg chl *a* m^{-3} *versus* 0,09 mg chl *a* m^{-3}, respectivement) et le rapport chlorophylle sur phéopigments plus faibles. En zone côtière, ces mêmes auteurs ont distingué différentes régions présentant des caractéristiques hydrographiques, chimiques et biologiques différentes. Les biomasses chlorophylliennes les plus faibles ont été observées dans la région de Chesterfield Inlet et la côte nord-est et les plus fortes dans les régions des îles Belcher et des îles Southampton, Coats et Mansel. En fin de période estivale, Harvey et al. (1997) ont réalisé une radiale du sud-est de la baie vers l'embouchure du détroit d'Hudson et ont également distingué différentes régions présentant des caractéristiques hydrographiques, chimiques et biologiques différentes. Dans le détroit d'Hudson, la colonne d'eau était bien mélangée, les biomasses chlorophylliennes étaient supérieures à

celles observées dans la baie (i.e. > 2,0 mg chl *a* m^{-3}) et la communauté phytoplanctonique était dominée par les cellules de grande taille (i.e. diatomées). Dans la baie d'Hudson, la colonne d'eau était généralement plus stratifiée, les biomasses chlorophylliennes plus faibles et la communauté phytoplanctonique était dominée par les cellules de plus petite taille principalement des flagellés. Cependant, dans la baie, différentes régions ont pu être distinguées comme dans les études précédentes avec, en autres, des biomasses chlorophylliennes maximales dans la région des îles Belcher (i.e. > 1,0 mg chl *a* m^{-3}).

Plus récemment, dans le cadre du programme de monitorage de l'Étude des mers intérieures du Canada (MERICA-nord), une radiale nord-sud dans le détroit d'Hudson, une radiale ouest-est dans la baie d'Hudson et une station dans le bassin de Foxe ont été échantillonnées en fin de période estivale entre 2003 et 2006. De 2004 à 2006, la production primaire estivale moyenne a varié de 301 à 1217 mg C m^{-2} j^{-1} dans la baie d'Hudson, de 412 à 2740 mg C m^{-2} j^{-1} dans le détroit d'Hudson et de 278 à 504 mg C m^{-2} j^{-1} dans le bassin de Foxe (Ferland 2010). Cette étude a également confirmé la forte stratification de la baie d'Hudson par rapport au détroit d'Hudson. Comparativement à d'autres mers arctiques et sub-arctiques, la baie d'Hudson présente une production primaire annuelle faible (50–70 g C m^{-2}) comparable à la mer de Beaufort (30–70 g C m^{-2}) (Sakshaug 2004). La production nouvelle annuelle a été estimée à 24–35 g C m^{-2} dans le secteur nord de la baie d'Hudson (Jones & Anderson 1994).

À notre connaissance, Tremblay et al. (1989) ont présenté les premières et seules données sur le flux vertical de matériel organique particulaire dans la baie d'Hudson. L'échantillonnage a été effectué à l'aide de pièges à particules fixés sous la glace de mer au sud-est de la baie au printemps. Les taux de sédimentation de pigments mesurés étaient < 0,6 mg chl *a* m^{-2} j^{-1} et < 0,3 mg phéopigments m^{-2} j^{-1}. Les premières données de vitesse de chute cellulaire ont été obtenues par Michel et al. (1993) sur des algues de glace au sud-est de la baie et ont varié entre 0,4 et 2,7 m j^{-1}. Enfin, le taux moyen d'enfouissement du COP dans les sédiments sur l'ensemble de la baie d'Hudson a été estimé à $1,3 \times 10^6$ t C a^{-1} dont environ 80% seraient d'origine marine (Kuzyk et al. 2009).

Problématique

Le réchauffement climatique prenant place à l'échelle du globe met en évidence la nécessité et l'urgence de comprendre l'impact de ces changements sur les écosystèmes arctiques et sub-arctiques et les communautés qui y vivent. C'est dans cette optique que le Réseau de centres d'excellence du Canada, ArcticNet, a été mis en place. L'objectif central du réseau ArcticNet est d'étudier les impacts des changements climatiques dans l'Arctique canadien côtier afin de contribuer au développement et à la diffusion des connaissances nécessaires à la formulation de stratégies d'adaptation face à ces changements. Par ailleurs, afin de pouvoir détecter, comprendre, suivre et prédire les changements environnementaux dans le SBH, le ministère des Pêches et Océans a initié en 2003 le programme de monitorage MERICA-nord. Ces deux programmes ont servi de piliers pour cette thèse de recherche portant sur la production et l'exportation du matériel organique au sein du SBH.

Nous prévoyons que les modifications de la production et de la structure des communautés phytoplanctoniques liées aux changements climatiques conduiront à de nombreux changements en termes de la quantité, mais aussi de la qualité des voies d'exportation du matériel organique. Ces changements auront assurément des conséquences importantes pour les communautés pélagiques et benthiques, notamment en termes d'interactions trophiques et par conséquent de distribution et de composition taxonomique, particulièrement dans un milieu peu profond comme le SBH. Cependant, avant d'envisager différents scénarios portant sur les modifications du couplage entre la production primaire et les réseaux pélagiques et benthiques, nous devons acquérir des connaissances supplémentaires sur la situation actuelle.

Objectifs du projet doctoral

L'objectif central de cette thèse est de caractériser et de quantifier la relation entre la production primaire et l'exportation du matériel organique hors de la zone euphotique dans une mer subarctique en période libre de glace. De nombreux programmes internationaux ont été mis en place afin d'étudier la problématique du couplage entre la production primaire et son exportation dans différents milieux marins (e.g. VERTEX, JGOFS, VERTIGO, MEDFLUX) mais ce genre d'étude n'avait, jusqu'à ce jour, jamais été mené dans la baie d'Hudson.

Cette thèse de doctorat comprend trois parties. Dans le premier chapitre, j'ai étudié la variabilité spatiale de la sédimentation du phytoplancton et du matériel particulaire sous la zone euphotique. L'objectif de ce chapitre était de quantifier et de caractériser le matériel organique qui sédimente hors de la zone euphotique à l'aide de pièges à particules dérivant à court terme déployés dans différentes régions hydrographiques du SBH. J'ai quantifié et caractérisé l'exportation de matériel organique à différentes profondeurs (i.e. 50, 100 et 150 m) ainsi que son atténuation avec la profondeur. Cette étude m'a permis de tester l'hypothèse selon laquelle l'exportation verticale du matériel organique est une source importante de matériel peu dégradé pour les communautés benthiques compte tenu de la faible profondeur du SBH.

Le second chapitre concerne l'étude du couplage entre la production primaire et la sédimentation du matériel particulaire dans le SBH. L'objectif de ce chapitre était de quantifier et de caractériser la production primaire au sein de la zone euphotique pour ensuite déterminer l'influence de l'intensité de la production et la structure de la communauté planctonique sur l'exportation du matériel organique hors de la zone euphotique. J'ai également testé l'influence de variables du milieu telles que le mélange vertical et la disponibilité des sels nutritifs sur ce couplage. Cette étude a permis de tester l'hypothèse selon laquelle une forte exportation verticale est associée à une production primaire élevée et/ou une biomasse importante des grandes cellules phytoplanctoniques.

Enfin, dans le dernier chapitre de cette thèse, j'ai étudié le rôle des bactéries attachées aux particules dans l'exportation du matériel organique. Cet aspect généralement négligé lors des études sur l'exportation verticale de la matière organique a fait l'objet de controverse au cours de la dernière décennie. Dans le cadre du premier chapitre de cette thèse, j'ai pu mettre en évidence des flux de carbone bactérien significatifs et supérieurs aux flux de carbone associés aux protistes intacts et aux pelotes fécales d'herbivores. Ces résultats m'ont donc poussé à approfondir mes recherches sur le rôle des bactéries dans l'exportation verticale de matériel organique en tant que recycleurs mais également en temps que contributeurs. L'objectif de ce chapitre était donc de déterminer les vitesses de chute des bactéries attachées aux protistes et d'estimer leur contribution en termes de biomasse au flux de COP par rapport aux pertes occasionnées par leur respiration. Cette étude m'a permis de tester les hypothèses selon lesquelles : (1) les bactéries peuvent avoir des vitesses de chute supérieures à celles prédites par la loi de Stoke en s'attachant aux particules qui sédimentent, et (2) les bactéries ont principalement un rôle dans la reminéralisation du matériel organique et contribuent peu au flux de COP.

CHAPITRE I

SPATIAL VARIABILITY IN ORGANIC MATERIAL SINKING EXPORT IN THE HUDSON BAY SYSTEM, CANADA, DURING FALL

RÉSUMÉ

Les variations spatiales de l'exportation verticale du matériel organique ont été étudiées dans le système de la baie d'Hudson (i.e. baie d'Hudson, détroit d'Hudson et bassin de Foxe) au cours de la deuxième expédition océanographique d'ArcticNet, à bord du NCCG *Amundsen* au début de l'automne 2005. Les flux verticaux de matériel organique particulaire ont été mesurés à l'aide de pièges à particules dérivants à court terme déployés à 50, 100 et 150 m pendant 8 à 20 h à huit stations. Des mesures de chlorophylle *a* (chl *a*), phéopigments (pheo), carbone organique particulaire (COP), silice biogénique (BioSi), protistes, pelotes fécales et bactéries ont été réalisées sur le matériel collecté. En parallèle, la salinité et la température de la couche de surface ont été déterminées à 121 stations dans le système de la baie d'Hudson. Trois régions hydrographiques présentant des patrons d'exportation différents ont pu être identifiées à partir de la salinité et de la température de surface. Le détroit d'Hudson était caractérisé par une signature marine avec une salinité élevée (moyenne = 32,3) et une faible température (moyenne = 2,1°C). L'est de la baie d'Hudson était très influencé par les apports fluviaux et présentait la salinité moyenne la plus faible (26,6) et la température moyenne la plus élevée (7,6°C) des trois régions. L'ouest de la baie d'Hudson présentait une salinité et une température intermédiaires (moyenne = 29,4 et 4,4°C, respectivement). Les flux verticaux de pigments totaux (chl *a* + pheo = 3,37 mg m^{-2} d^{-1}), de carbone associé aux diatomées (19,8 mg m^{-2} d^{-1}) et de BioSi (50,2 mg m^{-2} d^{-1}) à 50 m étaient les plus élevés dans le détroit d'Hudson. L'est de la baie d'Hudson montrait des flux verticaux de pigments totaux (0.52 mg m^{-2} d^{-1}), de carbone associé aux diatomées (3,29 mg m^{-2} d^{-1}) et de BioSi (36,6 mg m^{-2} d^{-1}) plus élevés qu'à l'ouest (0,19, 0,05 et 7,76 mg m^{-2} d^{-1}, respectivement). Les flux verticaux de COP à 50 m étaient faibles et relativement uniformes sur l'ensemble du système de la baie d'Hudson (37,5–76,8 mg C m^{-2} d^{-1}). Cependant, des variations spatiales de la composition du matériel organique exporté ont été observées. Une grande partie (37–78%) du COP exporté n'était pas identifiable lors de l'observation par microscopie et a été qualifiée de détritus amorphes. En ne considérant que le matériel identifiable, les principaux contributeurs du COP exporté étaient les protistes sous forme de cellules intactes dans le détroit d'Hudson (28%), les pelotes fécales à l'est de la baie d'Hudson (52%) et les bactéries à l'ouest de la baie d'Hudson (17%). Une atténuation significative des flux verticaux de COP avec la profondeur (diminution moyenne entre 50 et 150 m = 32%) ainsi qu'une augmentation significative des rapports BioSi : COP (augmentation moyenne entre 50 et 150 m = 76%) ont été observées uniquement dans le détroit d'Hudson et l'est de la baie d'Hudson. Pour tous les autres flux verticaux et rapports de composition, nous n'avons pas trouvé de

différence significative avec la profondeur. Ces résultats montrent que pendant l'automne, l'exportation verticale de COP total provenant de la zone euphotique était constante sur l'ensemble du système de la baie d'Hudson alors que les autres constituants du matériel organique exporté (e.g. chl *a*, BioSi, pelotes fécales, protistes) présentaient des variations spatiales marquées.

ABSTRACT

Spatial variations in the sinking export of organic material were assessed within the Hudson Bay system (i.e. Hudson Bay, Hudson Strait and Foxe Basin) during the second oceanographic expedition of ArcticNet, on board the CCGS *Amundsen* in early fall 2005. Sinking fluxes of particulate organic material were measured using short-term free-drifting particle interceptor traps deployed at 50, 100 and 150 m for 8 to 20 h at eight stations. Measurements of chlorophyll *a* (chl *a*), pheopigments (pheo), particulate organic carbon (POC), biogenic silica (BioSi), protists, fecal pellets and bacteria were performed on the collected material. In parallel, sea surface salinity and temperature were determined at 121 stations in the Hudson Bay system. Three hydrographic regions presenting different sedimentation patterns were identified based on average surface salinity and temperature. Hudson Strait was characterized by a marine signature, with high salinity (average 32.3) and low temperature (average 2.1°C). Eastern Hudson Bay was strongly influenced by river runoff and showed the lowest average salinity (26.6) and highest average temperature (7.6°C) of the three regions. Western Hudson Bay showed intermediate salinity (average 29.4) and temperature (average 4.4°C). Sinking fluxes of total pigments (chl *a* + pheo 3.37 mg m^{-2} d^{-1}), diatom-associated carbon (19.8 mg m^{-2} d^{-1}) and BioSi (50.2 mg m^{-2} d^{-1}) at 50 m were highest in Hudson Strait. Eastern Hudson Bay showed higher sinking fluxes of total pigments (0.52 mg m^{-2} d^{-1}), diatom-associated carbon (3.29 mg m^{-2} d^{-1}) and BioSi (36.6 mg m^{-2} d^{-1}) compared to western Hudson Bay (0.19, 0.05 and 7.76 mg m^{-2} d^{-1}, respectively). POC sinking fluxes at 50 m were low and relatively uniform throughout the Hudson Bay system (37.5–76.8 mg C m^{-2} d^{-1}), but spatial variations in the composition of the sinking organic material were observed. A large part (37–78%) of the total sinking POC was unidentifiable by microscopic observation and was qualified as amorphous detritus. Considering only the identifiable material, the major contributors to the POC sinking flux were intact protist cells in Hudson Strait (28%), fecal pellets in eastern Hudson Bay (52%) and bacteria in western Hudson Bay (17%). A significant depth-related attenuation of the POC sinking fluxes (average loss between 50 and 150 m = 32%) and a significant increase in the BioSi:POC ratio (average increase between 50 and 150 m = 76%) were observed in Hudson Strait and eastern Hudson Bay. For all other sinking fluxes and composition ratios, we found no statistically significant difference with depth. These results show that during fall, the sinking export of total POC from the euphotic zone remained fairly constant throughout the Hudson Bay system, whereas other components of the organic sinking material (e.g. chl *a*, BioSi, fecal pellets, protist cells) showed strong spatial variations.

1.1 Introduction

Over the last few decades, there has been a growing interest in climate change and its effect on arctic and subarctic environments (e.g. Johannessen et al. 1995, Moritz et al. 2002, Serreze et al. 2007). Environmental changes already observed include a decline in the volume and extent of the sea-ice cover (Johannessen et al. 1999, Comiso et al. 2008), an advance in the melt period (Overpeck et al. 1997, Comiso 2006b), and an increase in river discharge to the Arctic Ocean (Peterson et al. 2002, McClelland et al. 2006) due to increasing precipitation and terrestrial ice melt (Peterson et al. 2006).

Hudson Bay, Hudson Strait and Foxe Basin (the Hudson Bay system) make up a large inland sea in the Canadian subarctic region (Jones & Anderson 1994). Hudson Bay is a shallow embayment (average depth 120 m, Prinsenberg 1984) strongly influenced by riverine input, mainly from the Nelson, Severn, Churchill, Great Whale, Winisk, and James Bay rivers (Fig. 1; Déry et al. 2005). Hudson Strait, with an average depth of 400 m, links Hudson Bay and Foxe Basin with the Labrador Sea (Drinkwater & Jones 1987, Jones & Anderson 1994). The climate of this system is anomalously cold in comparison to other regions of similar latitudes because of the presence of a seasonally varying ice cover (Rouse 1991). Its subarctic location and the presence of a seasonal ice cover make the Hudson Bay system particularly vulnerable to climate-related changes. Indeed, the sea-ice extent in Hudson Bay decreased by 2000 ± 900 km^2 y^{-1} between 1978 and 1996 (Parkinson et al. 1999). An increase in the mean annual sea surface temperature, earlier ice breakup and delayed freeze-up were also detected in Hudson Bay between 1971 and 2003 (Gagnon

& Gough 2005a). The average surface water temperature projected for 2070–2099 is between 4.8 and 8.0°C higher than the average for 1961–1990 (Gagnon & Gough 2005b).

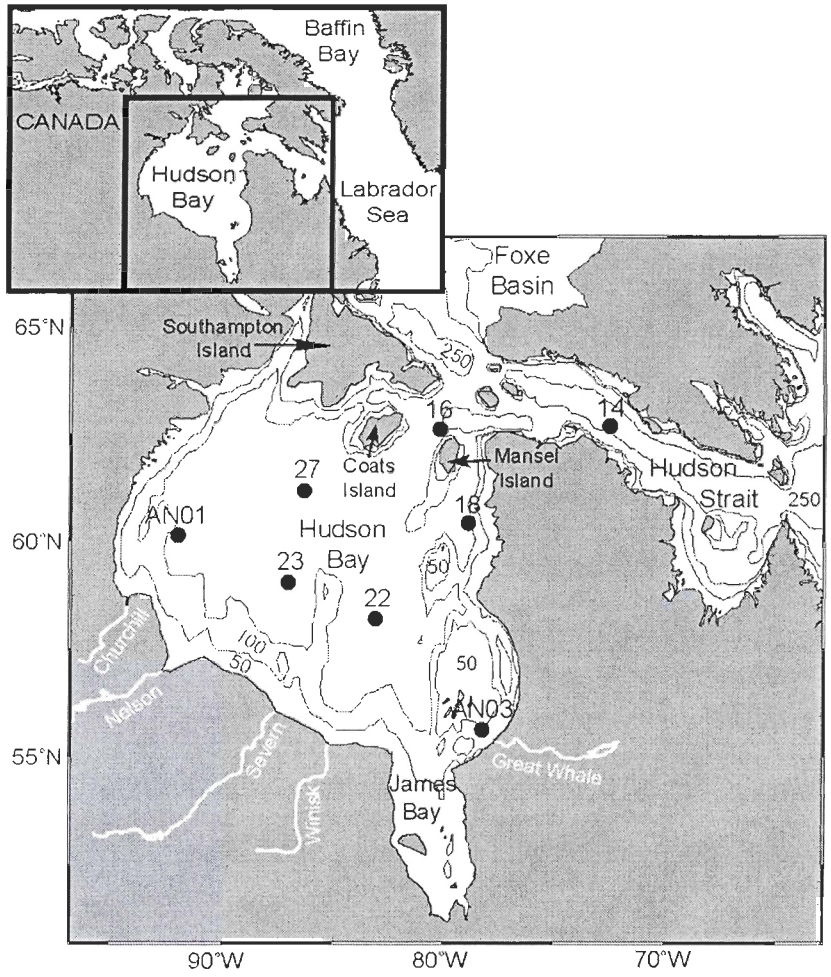

Fig. 1. Location of the sampling stations in the Hudson Bay system during early fall 2005. Isobaths are in meters.

The global carbon cycle, and particularly the increase in atmospheric CO_2 concentrations, plays a key role in the warming trend observed over the past decades (IPCC 2007). As part of the global carbon cycle, atmospheric CO_2 is transferred to the surface

ocean by diffusion and can be converted into organic carbon by primary producers. The fate of surface primary production, i.e. channeling through grazers, recycling in the water column or sinking export to depth, is influenced by a variety of factors, including the taxonomic composition of the phytoplankton (e.g. Boyd & Newton 1995) and zooplankton communities (e.g. Pasternak et al. 2002, Wexels Riser et al. 2002) as well as transformation processes taking place during sinking (e.g. Boyd et al. 1999). Since phytoplankton cells and fecal pellets from herbivores constitute important channels for the sinking export of organic material to depth, these constituents are typically quantified in sinking export studies (e.g. Turner 2002, Caron et al. 2004). Nevertheless, a few studies have shown that the contribution of bacteria to the sinking export of organic material can also be important (e.g. Pedrós-Alió et al. 1989, Turley & Mackie 1994). Hence, it is important to quantify bacterial sinking fluxes to better quantify and understand processes controlling the sinking export of organic material. The amount and composition of sinking particles are commonly characterized using particle interceptor traps, while transformation during sinking is assessed from changes in particle sinking fluxes with depth (e.g. Martin et al. 1987, Michel et al. 2002, Juul-Pedersen et al. 2008).

In the Hudson Bay system, several studies have focused on the phytoplankton (e.g. Anderson & Roff 1980, Drinkwater & Jones 1987, Harvey et al. 1997) and zooplankton communities (e.g. Rochet & Grainger 1988, Harvey et al. 2001). The only published study on the sedimentation of organic material in Hudson Bay was carried out at a land-fast ice station in the southeastern part (Tremblay et al. 1989). To our knowledge, no study on the

sinking export of organic material has been published for the Hudson Bay system in open water conditions.

In the present study, we investigated the spatial variability in the sinking export of organic material in the Hudson Bay system during the open water period. The three main objectives of this work were to (1) characterize spatial variations in the sedimentation of organic material in the Hudson Bay system, (2) investigate how spatial variations in the magnitude and composition of organic material sinking fluxes may reflect hydrographic forcing in the Hudson Bay system, and (3) assess the attenuation of organic material sinking fluxes with depth and, consequently, the significance of degradation of the material exported below the euphotic zone in this shallow and cold inland sea. Our working hypotheses were that (1) the existence of different hydrographic regions in the Hudson Bay system would play a role in shaping the sedimentation patterns of organic material in this environment and (2) the degradation of organic material during sinking would be of minor importance in such a shallow sub-polar sea.

1.2 Material and methods

1.2.1 Study area

The Hudson Bay system is under the influence of various water inputs, i.e. the Arctic Ocean, the Labrador Sea, river runoff and precipitation. Arctic Ocean water enters

the system through Fury and Hecla straits and moves southward through Foxe Basin (Sadler 1982, Prinsenberg 1986a). Some of this water mass exits the system through Hudson Strait, while the remaining joins the cyclonic circulation around the bay (Prinsenberg 1986b, Ingram & Prinsenberg 1998). Labrador Sea water enters the bay along the north side of Hudson Strait, joining arctic water from Foxe Basin (Prinsenberg 1986b, Jones & Anderson 1994). In addition, Hudson Bay receives a large freshwater contribution from river runoff (*ca.* 562 km^3 y^{-1}; Déry et al. 2005). Freshwater input from rivers, sea-ice melt and precipitation contributes to a strongly stratified water column in Hudson Bay (Prinsenberg 1984). Conversely, the strong tidal currents (> 2–3 m s^{-1}) and large tidal range (> 4 m) in Hudson Strait generate strong vertical mixing that influences vertical profiles of temperature, salinity and nutrients and, consequently, primary production processes (Drinkwater & Jones 1987, Arbic et al. 2007).

1.2.2 Sampling

Sampling was carried out on board the research icebreaker CCGS *Amundsen* from 23 September to 16 October 2005. Short-term free-drifting particle interceptor traps were deployed at eight stations for 8 to 20 h at two or three depths below the euphotic zone (from 50 to 150 m), depending on water depth at the station (Fig. 1). The deployment duration was ultimately contingent upon the expedition plan and sampling schedule. Details for each deployment are presented in Table 1. The particle interceptor traps were polyvinyl chloride (PVC) cylinders with an internal diameter of 10 cm and an aspect ratio (height:diameter) of 7. Four particle interceptor traps, centered at the mooring depth, were

installed on the trap line in order to collect enough material for the analyses. Particle interceptor trap deployments and handling were performed according to JGOFS protocols (Knap et al. 1996) and following the recommendations of Gardner (2000). The free-drifting particle interceptor trap array was surface-tethered with a series of small floats to minimize vertical motion on the trap line. Before deployment, the traps were filled with seawater collected at depth and filtered through 0.22 μm polyvinyliden fluoride (PVDF) Millipore Durapore membrane filters. No poison or preservative was used during the deployments. Upon recovery, the traps were covered with a tight clean lid and placed in the dark at 4°C for a sedimentation period of 8 h. After the sedimentation period, the supernatant was carefully removed and the bottom volume of the trap samples, which was sieved through a 450 μm mesh to remove large swimmers, was kept for further analyses. Individual samples collected from traps deployed in the same depth horizon were pooled to obtain one sample per depth, which was used for subsequent analyses.

During the expedition, sea surface salinity and temperature were measured using a CTD (Sea-Bird 911 plus) and transmissiometry was measured with a WET Labs CST-558DR probe at 121 stations in Hudson Strait, Hudson Bay and at the mouth of Foxe Basin. Euphotic zone depth (i.e. depth of 1% surface irradiance) was established according to the light attenuation in the water column measured using a Secchi disk (Holmes 1970). Benthic nepheloid layer depths were estimated from vertical transmissiometer profiles at each particle interceptor trap station (Table 1).

Table 1. Characteristics of free-drifting particle interceptor trap moorings in the Hudson Bay system during early fall 2005.

Station	Deployment date	Water depth (m)	Nepheloid depth (m)	Euphotic zone depth (m)	Deployment		Recovery		Duration (d)	Deployment depth (m)
					Latitude (°N)	Longitude (°W)	Latitude (°N)	Longitude (°W)		
14	23 Sept	342	212	24	62°16.62'	71°59.11'	62°14.82'	71°57.17'	0.45	50 – 100 – 150
16	26 Sept	220	167	50	62°39.18'	80°03.46'	62°39.83'	80°46.06'	0.38	50 – 100 – 150
18	28 Sept	148	117	48	60°07.52'	79°10.37'	60°10.51'	79°10.71'	0.47	50 – 100
AN03	30 Sept	86	72	25	55°20.09'	78°13.58'	56°22.60'	78°05.94'	0.86	50
22	06 Oct	182	150	45	58°23.83'	83°17.28'	58°22.76'	83°18.28'	0.32	50 – 100 – 150
23	11 Oct	200	166	37	59°00.66'	87°37.45'	59°01.92'	87°32.36'	0.38	50 – 100 – 150
AN01	13 Oct	104	78	40	60°00.03'	91°57.06'	60°00.03'	91°58.40'	0.31	50
27	16 Oct	242	221	48	61°03.72'	86°11.31'	61°04.18'	86°14.13'	0.44	50 – 100 – 150

1.2.3 Laboratory analyses

Duplicate trap subsamples were filtered onto Whatman GF/F glass fiber filters for fluorometric determination of chlorophyll *a* (chl *a*) and pheopigments (pheo) after a 24 h extraction in 90% acetone at 4°C in the dark (Parsons et al. 1984). Chl *a* and pheo were determined on board the ship using a 10-AU Turner Designs fluorometer calibrated with chl *a* extract from *Anacystis nidulans* (Sigma). Total particulate carbon (TPC) and particulate organic carbon (POC) were determined on trap subsamples filtered onto precombusted (450°C for 24 h) Whatman GF/F filters then dried at 60°C for 24 h during the expedition. In the laboratory, we acidified filters for POC measurement. All samples were analyzed on a PerkinElmer Model 2400 CHN analyzer. Particulate inorganic carbon (PIC) was determined by subtracting POC from TPC values. Biogenic silica (BioSi) was determined on duplicate subsamples filtered onto 0.6 μm Nuclepore polycarbonate membrane filters that were then dried at 60°C for 24 h and stored until analysis. The material retained on filters was analyzed according to Ragueneau & Tréguer (1994), with hydrolysis using a 0.2 N NaOH solution and spectrophotometric determination of a silico-molybdate complex (Varian Cary 100). Microscopic examination of our samples did not reveal the presence of lithogenic material or residual biogenic silica after hydrolysis. Subsamples (100 mL) from the 50 m depth horizon were preserved with acidic Lugol's solution (Parsons et al. 1984) for later identification and enumeration of protist cells > 4 μm with an inverted microscope (Leica DM IRB) according to Lund et al. (1958). For each sample, a minimum of 400 cells and three transects were counted. The abundance of each taxon was calculated according to the equation of Horner (2002). Average cell sizes were

obtained by measuring 30 individual cells from the most abundant species and average cell biovolumes were estimated using appropriate geometric equations (Hillebrand et al. 1999). For the least abundant taxa, average cell sizes were obtained from the literature (Tomas 1997, Bérard-Therriault et al. 1999). Protist carbon biomass was estimated using the conversion factors of Menden-Deuer & Lessard (2000), except for ciliates for which we used the specific conversion factor from Putt & Stoecker (1989). All protist cells except spores and empty diatom cells were included in the total protist community carbon estimate. The number and size of fecal pellets were determined from 250 mL subsamples preserved with buffered formaldehyde (1% final concentration) using an inverted microscope (Leica DM IRB). The biovolume of whole and broken fecal pellets was estimated using appropriate geometric equations and the carbon contribution of the fecal pellets was estimated using the conversion factors of 0.029 mg C mm^{-3} for elliptical and round fecal pellets and 0.057 mg C mm^{-3} for cylindrical fecal pellets from González & Smetacek (1994). Most cylindrical fecal pellets were broken (> 90% of pellet numbers). In order to determine if sinking fecal pellets contained diatom frustules, fecal pellets from traps deployed at 50 m were examined using scanning electron microscopy (SEM; JEOL 6460LV). At each station, subsamples were filtered onto 5 μm Nuclepore polycarbonate membrane filters to concentrate the fecal pellets and gently rinsed with distilled water to eliminate salt crystals. An aliquot of fecal pellet material was placed on an aluminum stub and air-dried before SEM examination; no coating was necessary. Five to ten fecal pellets per station were examined in order to provide qualitative information on their content. Bacteria were counted with an epifluorescence microscope (Leica DHLS). Duplicate

subsamples for bacterial counts were fixed with buffered formaldehyde (1% final concentration), stained with DAPI (4,6-diamidino-2-phenylindole) at a final concentration of 1 μg mL^{-1}, and filtered onto 0.2 μm black Nuclepore polycarbonate membrane filters. Bacterial carbon was estimated using a conversion factor of 0.02 pg C $bacteria^{-1}$ (Lee & Fuhrman 1987). The bacterial carbon contribution was corrected for potential bacterial growth and mortality during the trap deployment period. We used the equation of Pedrós-Alió & Mas (1993) with the initial concentration of bacteria in the filtered seawater used to fill the traps, a specific growth rate of 0.1 d^{-1} (Rivkin et al. 1996a, Rich et al. 1997) and a specific mortality rate of 28% (Steward et al. 1996). Without this correction, bacteria sinking fluxes would have been estimated to be between 2 and 6% (average 3%) higher than those presented here. The POC contribution of amorphous detritus was estimated by subtracting fecal pellet, protist and bacterial carbon from the total POC sinking flux. Sinking fluxes were calculated using the following equation (Juul-Pedersen et al. 2008):

$$\text{Sinking rate (mg m}^{-2}\text{ d}^{-1}) = (C_{trap} \times V_{trap})/(A_{trap} \times T_{dep})$$

where C_{trap} (mg m^{-3}) is the concentration of the measured variable in the particle interceptor trap, V_{trap} (m^3) is the volume of the particle interceptor trap sample, A_{trap} (m^2) is the particle interceptor trap surface area and T_{dep} (d) is the deployment time.

1.2.4 Statistical analyses

Our spatial analysis focused on the sinking fluxes measured at 50 m, which represent the sinking export from the euphotic zone since the euphotic zone depth ranged from 24 to 50 m at all stations visited (Table 1). The R software (Casgrain & Legendre 2000) was used to analyze the horizontal variability in sinking fluxes by spatial autocorrelation using Moran's I coefficient (Legendre & Legendre 1998). The number of distance classes for the spatial autocorrelation analysis between stations was calculated using Sturge's rule with $\alpha = 0.05$ as the critical level of significance. A model II linear regression was used to estimate the percent contribution of PIC to TPC sinking flux throughout the sampling area. The Wilcoxon signed-ranks test was used to compare paired variates and to compare composition ratios of the sinking material with values from the literature. The Mann-Whitney test was used to identify differences between two groups of stations (Sokal & Rohlf 1981). All maps presented in this paper were produced with Ocean Data View Software (Schlitzer 2010).

1.3 Results

Surface waters (≤ 5 m) were more saline and cooler in Hudson Strait than in Hudson Bay (Fig. 2; Table 2). In southeast Foxe Basin, the average surface salinity was 31.8 and the average temperature 1.15°C. Surface waters were less saline and warmer in eastern Hudson Bay than in western Hudson Bay (Fig. 2; Table 2). Benthic nepheloid layer depths

ranged from 72 to 221 m at deployment trap stations and were below the deepest interceptor trap deployment except at station 22 (Table 1).

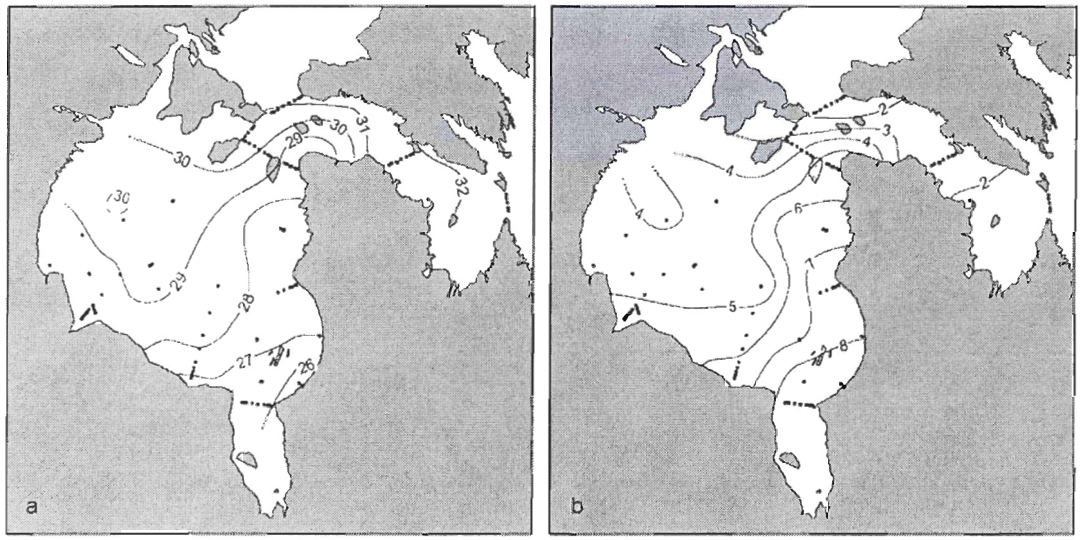

Fig. 2. Sea surface distribution of (a) salinity and (b) temperature (°C) in the Hudson Bay system during early fall 2005.

Total pigment (chl *a* + pheo) sinking fluxes were significantly higher in Hudson Strait (station 14) than in Hudson Bay (Fig. 3a; Table 2). In Hudson Bay, sinking fluxes of total pigments showed a significant longitudinal gradient, with decreasing rates from east (stations 22, AN03, 18 and 16) to west (stations AN01, 23 and 27) (spatial autocorrelations, $p < 0.05$) (Fig. 3a; Table 2). The highest chl *a* sinking flux was measured at station 16, near Mansel Island (0.30 mg m^{-2} d^{-1}), and the lowest at the deep offshore station 27 (0.04 mg m^{-2} d^{-1}). At station 23, the pheo sinking flux was ≤ 0.01 mg m^{-2} d^{-1}.

Table 2. General hydrographic conditions, sinking fluxes and composition ratios of the particulate material in particle interceptor traps deployed at 50 m in three regions of the Hudson Bay system during early fall 2005. The range of values and mean (in italics), are shown for each region. n: number of stations.

	Western Hudson Bay	Eastern Hudson Bay	Hudson Strait
Hydrographic condition	n = 34	n = 61	n = 26
Surface temperature (°C)	3.56 – 5.01 *4.42*	4.26 – 8.93 *7.59*	1.08 – 2.85 *2.10*
Surface salinity	28.4 – 30.4 *29.4*	23.9 – 28.4 *26.9*	31.3 – 33.2 *32.3*
Sinking flux (mg m^{-2} d^{-1})	n = 3	n = 4	n = 1
Chlorophyll *a* (chl *a*)	0.04 – 0.20 *0.12*	0.06 – 0.30 *0.17*	1.34
Pheopigment	0 – 0.16 *0.07*	0.20 – 0.50 *0.35*	2.03
Total particulate organic carbon (POC)	50.0 – 52.0 *51.1*	37.5 – 71.3 *55.0*	76.8
Total protist carbon	2.39 – 8.02 *5.29*	1.75 – 8.24 *4.82*	21.5
Diatom carbon	0.01 – 0.11 *0.05*	1.19 – 6.65 *3.29*	19.8
Fecal pellet carbon	2.94 – 6.46 *4.53*	1.83 – 32.1 *19.3*	7.82
Bacterial carbon	6.96 – 10.7 *8.68*	2.32 – 9.58 *5.32*	6.46
Amorphous detrital carbon	28.9 – 35.7 *32.6*	1.37 – 47.3 *25.6*	40.9
Biogenic silica (BioSi)	4.63 – 11.6 *7.8*	20.3 – 43.7 *36.6*	50.2
Ratio	n = 3	n = 4	n = 1
BioSi:POC (mol:mol)	0.04 – 0.10 *0.06*	0.14 – 0.47 *0.31*	0.28
POC:chl *a* (g:g)	252 – 1359 *683*	200 – 583 *389*	57.4

POC sinking fluxes ranged from 50.0 mg m^{-2} d^{-1} (stations AN03 and 23) to 76.8 mg m^{-2} d^{-1} (station 14), with no significant spatial pattern (spatial autocorrelation, $p > 0.05$) (Fig. 3b). Over the whole Hudson Bay system, PIC made up, on average, 15% of the TPC sinking fluxes (data not shown). The highest diatom-associated carbon and BioSi

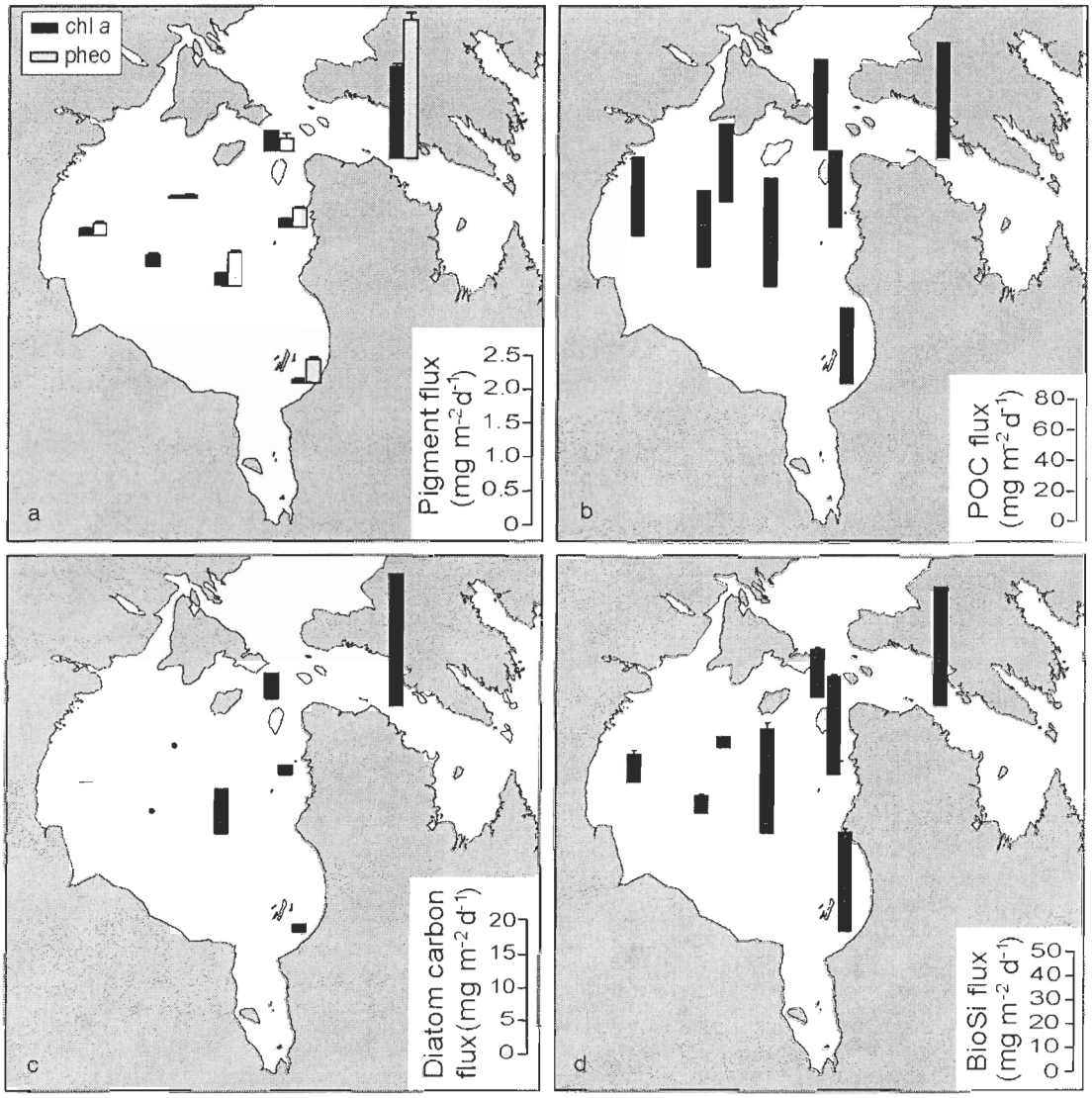

Fig. 3. Spatial variation in sinking fluxes of (a) chlorophyll *a* (chl *a*) and pheopigment (pheo), (b) particulate organic carbon (POC), (c) diatom-associated carbon, and (d) biogenic silica (BioSi) at 50 m in the Hudson Bay system during early fall 2005. In (a), pheo sinking flux at station 23 was ≤ 0.01 mg m^{-2} d^{-1}. In (c), diatom-associated carbon sinking fluxes at stations 23 and 27 were ≤ 0.01 mg C m^{-2} d^{-1}. In (a) and (d), stacked and error bars represent the mean and the maximum value, respectively.

sinking fluxes were measured in Hudson Strait (station 14; Fig. 3c, d; Table 2). In Hudson Bay, both diatom-associated carbon and BioSi sinking fluxes decreased longitudinally from east (stations 22, AN03, 18 and 16) to west (stations AN01, 23 and 27; spatial autocorrelations, $p < 0.05$) (Fig. 3c, d; Table 2).

BioSi:POC molar ratios of the sinking material at 50 m were significantly higher than the value of 0.13 measured in light-limited diatoms (Brzezinski, 1985) in Hudson Strait and eastern Hudson Bay (stations 22, AN03, 18 and 16) but significantly lower than this critical value in western Hudson Bay (stations AN01, 23 and 27) (Wilcoxon signed-ranks tests, $p < 0.05$; Fig. 4a; Table 2). POC:chl *a* mass ratios of the sinking material were consistently higher than the value of 40 observed in light-limited phytoplankton (Lorenzen 1968) throughout the sampling area (Wilcoxon signed-ranks test, $p < 0.05$; Fig. 4b; Table 2). The highest POC:chl *a* ratio was measured at station 27 (1359 g:g) in western Hudson Bay and the lowest at station 14 (57.4 g:g) in Hudson Strait (Fig. 4b).

The material collected in the traps deployed at 50 m was composed of bacteria, protists, fecal pellets and amorphous detritus (Fig. 5). Amorphous detritus contributed > 50% of the total POC sinking fluxes in the Hudson Bay system, except at stations 22 and AN03 in eastern Hudson Bay, where fecal pellets were the largest carbon component (38 and 85% of total POC, respectively). At three stations in eastern Hudson Bay (stations AN03, 22 and 18), the fecal pellet contribution to total POC sinking flux was significantly

higher (average 52%) than in the other two regions of the system (average 8%) (Mann-Whitney test, $p < 0.05$). Station 16 near Mansel Island showed the highest relative contribution in amorphous detritus (78%) and the lowest contribution in fecal pellet (3%) to total POC sinking flux over the sampling area. The protist contribution to total POC sinking flux ranged from 5 to 28%, with the highest value at station 14 in Hudson Strait. The bacterial carbon contribution to the total POC sinking flux was significantly higher in western Hudson Bay (stations AN01, 23 and 27; average 17%) than in the other two regions (average 9%) (Mann-Whitney test, $p < 0.05$), with the maximum value at station AN01 (21%).

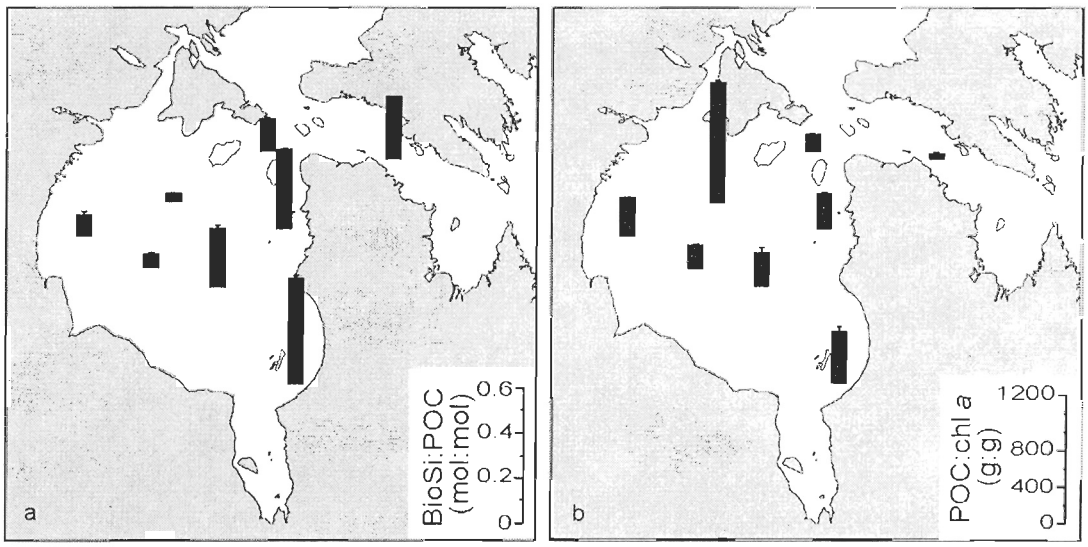

Fig. 4. Spatial variation in the ratios of (a) biogenic silica (BioSi) to particulate organic carbon (POC) and (b) POC to chlorophyll *a* (chl *a*) in particle interceptor traps deployed at 50 m in the Hudson Bay system during early fall 2005. Stacked and error bars represent the mean and the maximum value, respectively.

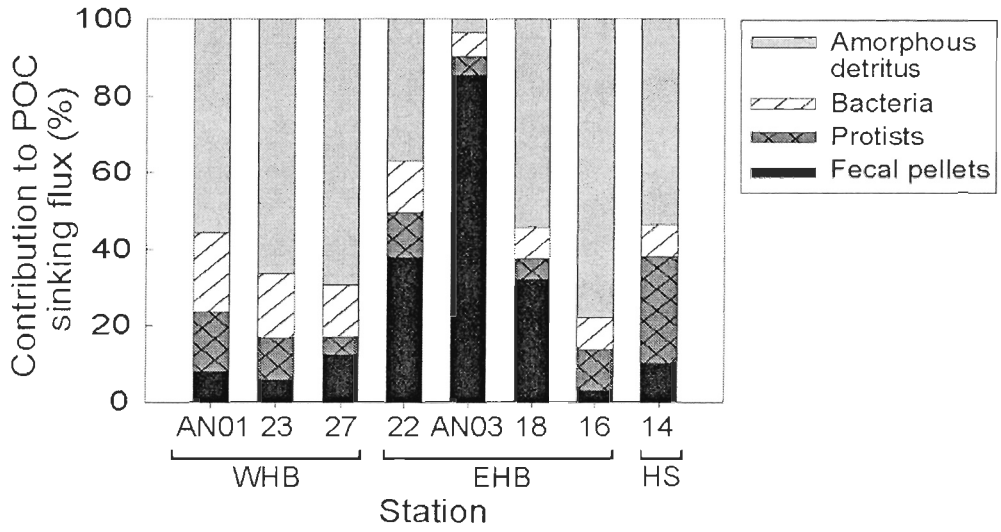

Fig. 5. Relative contribution of fecal pellets, protists, bacteria and amorphous detritus to total particulate organic carbon (POC) sinking flux at 50 m in the Hudson Bay system during early fall 2005. WHB: western Hudson Bay; EHB: eastern Hudson Bay; HS: Hudson Strait.

The main protist species collected in the traps deployed at 50 m were the prymnesiophytes *Phaeocystis pouchetii* and *Chrysochromulina* spp. in Hudson Strait, the pennate diatom *Cylindrotheca closterium* and the centric diatoms *Chaetoceros contortus*, *C. wighamii*, *C. furcillatus* and *Skeletonema costatum* in eastern Hudson Bay, and the dinoflagellate *Gymnodinium galeatum* in western Hudson Bay (Table 3). Unidentified nanoflagellates and other unidentified protists were present at each station and made up 33 to 71% of the total protist abundance in the sinking material (Table 3). The relative contribution of the major protist groups to the total protist abundance in the 50 m traps is presented in Fig. 6 and the dominant protist taxa at each station are shown in Table 3. The main groups contributing to the total protist sinking flux, by numbers, were flagellates (88%) in Hudson Strait, intact and empty diatoms (9–38% and 15–21%, respectively) and

flagellates (19–45%) in eastern Hudson Bay, and unidentified protists (21–49%) and flagellates (22–32%) in western Hudson Bay (Fig. 6a). In terms of carbon biomass, the main groups contributing to the total protist carbon sinking flux were intact diatoms (92%) in Hudson Strait, intact diatoms (54–81%) and dinoflagellates (16–40%) in eastern Hudson Bay, and dinoflagellates (43–67%) and ciliates+choanoflagellates (31–52%) in western Hudson Bay (Fig. 6b).

Table 3. Percent abundance (% total intact cells) of dominant protist taxa in particle interceptor traps at 50 m in the Hudson Bay system in early fall 2005. WHB: western Hudson Bay; EHB: eastern Hudson Bay; HS: Hudson Strait; n.d.: not detected.

Taxon	Station							
	WHB			EHB				HS
	AN01	23	27	22	AN03	18	16	14
Chaetoceros contortus Schütt	n.d.	n.d.	n.d.	< 5	n.d.	< 5	13	n.d.
Chaetoceros furcillatus Bailey	n.d.	n.d.	n.d.	5	n.d.	< 5	< 5	< 5
Chaetoceros wighamii Brightwell	< 5	n.d.	n.d.	< 5	n.d.	9	7	< 5
Cylindrotheca closterium (Ehrenberg) Reimann & Lewin	< 5	n.d.	n.d.	5	< 5	< 5	< 5	n.d.
Skeletonema costatum Greville	< 5	< 5	n.d.	n.d.	8	n.d.	< 5	n.d.
Gymnodinium galeatum Larsen	6	5	8	6	5	< 5	< 5	< 5
Cryptophyceae spp.	< 5	< 5	< 5	< 5	20	< 5	< 5	< 5
Imantonia rotunda Reynolds	< 5	< 5	< 5	< 5	< 5	< 5	< 5	19
Phaeocystis pouchetii (Hariot) Lagerheim	< 5	< 5	< 5	< 5	< 5	n.d.	< 5	21
Unidentified nanoflagellates	17	11	13	17	25	19	13	36
Unidentified protists	22	60	43	24	16	33	20	< 5

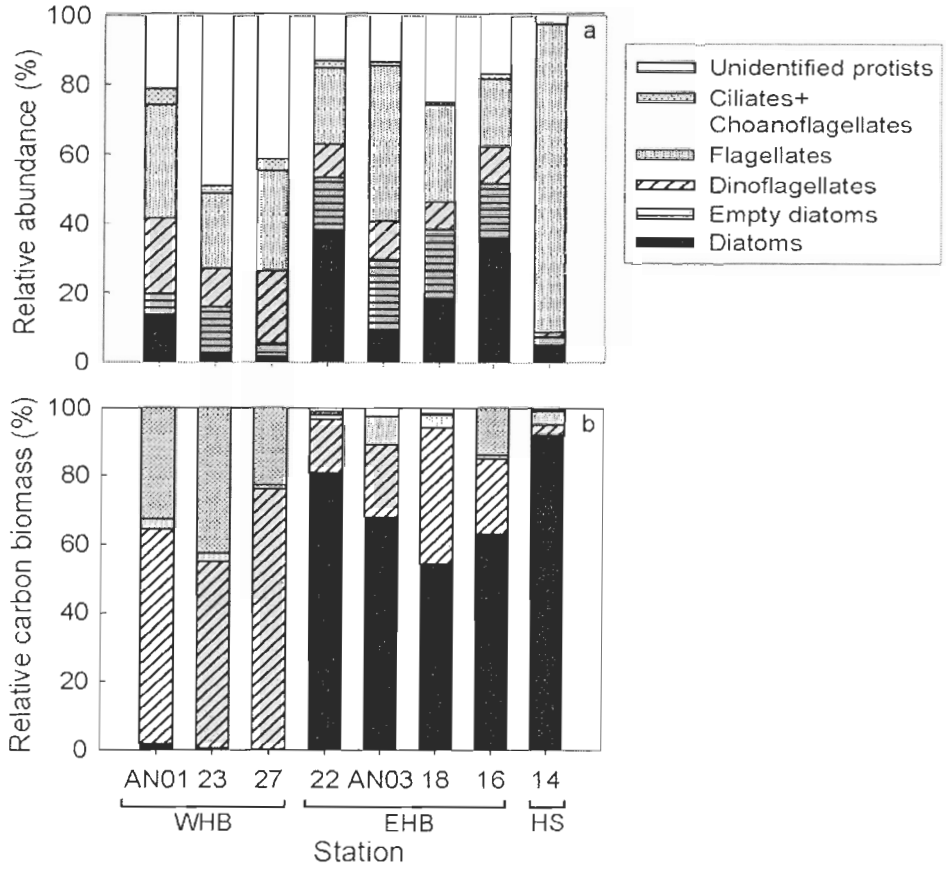

Fig. 6. Relative contribution of different protist groups to their total sinking flux in terms of (a) abundance and (b) carbon biomass at 50 m in the Hudson Bay system during early fall 2005. The term "unidentified" corresponds to cells that we were unable to identify. In (b), empty diatoms are not shown since they do not contribute to carbon biomass. WHB: western Hudson Bay; EHB: eastern Hudson Bay; HS: Hudson Strait.

In the Hudson Bay system, fecal pellets sinking at 50 m were mainly long cylinders. Cylindrical fecal pellets accounted for 79 to 100% of the total fecal pellet abundance (data not shown); other fecal pellets were elliptical or round. The fecal pellet carbon sinking fluxes were highly variable in the Hudson Bay system, ranging from a minimum of 1.83 mg C $m^{-2} d^{-1}$ at station 16 near Mansel Island to a maximum of 32.1 mg C $m^{-2} d^{-1}$ at station AN03 near the Great Whale River (Fig. 7a). Fecal pellet sinking fluxes were, on

average, twice as high at stations 22, AN03 and 18 compared to stations located in Hudson Strait and western Hudson Bay (Fig. 7a; Table 2). The size-distribution of sinking fecal pellets at 50 m is presented for each region in Fig. 7b. Large fecal pellets (> 100 μm in width) made up > 92% of the total fecal pellet sinking flux in Hudson Bay whereas they represented only 61% in Hudson Strait. The sinking flux of these large fecal pellets was significantly higher in eastern Hudson Bay (average 19.1 mg C $m^{-2} d^{-1}$) than in western Hudson Bay (average 4.21 mg C $m^{-2} d^{-1}$) and in Hudson Strait (average 4.77 mg C $m^{-2} d^{-1}$) (Mann-Whitney test, $p < 0.001$). It is interesting to note that fecal pellets from the two larger size-classes (> 100 μm in width) were always fragmented and were more loosely packed than smaller (< 100 μm) cylindrical fecal pellets.

In Hudson Strait and eastern Hudson Bay, POC sinking fluxes were significantly lower at 150 m than at 50 m (average loss 32%) and BioSi:POC ratios of the sinking material were significantly higher at 150 m than at 50 m (average increase 76%; Wilcoxon signed-ranks tests, $p < 0.05$; Table 4). In western Hudson Bay, both variables were significantly higher at 150 m than at 50 m (average increase of 17% and 102%, respectively; Wilcoxon signed-ranks tests, $p < 0.05$; Table 4). There was no significant difference in the sinking fluxes between these two depths with respect to pigments, diatom-associated carbon and BioSi, or for the POC:chl *a* ratios of the sinking material (Wilcoxon signed-ranks tests, $p > 0.05$).

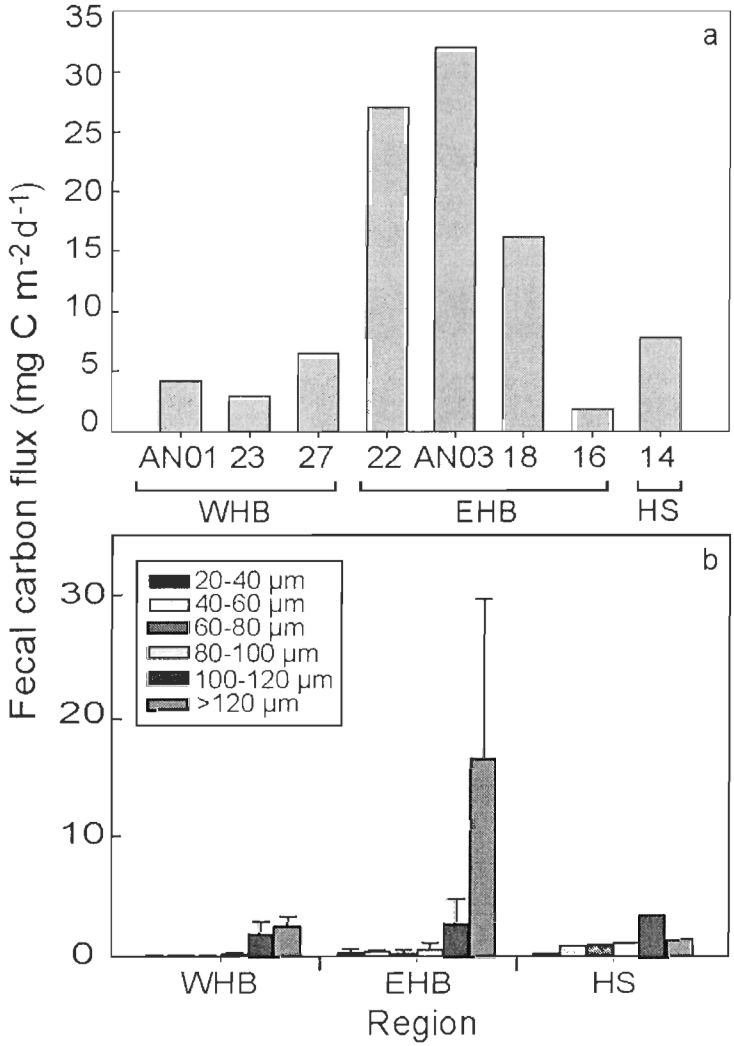

Fig. 7. Variations in (a) fecal pellet carbon sinking flux and (b) different pellet size-classes fecal pellet carbon sinking export in particle interceptor traps deployed at 50 m in the Hudson Bay system during early fall 2005. WHB: western Hudson Bay; EHB: eastern Hudson Bay; HS: Hudson Strait.

Table 4. Particulate organic carbon (POC) sinking flux and biogenic silica (BioSi):POC ratio of the sinking material at different depths and sampling stations of the Hudson Bay system in early fall 2005. n.v.: no value since water depth was < 150 m.

Station	50 m		100 m		150 m	
	POC (mg m^{-2} d^{-1})	BioSi:POC (mol:mol)	POC (mg m^{-2} d^{-1})	BioSi:POC (mol:mol)	POC (mg m^{-2} d^{-1})	BioSi:POC (mol:mol)
Hudson Strait						
14	76.8	0.28	63.9	0.35	43.2	0.44
Eastern Hudson Bay						
16	60.7	0.14	63.4	0.17	49.0	0.37
18	50.5	0.35	37.7	0.41	n.v.	n.v.
22	71.3	0.26	70.4	0.13	47.0	0.30
Western Hudson Bay						
23	50.0	0.06	47.1	0.08	66.8	0.08
27	51.5	0.04	69.4	0.05	60.0	0.10

1.4 Discussion

To our knowledge, this study is the first to present results on the sinking export of organic material in the Hudson Bay system during open water conditions. Sediment trap studies are always challenging from a methodological stand-point, and one might argue that the variable duration of the trap deployments (from 8 to 20 h) introduced a bias to the interpretation of the sinking fluxes. Deployment duration was similar at all stations, with an average of 9.5 h ± 1.5 h, except at station AN03 located in southeastern Hudson Bay, where the deployment duration was 20 h (Table 1). The fluxes and the composition ratios of the sinking material at this station were very similar to those at other stations in eastern Hudson Bay (Figs. 3–7). We are therefore inclined to believe that the longer deployment period at station AN03 did not influence our interpretation of the results. Sinking fluxes estimated

during our study are at the low end of sinking flux values reported from other short-term particle interceptor trap studies. For example, POC sinking fluxes (50–77 mg C m^{-2} d^{-1} at 50 m; Table 2) were similar to background winter values observed in the Barents Sea (30–70 mg C m^{-2} d^{-1}; Olli et al. 2002). In open water conditions, Lalande et al. (2007a) reported POC sinking fluxes ranging from 129 to 442 mg C m^{-2} d^{-1} at 50 m in the Chukchi Sea in July–August and Caron et al. (2004) reported values averaging 219 mg C m^{-2} d^{-1} at 50 m in northern Baffin Bay in August–September. Lower primary productivity in the Hudson Bay system compared to the Chukchi Sea and northern Baffin Bay (Sakshaug 2004) likely explains the differences observed. Notwithstanding the low sinking fluxes of organic material observed, strong spatial variations were found for the Hudson Bay system during early fall. This will be discussed in the next sections.

1.4.1 Hydrographic regions

Sea surface temperature and salinity measurements revealed three different hydrographic regions in the Hudson Bay system: Hudson Strait, eastern Hudson Bay and western Hudson Bay. Hudson Strait was characterized by low temperature and high salinity due to the dominant marine influence in this region, while eastern Hudson Bay was characterized by high temperature and low salinity associated with strong riverine input (Granskog et al. 2007). The intermediate temperature and salinity characterizing western Hudson Bay reflect water mass modification during cyclonic circulation around the bay (Fig. 2; Table 2). These general hydrographic conditions correspond to the spatial

delineations proposed by Prinsenberg (1986b). In the three hydrographic regions described, contrasting sedimentation patterns were observed, as evidenced by differences in the magnitude and composition of sinking fluxes.

1.4.2 Regional sedimentation patterns

1.4.2.1 Hudson Strait

During this study, Hudson Strait was characterized by the highest sinking fluxes of pigments, BioSi and diatom-associated carbon (Fig. 3a, c, d; Table 2). In general, high export is associated with high primary production and/or phytoplankton biomass in the euphotic zone (e.g. Betzer et al. 1984, Wassmann 1990). These observations are consistent with the results of Harvey et al. (1997, 2006), who showed higher phytoplankton production and biomass (chl *a*) in Hudson Strait than in Hudson Bay in late summer. During our study, the most abundant protist in the sinking material in Hudson Strait was the prymnesiophyte *Phaeocystis pouchetii* (Fig. 6a). This contrasts with observations by Harvey et al. (1997), who reported a numerical dominance of diatoms in the phytoplankton assemblage during the same period of the year. Such a discrepancy may be due to spatial variability. Harvey et al. (1997) studied the southern part of Hudson Strait, whereas our station was located in the center of Hudson Strait. According to Harvey et al. (2006), suspended chl *a* biomass decreased from the north to the south of Hudson Strait in late summer, and these variations were associated with different hydrographic conditions

controlled by tidal mixing (Drinkwater & Jones 1987). Interannual variability may also come into play to explain the differences observed. However, our results do not allow us to scale the effects of spatial *versus* interannual variability as this would require sampling an array of stations in Hudson Strait over multiple years. Another explanation may reside in the differential export of various phytoplankton species due to differential sinking velocities and/or the preferential grazing of one species compared to another. Nevertheless, it is interesting to note that although flagellates were the most abundant cells in the sinking material during our study, diatoms contributed the most to carbon biomass (Fig. 6). Colonial or solitary *Phaeocystis* cells are very common in arctic and subarctic regions and are frequently observed in shallow particle interceptor traps, but their contribution in terms of carbon sinking flux is usually small (e.g. Reigstad & Wassmann 2007). In Hudson Strait, the high contribution of intact protist cells to the sinking POC (Fig. 5) and the low fecal pellet sinking flux (Fig. 7a) indicated that the protist community was dominated, in terms of biomass, by autotrophs and that the grazing pressure was low in this region.

In Hudson Strait, the intermediate BioSi:POC ratios obviously resulted from the high relative biomass of diatoms and the abundance of intact protist cells in the sinking material (Figs. 4a, 5 and 6b). The high biomass of autotrophs in the material sinking out of the euphotic zone in Hudson Strait would also explain the low POC:chl *a* ratios observed (Fig. 4b). We cannot differentiate the influence of diatoms from that of prymnesiophytes on the POC:chl *a* ratios observed. However, diatoms, with their larger biovolume (highest relative contribution to POC, Fig. 6b) and their low POC:chl *a* ratios compared to

prymnesiophytes (Johnsen et al. 1992), would likely contribute to the low POC:chl *a* ratios observed.

1.4.2.2 Eastern Hudson Bay

Eastern Hudson Bay was characterized by higher pigments, BioSi and diatom-associated carbon sinking fluxes than western Hudson Bay (Fig. 3; Table 2). These observations are in line with those of Anderson & Roff (1980), who reported higher chl *a* biomass on the eastern side of Hudson Bay during late summer. The composition of the protist community collected in the particle interceptor traps (Fig. 6a) is also consistent with previous observations showing a dominance of diatoms and flagellates in the euphotic zone of this region (Harvey et al. 1997). In eastern Hudson Bay, the sinking protist carbon biomass was dominated by diatoms; similar to Hudson Strait, but the sinking organic carbon was mainly from fecal pellets (Figs. 5 and 6b).

The higher fecal pellet sinking fluxes measured in eastern Hudson Bay compared to the other two regions (Fig. 7a) suggests that the grazing pressure by zooplankton was higher in this region. In addition, abundant diatom frustules in the fecal pellets of this region that we observed by SEM reflect active zooplankton grazing on diatoms. The degradation of primary-produced organic material by zooplankton grazing is further supported by the higher POC:chl *a* ratios of the sinking material in eastern Hudson Bay compared to Hudson Strait (Fig. 4b).

The shape and size of fecal pellets in particle interceptor traps can provide an indication of the taxonomic composition of the zooplankton community present in the upper water column. However, it is difficult to directly link sinking fecal pellet shape and abundance to zooplankton group abundance in the euphotic zone because degradation processes (e.g. coprohexy, coprochaly; Noji et al. 1991) occur during sinking, thereby modifying the composition of the collected fecal pellets. The higher contribution of large (> 100 μm) fecal pellets to the fecal carbon sinking flux in eastern Hudson Bay (Fig. 7b) suggests a higher production/abundance of larger pellets and, consequently, a dominance of larger zooplankton organisms compared to Hudson Strait. This hypothesis is in accordance with observations of Harvey et al. (2001), who reported a higher proportion of large-sized copepods, namely *Calanus glacialis* Jaschnov and *C. finmarchicus* Gunnerus, in eastern Hudson Bay compared to Hudson Strait. The occurrence of fecal pellet fragments of 200–300 μm in width and of 800–1000 μm in length suggests that some of the fecal pellets were produced by the chaetognath *Sagitta elegans* Varrill, which was found to be particularly abundant in eastern Hudson Bay during this expedition (Gérald Darnis, Université Laval, personal communication). This zooplankton species is more abundant in eastern Hudson Bay than in Hudson Strait in late summer (Harvey et al. 2001). Even though the large pellets were not abundant, they contributed significantly to the total fecal carbon sinking flux (Fig. 7b). The fact that all large (> 100 μm in width) fecal pellets were fragmented and loosely packed suggests that these pellets were prone to degradation in the euphotic zone. According to Dilling & Alldredge (1993), pellets of chaetognaths, which are carnivorous macrozooplankton, contain copepod exoskeletal remains and are packed less densely than

copepod pellets that contain phytoplankton cells. Therefore, chaetognath fecal pellets would have longer residence time in the water column favouring degradation and recycling rather than direct sinking.

In contrast with the rest of the system, diatom-associated carbon sinking fluxes in eastern Hudson Bay showed a trend opposite to that of BioSi sinking fluxes (i.e. low diatom sinking fluxes were associated with high BioSi sinking fluxes; stations 18 and AN03, Fig. 3c, d). This decoupling was likely linked to the abundance of diatom-containing fecal pellets and empty frustules in the sinking material (Figs. 6a and 7a). This hypothesis is supported by the SEM examination of fecal pellets. Indeed, we observed diatom spores and intact or fragmented frustules in fecal pellets throughout the Hudson Bay system, but in higher proportion at stations 18 and AN03. Active grazing on diatoms would contribute to the high BioSi:POC ratios measured in the sinking material in eastern Hudson Bay (Table 2) since carbon is assimilated by zooplankton while silica is excreted (Conover et al. 1986, Brown et al. 2006).

1.4.2.3 Western Hudson Bay

The lowest pigments, BioSi and diatom-associated carbon sinking fluxes of the system were measured in western Hudson Bay (Fig. 3). To our knowledge, the only biological oceanographic study encompassing western Hudson Bay showed low chl *a* biomass in this part of the Hudson Bay system in late summer (Anderson & Roff 1980). In

contrast with other regions, the sinking protist carbon biomass in western Hudson Bay was dominated by dinoflagellates, ciliates and choanoflagellates (Fig. 6b), and consequently low BioSi:POC ratios were observed (Figs. 4b and 6b). Interestingly, bacteria contributed more than fecal pellets or protists to the total POC sinking flux in western Hudson Bay (Fig. 5), challenging the view that bacteria are minor contributors to the sinking flux of particles. According to Stoke's Law, the sinking velocity of small cells like bacteria is negligible (Pedrós-Alió & Mas 1993). However, increased bacterial carbon sinking export can be explained by the attachment of bacterial cells to other particles or aggregates (e.g. Kiørboe et al. 2002, Grossart et al. 2003b). Indeed, bacterial attachment to particles was observed during microscopic observation of our samples. Our values of bacterial carbon sinking fluxes for western Hudson Bay (7.0–10.7 mg C m^{-2} d^{-1}) are in the range of values reported by Ducklow et al. (1982) at 10 m in the Hudson River plume of the New York bight in March (1.5–10.0 mg C m^{-2} d^{-1}), but higher than those measured by Turley & Mackie (1994) at 50 m in the northeast Atlantic in May (0.03–0.99 mg C m^{-2} d^{-1}). These two studies also used unpoisoned short-term free-drifting particle interceptor traps. Collected bacteria entered interceptor traps by sedimentation, but since the traps were not poisoned, bacterial growth during the deployment period could bias sedimentation estimates. We corrected our bacteria sinking fluxes using potential growth and mortality rates from literature, whereas Ducklow et al. (1982) used a specific growth rate directly measured from bacteria collected in their traps. The correction of Ducklow et al. (1982) was more precise, but in both cases the bacterial growth in interceptor traps was insignificant when compared to bacterial sinking flux. The low contribution of algal carbon

to sinking POC explains the low pigment sinking fluxes and, consequently, the high POC:chl *a* ratios observed in western Hudson Bay, especially at station 27 (Figs. 3a and 4b; Table 2).

While sinking fluxes of pigments, BioSi and diatom-associated carbon all showed strong horizontal patterns at 50 m, spatial variations in POC sinking fluxes were modest throughout the Hudson Bay system (Fig. 3). As shown above, it is the composition rather than the magnitude of the sinking POC that varied regionally during our study. Rivkin et al. (1996b) reported similar results, showing a strong variability in chl *a* and fecal pellet sinking fluxes while the POC sinking flux remained fairly constant during the bloom and post-bloom period in the Gulf of St. Lawrence. These authors proposed that, over the duration of their study, neither food web structure nor new production could be used to predict the magnitude or patterns of POC sinking export from the euphotic zone. This hypothesis is supported by our results. However, further studies integrating primary production, plankton community structure and export data are needed to test this hypothesis in the Hudson Bay system. The potential implications of spatial variations and depth-transformation of the sinking material with respect to benthic communities will be treated in the next section.

1.4.3 Linkages with the benthos

A decrease in POC sinking fluxes with depth was only observed in regions characterized by a high sinking export of algal material (i.e. chl *a*, diatom-associated carbon and BioSi), i.e. Hudson Strait and eastern Hudson Bay (Table 4). In contrast, an increase in sinking POC with depth was observed in western Hudson Bay. Close examination of the benthic nepheloid layer depths (Table 1) did not show clear evidence of resuspension in the deepest particle interceptor traps throughout the Hudson Bay system. We therefore hypothesize that lateral advection of POC may have occurred in western Hudson Bay, although further investigation is required to confirm this process. Lateral advection may also have influenced chl *a* sinking export at depth since our results did not consistently show depth attenuation of chl *a* sinking fluxes at the stations visited. Lalande et al. (2007a) also reported depth-related attenuation of POC but not of chl *a* sinking fluxes in the Chukchi Sea during ice-free conditions, although the cause for such discrepancy was not fully elucidated.

Little dissolution of BioSi in sinking particles appeared to take place during the fall in the Hudson Bay system since no significant decrease in BioSi sinking fluxes was observed with depth. This, together with longitudinal differences in the sinking export of diatom-associated material (i.e. more diatom-associated material in the east compared to the west) and in POC attenuation (i.e. higher POC attenuation in the east than west) resulted in very different BioSi:POC ratios at depth in eastern and western Hudson Bay

(Table 4). Clearly, a combination of factors including the amount and composition of the material leaving the euphotic zone and degradation processes during sinking shaped the composition of the material reaching the benthos, producing high BioSi:POC molar ratios at depth in the east (BioSi:POC > 0.30) and low ratios in the west (BioSi:POC < 0.13).

It is well established that the distribution and composition of benthic communities are influenced by a complex of abiotic (e.g. hydrographic conditions, ice cover, light regime, temperature, bottom substrate, water depth) and biotic (e.g. magnitude of primary production, pelagic food web structure) factors (Grebmeier & Barry 1991). The food supply to the benthos, which is entirely dependent upon the sinking of organic matter originating in the euphotic zone, is generally considered to be the most important factor for a vast majority of benthic communities (Piepenburg 2005). Therefore, although our results provide only a snapshot of sedimentation patterns during a short period in the fall, we surmise that the spatial variations in the magnitude and composition of the sinking fluxes of organic material observed are likely to shape the spatial patterns observed in the abundance and composition of benthic communities. To our knowledge, there are only a few studies on benthic communities in Hudson Bay. Cusson et al. (2007) documented strong differences among macrofaunal communities in various regions of the Hudson Bay system. Benthic communities were also studied in Hudson Strait and along a longitudinal transect in Hudson Bay in 2003 (P. Archambault, Université du Québec à Rimouski, unpublished data). Macrobenthic communities were more abundant and diverse in Hudson Strait than in Hudson Bay, and within Hudson Bay, macrobenthic communities were more abundant

although less diverse in the west compared to the east (P. Archambault, unpublished data). In addition, crustaceans Tanaidacean, known to be consumers of pelagic-sedimented diatoms (Blazewicz-Paszkowycz & Ligowski 2002), were mainly found in Hudson Strait and in eastern Hudson Bay (P. Archambault, unpublished data). The spatial trends observed during our study, e.g. higher sinking fluxes of pigments, POC and diatom-associated carbon, and higher BioSi:POC composition ratios in the east compared to the west, agree with these studies. These initial comparisons, which need to be substantiated with additional studies of vertical export and benthic communities, suggest that the prevalent spatial patterns in the sedimentation of organic material in Hudson Bay may be indicative of the taxonomic composition and abundance of benthic communities in this large inland sea.

In the Hudson Bay system, different export pathways emerged in the three distinct regions. In Hudson Strait, direct sinking of intact diatoms played an important role in the sinking export of POC. Regions dominated by large phytoplankton, in particular diatoms, are usually high export environments (Buesseler 1998). In contrast, in western Hudson Bay, high contributions of flagellates and bacteria to the sinking material is characteristic of an environment dominated by a microbial food web, where POC was exported to depth in the form of amorphous detritus. Therefore, this region is more typical of a high recycling environment and, as a corollary, a low export environment. Finally, eastern Hudson Bay appeared to be intermediate to the other two regions, with diatoms being transferred to

pelagic grazers and a large contribution of diatom-containing fecal pellets in the POC sinking export.

1.5 Conclusion

This study presents the first results on the sinking export of organic material and its vertical degradation in the Hudson Bay system in open water conditions. The Hudson Bay system, which is considered to be a region of low primary production, showed low organic material sinking fluxes compared to other arctic and subarctic regions. Nevertheless, horizontal heterogeneity in the magnitude and composition of organic material sinking fluxes was observed. Three regions characterized by different hydrographic conditions and contrasting sinking export pathways were identified: Hudson Strait, eastern Hudson Bay and western Hudson Bay. Hudson Strait emerged as the region of highest sinking export of the system, including a high contribution of intact diatoms to the POC sinking export. Western Hudson Bay was characterized by the lowest sinking fluxes of organic material and a POC export mainly in the form of amorphous detritus and bacterial carbon, therefore pointing to an environment of high recycling. Finally, eastern Hudson Bay was somewhat intermediate between these two systems, characterized by a significant transfer of diatoms to pelagic grazers and sedimentation of fecal pellets. These results support our first hypothesis, which was that different hydrographic regions in the Hudson Bay system play a role in shaping the sedimentation patterns of organic material in this environment. However, our results do not indisputably support our second hypothesis, which proposed

that degradation of organic material during sinking would be of minor importance in this system, given that we observed a variable loss of organic matter during its sinking in different regions of the Hudson Bay system.

CHAPITRE II

PRIMARY PRODUCTION AND SINKING EXPORT DURING FALL IN THE HUDSON BAY SYSTEM, CANADA

RÉSUMÉ

La production primaire et l'exportation verticale du matériel organique ont été étudiées dans le système de la baie d'Hudson (i.e. baie d'Hudson, détroit d'Hudson et bassin de Foxe) en période libre de glace à l'automne 2005. La production primaire a été mesurée par assimilation du ^{14}C et les flux verticaux de matériel organique ont été déterminés à l'aide de pièges à particules dérivant à court terme déployés sous la zone euphotique à 50 m. Une analyse de groupement des K-moyennes a révélé des patrons spatiaux de la production primaire et de la biomasse chlorophyllienne, au sein de la zone euphotique, liés aux conditions physico-chimiques du milieu. Nos résultats ont montré que les rapports d'exportation (i.e. flux vertical de carbone organique particulaire divisé par la production primaire) les plus élevés (moyenne de 0,51) ont été observés pour les stations où la production primaire était faible et dominée par les petites cellules et où les protistes hétérotrophes dominaient en termes de biomasse. Ces résultats montrent qu'à court terme, une exportation verticale élevée n'est pas nécessairement associée à une production primaire élevée et/ou une biomasse importante des grandes cellules phytoplanctoniques.

ABSTRACT

Primary production and organic material sinking export were investigated in the Hudson Bay system (i.e. Hudson Bay, Hudson Strait and Foxe Basin) under ice-free conditions during early fall 2005, using ^{14}C-uptake method and short-term free-drifting particle interceptor traps deployed below the euphotic zone at 50 m. K-means clustering revealed spatial patterns of primary production and chlorophyll *a* (chl *a*) biomass in the euphotic zone that were shaped by physical and chemical conditions. Our results also showed that the highest ratios of POC sinking export to primary production (i.e. export ratios) which averaged 0.51 were observed for stations where primary production was low and dominated by small cells, and where heterotrophic protist dominated in biomass. These results show that, at short temporal scales, high sinking export is not necessarily associated with high primary production rates and/or a high biomass of large phytoplankton cells.

2.1 Introduction

The export of photosynthetically fixed carbon from surface waters to depth constitutes an important process in marine ecosystems as it influences atmosphere–ocean carbon fluxes (Falkowski et al. 1998, Sarmiento & Gruber 2006, Buesseler 2008) and supplies energy to benthic communities (e.g. Piepenburg 2005, Renaud et al. 2008). Over the last decades, several empirical algorithms were developed to assess the relationship between total primary production and the sinking export of particulate organic carbon (POC). Algorithms relating POC sinking export to total primary production in a non-linear fashion (e.g. Eppley & Peterson 1979, Suess 1980, Wassmann 1990) can provide reasonable estimates of POC export (e.g. Bishop 1989). However their poor performance in other situations (e.g. Boyd & Newton 1995, Olesen & Lundsgaard 1995, Karl et al. 1996) suggests that the magnitude of primary production may not necessarily be the determinant factor for POC export. It has been proposed that the structure of the plankton community can be the main factor controlling the magnitude and composition of the POC sinking export (e.g. Michaels & Silver 1988, Boyd & Newton 1995, 1999, Boyd et al. 2008). Large phytoplankton cells play an important role in the export of POC because they can readily sink as intact cells or be integrated in the herbivorous food web and exported as fast sinking fecal pellets produced by large zooplankton (Legendre & Le Fèvre 1991, Aksnes & Wassmann 1993, Buesseler 1998, 2008). Moreover, diatoms contain silica and often form aggregates, therefore sink faster than other phytoplankton cells (e.g. Passow & de la Rocha 2006, de la Rocha et al. 2008, Armstrong et al. 2009, Fischer et al. 2009). Diatoms may consequently have a disproportionate influence relative to other phytoplankton groups on

POC sinking export (Boyd & Newton 1995), as observed in a number of studies (e.g. Pommier et al. 2008, Maiti et al. 2009). In contrast, small cells are typically considered to be marginal contributors to the sinking export of organic matter, although this premise was recently revisited and the contribution of small cells to POC export was found to be proportional to their contribution to total primary production (Richardson & Jackson 2007).

One way to quantify the coupling between primary production and POC export is to calculate the export ratio, defined as the ratio of sinking POC measured by particle interceptor traps deployed below the euphotic zone to primary production rates measured in the euphotic zone (Wexels Riser et al. 2002). In general, export ratios range from less than 0.10 in oligotrophic regions to greater than 0.50 in productive coastal regions (Karl et al. 1996). Interestingly, Olesen & Lundsgaard (1995) and Karl et al. (1996) in the coastal and open ocean, respectively, failed to evidence a clear relation between primary production or size-structure of the plankton community and POC export ratios. Rivkin et al. (1996b) also failed to predict the magnitude of POC sinking export from primary production and planktonic food web structure in the Gulf of St. Lawrence during bloom and post-bloom conditions. Additional factors such as mineral ballast (Armstrong et al. 2002, 2009, François et al. 2002, Fischer et al. 2009), algal physiology (Waite & Nodder 2001, Kahl et al. 2008) or surface ocean properties (Laws et al. 2000, Tian et al. 2001, Dunne et al. 2005) all conspire to influence the sinking export of POC. Clearly, the coupling between primary production and sinking export depends on a complex concurrence of biological and environmental factors (Boyd & Trull 2007).

We showed previously that the magnitude of the POC sinking export was fairly homogeneous throughout the Hudson Bay system, whereas the composition of the sinking POC showed strong spatial patterns (Lapoussière et al. 2009, see Chapter I). Here we investigate, for the first time, the coupling between primary production and the POC sinking export during ice-free conditions in the Hudson Bay system. The three main objectives of our study were to: (1) quantify the primary production and biomass of size-fractioned (0.7–5 μm and ≥ 5 μm) phytoplankton cells and to assess protist taxonomic composition, (2) determine how environmental factors influence the magnitude and size-structure of phytoplankton primary production and biomass, and (3) investigate the relationship between primary production and sinking export of organic material, and quantify export ratios and daily loss rates in this shelf system. Our work was designed according to the following hypotheses: (1) water column structure and nutrient distribution influence the distribution, structure and production of phytoplankton communities in the Hudson Bay system, and (2) variations in the intensity and structure of phytoplankton production influence the magnitude of the organic material sinking export and consequently, export ratios and daily loss rates. To test the first hypothesis, we analyzed relationships between physical/chemical variables and total particulate production, production by large cells and protist (diatoms, dinoflagellates, flagellates, ciliates, and choanoflagellates) carbon biomass. To test the second hypothesis, we studied the export ratios and daily loss rates of organic material at 50 m in relation to the structure of phytoplankton communities.

2.2 Material and methods

2.2.1 Sampling

Sampling was carried out on board the research icebreaker CCGS *Amundsen* from 23 September to 16 October 2005. Thirteen stations were visited in the Hudson Bay system (Fig. 1), which includes Hudson Bay, Hudson Strait and Foxe Basin, and represents a large inland sea system in northern Canada (1.23×10^6 km^2; Jones & Anderson 1994, Granskog et al. 2007). At each station, water samples were collected at seven optical depths (100, 50, 30, 15, 5, 1 and 0.2% of surface irradiance, including the depth of chlorophyll fluorescence maximum concentration, Z_{CFM}) and at three to five depths in the aphotic zone, with a rosette sampler equipped with 24 12 L Niskin-type bottles (OceanTest Equipment), an in-situ fluorometer (SeaPoint 2443) and a high precision Sea-Bird Electronics SBE 911-plus CTD probe. The euphotic zone depth (i.e. depth of 0.2% surface irradiance, Z_{eu}) was estimated with a Secchi disk (Holmes 1970). Surface water samples (< 5 m) for nutrient determination were collected with the rosette system at the 13 full stations plus 10 auxiliary stations (see Fig. 2).

The sinking export of particulate organic material was estimated at 8 of the 13 full stations, using short-term free-drifting particle interceptor traps deployed below the euphotic zone (Fig. 1). The particle interceptor traps were consistently deployed at 50 m whereas Z_{eu} varied from 28 to 50 m. On average, the distance between the Z_{eu} and the trap deployment depth was < 7 m. Consequently, we assume that little remineralization

occurred over this short distance and that the material collected at 50 m was representative of the material exiting the euphotic zone. Four traps were installed in order to collect enough material for subsequent analyses. Particle interceptor traps were polyvinyl chloride (PVC) cylinders with an internal diameter of 10 cm and an aspect ratio (height:diameter) of 7. Particle interceptor trap design, deployment and handling were performed following the recommendations of Gardner (2000) and Buesseler et al. (2007). However, logistical issues constrained us to short deployment times (~8–20 h, average 9.5 h ± 1.5 h, except for station AN03 where deployment duration was 20 h). One might argue that this short deployment period did not take into account potential diurnal variability in export entailed by processes such as zooplankton vertical migration, and that estimates measured during the deployment period cannot be extrapolated to daily sinking fluxes. Based on the microscopic observation of all samples, there was no evidence of zooplankton repackaging of particles associated with vertical migration as we did not observe any change in fecal pellet characteristics with depth (from 50 to 150 m). Moreover, stations located in a same hydrographic region of the HBS showed similar patterns in sinking flux magnitude and composition despite the short and variable deployment periods. These observations support that the sinking fluxes measured over the study period can reasonably be extrapolated to daily sinking fluxes.

A series of small floats was used to minimize vertical motion on the trap line. To track the trap line and facilitate its recovery, a radio beacon (Novatech Designs Ltd. RF-700C1) and a CAST ARGOS drifter (Seimac Smart Cat PTT/GPS transmitter) were attached to the trap array. Before deployment, the traps were filled with 0.22 μm filtered

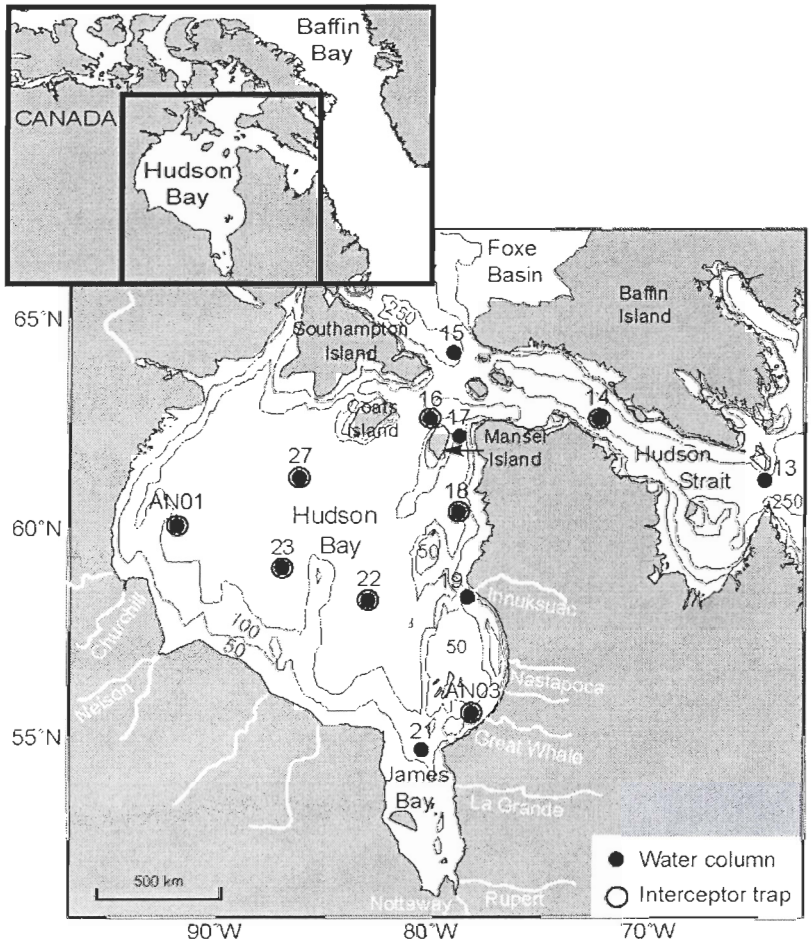

Fig. 1. Location of the sampling stations with isobaths (m) in the Hudson Bay system during early fall 2005 and location of rivers cited in the text.

seawater collected at depth at a previous station; no poison or preservative was added. After recovery, the particle interceptor traps were covered with a tight clean lid and placed in the dark at 4°C for a sedimentation period of 8 h. After that time, the supernatant was carefully removed and the bottom volume of the trap samples was sieved through a 450 μm mesh to remove large swimmers. The samples from the four traps were pooled together to obtain one sample, which was used for subsequent analyses. Additional details on the deployment

and handling of particle interceptor trap samples can be found in Lapoussière et al. (2009) (see Chapter I).

2.2.2 Physical and chemical measurements

Incident downwelling photosynthetically available radiation (PAR, 400–700 nm) was measured at 15 min intervals with a 2π LI-COR quantum sensor (LI 190SA). Water temperature and salinity were recorded over the water column and interpolated at 1-db intervals (*ca.* 1 m). The surface mixed layer depth (Z_{mix}) was determined according to the peak value observed in the Brunt-Väisälä frequency (N^2) vertical profile. An index of vertical stratification of the water column was estimated as the difference in the density (sigma-t, σ_t) between 80 and 5 m (Tritton 1988), except at shallow station 21 where the difference in σ_t was computed between 51 and 5 m.

Nutrient samples were drawn from each Niskin-type bottle using a syringe filter to remove large particles. Samples were stored at 4°C in the dark and analyzed for nitrate plus nitrite ($NO_3^-+NO_2^-$), nitrite (NO_2^-), silicic acid ($Si(OH)_4$) and phosphate (PO_4^{3-}) within a few hours on a Bran+Luebbe AutoAnalyzer 3 using standard colorimetric methods adapted for the analyzer (Grasshoff et al. 1999). Ammonium (NH_4^+) was determined manually with the fluorometric method of Holmes et al. (1999).

2.2.3 Biological water column analyses

At each sampling depth, duplicate subsamples for chlorophyll *a* (chl *a*) determination were filtered onto Whatman GF/F filters (total phytoplankton biomass: B_T) and a subsample was filtered onto Nuclepore polycarbonate 5 μm membrane filters (biomass of large phytoplankton: B_L). Concentrations of chl *a* were determined on board the ship on a 10-AU Turner Designs fluorometer, after 24 h extraction in 90% acetone at 4°C in the dark (acidification method; Parsons et al. 1984). The fluorometer was calibrated using chl *a* extract from *Anacystis nidulans* (Sigma). Biomass by small phytoplankton cells (0.7–5 μm; B_S) was calculated as the difference between B_T and B_L.

Particulate phytoplankton production was measured at seven optical depths (from 100 to 0.2% of surface irradiance) and at the Z_{CFM} using the ^{14}C uptake method (Knap et al. 1996, Pommier et al. 2009). Two light and one dark 500 mL Nalgene polycarbonate bottles were filled with seawater from each optical depth and inoculated with 20 μCi of $NaH^{14}CO_3$. The coefficient of variation between the two light bottles varied from 0 to 72% (average of 11%). In the dark bottle, we added 500 μL of 0.01 M 3,4-dichlorophenyl-1,1-dimethylurea (DCMU) to prevent the active incorporation of ^{14}C in the dark (Legendre et al. 1983). The initial activity was determined immediately after inoculation by pipetting 50 μL subsample into 10 mL of Ecolume scintillation cocktail (ICN™) containing 50 μl of ethanolamine. All incubation bottles were placed in a Plexiglass deck incubator (see Pommier et al. 2009 for details). Incubations started at the beginning of the day and ended at sunset to reduce the

variability in ^{14}C accumulation (Mingelbier et al. 1994), except for stations 13 and 27 where incubations started in the beginning of the afternoon. The incubation duration averaged 9.7 ± 2.9 h. After that period, subsamples (250 mL) were filtered onto Whatman GF/F filters and Nuclepore polycarbonate 5 μm membrane filters for the determination of total particulate primary production (P_T) and the production by large cells (≥ 5 μm; P_L), respectively. The filters were then put in 20 mL scintillation vials and acidified with 200 μL of 0.5 N HCl and left to evaporate until dry under the fume hood to remove excess ^{14}C. After the evaporation period, 10 mL of Ecolume (ICN^{TM}) were added and the samples were stored for a minimum of 12 h before counting on a liquid scintillation analyzer (Tri-Carb 2900TR, Packard). Production rates were corrected for incorporation in dark bottles, with the assumption that bacterial processes were occurring equally between light and dark bottles. Daily production rates were obtained by dividing the total C uptake by the fraction of daily irradiance received during the incubation (Pommier et al. 2009). Production and biomass by small phytoplankton cells (0.7–5 μm; P_S and B_S, respectively) was calculated as the difference between P_T from P_L and between B_T and B_L, respectively. Total and large cell production and biomass were integrated (trapezoidal integration) over the euphotic zone. P_L:P_T and B_L:B_T ratios were calculated with integrated data.

Total particulate carbon (TPC) concentration was determined on duplicate subsamples filtered onto pre-combusted (450°C for 5 h) Whatman GF/F filters. The samples, dried at 60°C for 24 h during the expedition, were later analyzed in the laboratory on a Perkin-Elmer Model 2400 CHN analyzer (Knap et al. 1996). Biogenic silica (BioSi)

concentration was determined on duplicate subsamples filtered onto Nuclepore polycarbonate 0.6 μm membrane filters which were dried at 60°C for 24 h, and stored until analysis. The material retained on filters was analyzed according to Ragueneau & Tréguer (1994), with hydrolysis using a 0.2 N NaOH solution and spectrophotometric determination of a silico-molybdate complex (Varian Cary 100).

Subsamples (100 mL) from the Z_{CFM} were preserved with acidic Lugol's solution (Parsons et al. 1984) for the identification and enumeration of phytoplankton and other protist cells (≥ 4 μm) with an inverted microscope (Leica DM IRB) according to Lund et al. (1958). For each sample, a minimum of 400 cells and three transects were counted and the abundance of each taxon was calculated according to the equation of Horner (2002). Averaged cell sizes were obtained by measuring 30 individual cells for the most abundant species and from the literature for the least abundant taxa (Tomas 1997, Bérard-Therriault et al. 1999). The biovolume of each taxon was then determined using appropriate geometric equations (Hillebrand et al. 1999). Protist carbon biomass was estimated using the conversion factors of Menden-Deuer & Lessard (2000), except for ciliates for which we used the specific conversion factor from Putt & Stoecker (1989). Choanoflagellate and ciliate biomasses are presented together as these two groups were composed of heterotrophic protists in the present study.

Twelve liters samples were collected at three depths (generally 10, 25 and 50 m) in the upper water column for fecal pellet determination. These samples were concentrated on a 50 μm mesh net and preserved with buffered formaldehyde (1% final concentration). The size (length and width) of each fecal pellet was determined using an inverted microscope (Leica DM IRB) and their biovolumes were estimated using appropriate geometric equations. Fecal pellet carbon (FPC) biomass was then calculated using a conversion factor of 0.057 mg C mm^{-3} for copepod (Gonzàles et al. 1994) and of 0.029 mg C mm^{-3} for appendicularian (Gonzàles & Smetacek 1994) pellets.

2.2.4 Sinking fluxes

Duplicate trap subsamples were filtered for total chl *a*, TPC and BioSi determination. A single trap subsample was filtered for large cell chl *a* (≥5 μm) and POC. Analytical methods were the same as for water column samples. POC was measured after acidification of filtered TPC sample with concentrated HCl for 24 h. Fecal pellet abundance and size were estimated on 250 mL subsamples preserved in formaldehyde (1% final concentration).

2.2.5 Mathematical and statistical analyses

Freshwater content (FWC) in the euphotic zone was defined as the integrated salinity fraction below a reference salinity of 34.8, as:

$$FWC\ (m) = \int_0^{Zeu} [(34.8 - S) / 34.8]\ dz$$

where dz (m) is the vertical layer thickness and S is the mean salinity of the layer.

Ratios of new to total primary production (i.e. *f*-ratios) were estimated from the size-structure of the phytoplankton community using the following equation (Tremblay et al. 1997):

$$f\text{-ratio} = 0.04 + 0.74\ (P_L / P_T)$$

Sinking fluxes (S_{flux}) were calculated using this equation (Juul-Pedersen et al. 2008):

$$S_{flux}\ (mg\ m^{-2}\ d^{-1}) = (C_{trap} \times V_{trap}) / (A_{trap} \times T_{dep})$$

where C_{trap} (mg m^{-3}) is the concentration of the measured variable in the particle interceptor trap, V_{trap} (m^3) is the volume of the particle interceptor trap sample, A_{trap} (m^2) is the particle interceptor trap surface area and T_{dep} (d) is the deployment time. Export ratios were calculated using the equation in Wexels Riser et al. (2002):

$$\text{Export ratio} = S_{flux} / P_T$$

The daily loss rate of suspended material due to sedimentation was estimated using the following equation (Olli et al. 2002):

$$\text{Daily loss rate (\% d}^{-1}\text{)} = S_{flux} \times 100 / C_{int}$$

where C_{int} (mg m^{-2}) is the integrated concentration of the variable considered from surface to the depth of the particle interceptor trap. The sinking velocity of organic material was estimated using this equation (Caron et al. 2004):

$$\text{Sinking velocity (m d}^{-1}\text{)} = S_{flux} / (C_{int} / z)$$

where z (m) is the deployment depth of the particle interceptor trap.

In order to determine the influence of environmental factors on phytoplankton biomass and production distribution, a *k*-means clustering (Legendre & Legendre 1998) was used to identify groups of stations based on physical properties of the water column showing strong horizontal variability (i.e. euphotic zone average temperature, vertical stratification index and Z_{eu}:Z_{mix} ratio). For each physical, chemical and biological variable, a one-way ANOVA was performed to seek significant differences among the groups of stations discriminated by the clustering procedure. The normality of distribution and homogeneity of variance of each variable were tested and data were transformed when required. The ANOVA was completed by a post-hoc multiple comparison of means (Tukey's Honestly Significant Difference test for unequal sample size) (Legendre & Legendre 1998). Standard deviations (SD) on integrated phytoplankton production and biomass estimates were computed according to Kendall & Stuart (1977). Spearman's rank

order correlation (r_s) and model II linear regression (reduced major axis) were used to determine relationships between variables (Sokal & Rohlf 1981). Statistical tests were carried out using the Statistica 7 software (StatSoft, Tulsa, OK). All maps presented in this paper were produced using Ocean Data View 3.4.1 software (Schlitzer 2010).

2.3 Results

2.3.1 Environmental variables, biomass and primary production distribution

Physical characteristics of the water column showed large spatial variability in the Hudson Bay system during early fall 2005 (Table 1). The mean temperature of the euphotic zone, the vertical stratification index of the water column and FWC varied widely, from 1.19 to 8.87°C, from 0.46 to 5.71 kg m^{-3} and from 1.39 to 7.45 m, respectively. Maximum and minimum values were recorded in southeastern Hudson Bay (Stations 19, AN03 and 21) and Hudson Strait (Stations 13 to 16), respectively. The mean salinity of the euphotic zone was also highly variable, ranging from 25.7 in the plume of the Great Whale River in southeastern Hudson Bay (Station AN03) to 33.4 at the mouth of the Hudson Strait (Station 13). Z_{eu} was always deeper than Z_{mix}, except at stations 13 and 15 where the ratio of Z_{eu} to Z_{mix} where 0.49 and 0.69, respectively. Z_{CFM} was shallower at stations 19, AN03 and 21 in southeastern Hudson Bay (9–11 m) than at the other stations (20–50 m). Based on the clustering analysis (see Materials and Methods section), three groups of stations were distinguished: (1) Group I composed of stations 13 to 16 located in the Hudson Strait area,

(2) Group III composed of stations 19, AN03 and 21 situated in the vicinity of large rivers in southeastern Hudson Bay, and (3) Group II comprised all the other stations of the Hudson Bay area (Stations 17, 18, 22, 23, AN01 and 27) (Table 1; Fig. 1).

Table 1. Physical characteristics of the stations visited in the Hudson Bay system during early fall 2005.

Station	Group	Temperature (°C)	Salinity	Water depth (m)	Z_{eu} (m)	Z_{mix} (m)	Z_{eu}:Z_{mix}	Z_{CFM} (m)	FWC (m)	Strat (kg m^{-3})
13	I	1.19 (1.11 – 1.30)	33.4 (33.2 – 33.5)	450	35	72	0.49	26	1.39	0.46
14	I	1.99 (0.58 – 2.80)	32.4 (32.0 – 32.8)	343	50	22	2.27	50	3.32	0.97
15	I	1.39 (1.38 – 1.40)	31.8 (31.8 – 31.8)	245	24	35	0.69	24	1.97	0.93
16	I	2.42 (-0.11 – 4.01)	31.5 (31.1 – 32.3)	205	50	13	3.85	23	4.64	0.97
17	II	4.72 (-0.63 – 6.52)	28.5 (27.9 – 30.1)	156	35	24	1.46	40	6.02	4.08
18	II	1.77 (-1.31 – 6.72)	29.5 (27.7 – 31.3)	140	48	18	2.67	30	6.95	4.31
22	II	1.85 (-1.59 – 4.28)	30.0 (28.4 – 32.1)	181	45	25	1.80	34	5.82	3.86
23	II	2.76 (-1.04 – 4.91)	30.6 (29.5 – 32.2)	199	37	26	1.42	48	4.34	3.02
AN01	II	2.41 (-0.73 – 4.32)	30.0 (28.5 – 32.3)	107	41	24	1.71	20	5.33	4.21
27	II	2.41 (-1.12 – 4.57)	30.7 (29.6 – 32.4)	242	48	25	1.92	43	5.10	2.94
19	III	8.00 (7.18 – 8.24)	27.2 (26.9 – 27.9)	116	37	25	1.48	11	7.45	4.06
AN03	III	8.87 (8.80 – 9.17)	25.7 (25.5 – 26.1)	92	28	14	2.00	9	6.76	5.71
21	III	8.12 (3.80 – 8.99)	26.4 (25.4 – 28.6)	60	32	27	1.19	10	7.28	4.82

Temperature and salinity were averaged over the euphotic zone depth (Z_{eu}) and the range is in parentheses. The station groups were determined from physical variables (see Materials and Methods section). Z_{mix}: surface mixed layer depth; Z_{CFM}: depth of chlorophyll fluorescence maximum; FWC: freshwater content in the euphotic zone; Strat: vertical stratification index.

Surface nutrient concentrations (i.e. NO_3^-, $Si(OH)_4$, PO_4^{3-} and NH_4^+) showed a well-defined longitudinal gradient in Hudson Strait, with increasing concentrations from west to east (Fig. 2a–d). In southeastern Hudson Bay, surface $Si(OH)_4$ and NH_4^+ concentrations decreased towards offshore waters (Fig. 2b, d). Similarly, surface NH_4^+ concentrations decreased towards offshore waters in western Hudson Bay (Fig. 2d). Surface PO_4^{3-} concentrations increased towards offshore waters in western Hudson Bay, with maximum concentrations in northwestern Hudson Bay (Fig. 2c). In contrast to the other nutrients, surface NO_3^- in the Hudson Bay did not show any clear pattern (Fig. 2a). Surface NO_2^- concentrations ranged from ≤ 0.02 to 0.16 mmol m^{-3} (average of 0.07 mmol m^{-3}; data not shown). In surface waters, the molar ratios of total dissolved nitrogen ($DIN = NO_3^- + NO_2^- + NH_4^+$) to PO_4^{3-} and of DIN to $Si(OH)_4$ ranged from 0.15 to 5.55 and from 0.04 to 0.61, respectively.

P_T and B_T integrated over the euphotic zone and protist carbon biomass at the Z_{CFM} were variable throughout the Hudson Bay system (Fig. 3a–d). P_T ranged from 70 mg C m^{-2} d^{-1} at station 15 in Foxe Channel to 435 mg C m^{-2} d^{-1} at station 19 in eastern Hudson Bay (Fig. 3a), and B_T varied between 10.2 mg chl *a* m^{-2} at station 13 at the mouth of Hudson Strait to 47.1 mg chl *a* m^{-2} at station 14 in central Hudson Strait (Fig. 3b). Throughout the Hudson Bay system, P_T and B_T were dominated by small cells (57–89% of P_T and 55–91% of B_T), except at station 21, the southernmost station at the mouth of James Bay, where small cells contributed 48% of P_T and 31% of B_T (Fig. 3a, b). Diatom carbon biomass at the Z_{CFM} ranged from < 0.1 mg C m^{-3} at stations 23 and 27 in western Hudson

Bay to 107 mg C m^{-3} at station 14 in central Hudson Strait (Fig. 3c). Dinoflagellate carbon biomass was minimum at station 27 (0.80 mg C m^{-3}) and maximum at station 14 (5.25 mg C m^{-3}). Flagellate carbon biomass ranged from 0.20 mg C m^{-3} at station 17 in northeastern Hudson Bay to 16.8 mg C m^{-3} at station 14 in central Hudson Strait (Fig. 3d). Ciliate + choanoflagellate carbon biomass ranged from 0.68 mg C m^{-3} at station 22 in central Hudson Bay to 30.7 mg C m^{-3} at station 23 in western Hudson Bay (Fig. 3d).

Protist carbon biomass at the Z_{CFM} was dominated by the centric diatom *Thalassiosira bioculata* (Grunow) Ostenfeld at stations 13 and 14 in Hudson Strait and at stations 19, AN03 and 21 in southeastern Hudson Bay, whereas the oligotrichous ciliate *Strombidium conicum* (Lohmann) Wulff was dominating at the other stations, making up 57–77% and 64–93% of the total protist biomass, respectively. The dominant diatom species at stations 15, 16, 17, 18, 22 and 27 belonged to the genus *Chaetoceros* Ehrenberg, making up 52–94% of total diatom biomass. The pennate diatom *Nitzschia longissima* (Brébisson) Ralfs dominated the diatom carbon biomass at stations AN01 (51%) and 23 (100%). The main species contributing to total flagellate carbon biomass was the colonial prymnesiophyte *Phaeocystis pouchetii* (Hariot) Lagerheim at station 14 (46%), the dictyochophyceae *Dictyocha speculum* Ehrenberg at stations 15, 19 and AN03 (36, 55 and 28%, respectively) and the cryptophyceae *Teleaulax acuta* (Butcher) Hill at stations 18, 21, 22, 23, 27 and AN01 (28–46%). Total dinoflagellate carbon biomass was mainly associated with species belonging to the genera *Gyrodinium* Kofoid & Swezy (28–77%) and *Gymnodinium* Stein (11–36%).

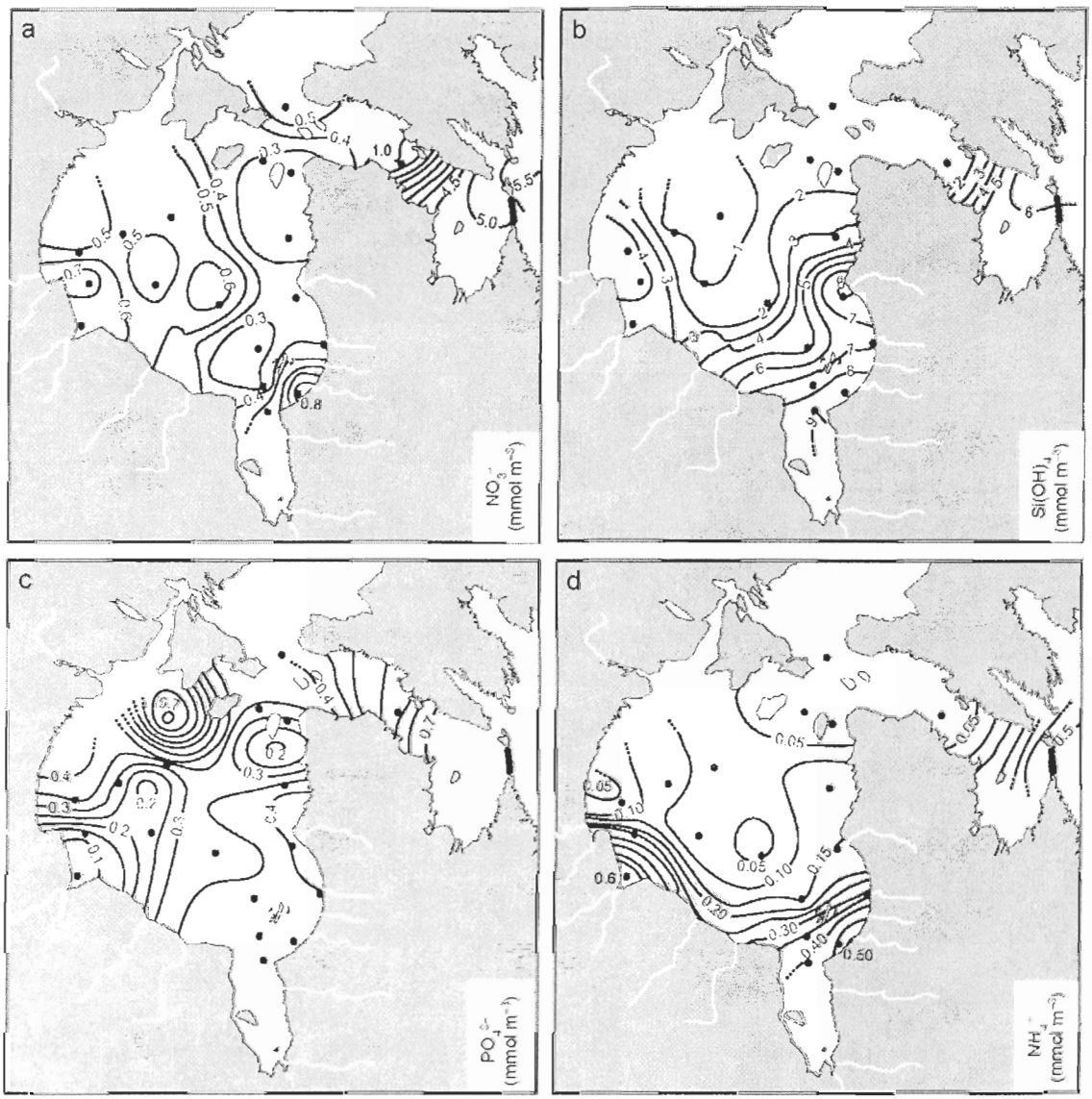

Fig. 2. Sea surface distribution of (a) nitrate (NO_3^-), (b) silicic acid ($Si(OH)_4$), (c) phosphate (PO_4^{3-}), and (d) ammonium (NH_4^+) concentrations in the Hudson Bay system during early fall 2005.

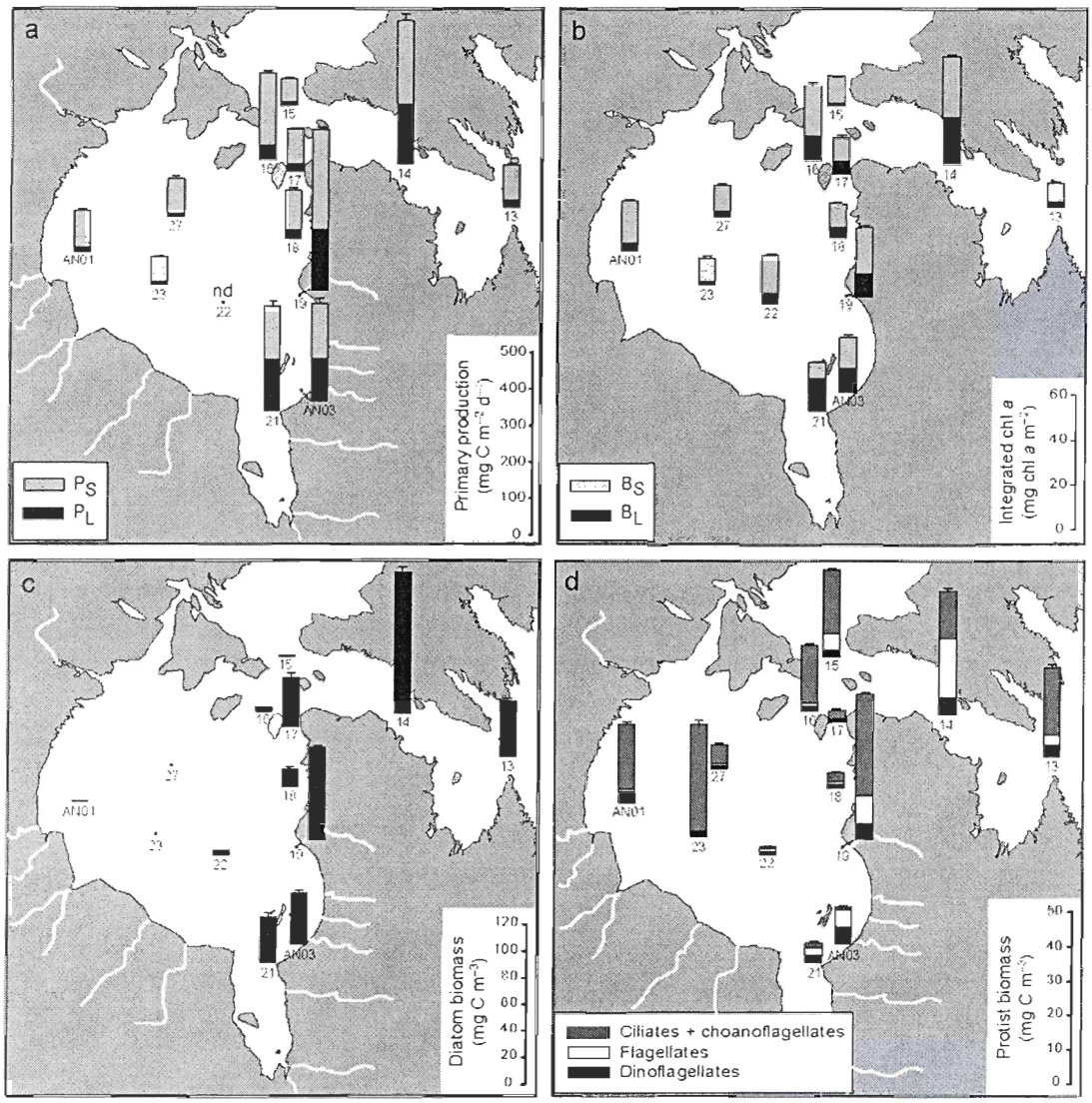

Fig. 3. Spatial variations in (a) particulate primary production, (b) chlorophyll *a* (chl *a*) biomass integrated over the euphotic zone depth, (c) carbon biomass of diatoms, and (d) carbon biomass of other protists at the depth of chl fluorescence maximum in the Hudson Bay system during early fall 2005. Production and biomass were determined for small (P_S and B_S; 0.7–5 μm) and large (P_L and B_L; ≥ 5 μm) phytoplankton cells. Primary production was not measured at station 22 (nd). In (c), diatom carbon biomass was < 0.1 mg C m^{-3} at stations 23 and 27. In (a) and (b) error bars represent SD of duplicate samples. In (c) and (d) error bars represent SD calculated from replicate transects counted for each sample.

Table 2. Average and, in parentheses, range of physical, chemical and biological variables in three groups of stations in the Hudson Bay system during early fall 2005.

Variable	Group I (Stations 13, **14**, 15, **16**)	Group II (Stations 17, **18**, **22**, **23**, **AN01**, **27**)	Group III (Stations 19, **AN03**, 21)
Temperature (°C)	1.75 (1.19 – 2.42)	2.65 (1.77 – 4.72)	8.33 (8.00 – 8.87)*[1,2]
Salinity	32.3 (31.5 – 33.4)*[2]	29.9 (28.5 – 30.7)	26.4 (25.4 – 27.2)*[1,2]
Stratification index (kg m^{-3})	0.83 (0.46 – 0.97)*[2,3]	3.71 (2.94 – 4.31)	4.87 (4.06 – 5.71)
Freshwater content (m)	2.83 (1.39 – 4.64)*[2,3]	5.59 (4.34 – 6.95)	7.16 (6.76 – 7.45)
Z_{eu}:Z_{mix} ratio	1.82 (0.49 – 3.85)	1.83 (1.42 – 2.67)	1.56 (1.19 – 2.00)
Nitrate (mmol m^{-3})	2.28 (0.50 – 6.80)	0.99 (0.08 – 2.31)	0.64 (0.38 – 1.11)
Ammonium (mmol m^{-3})	0.12 (0.02 – 0.24)	0.06 (0.01 – 0.10)	0.32 (0.11 – 0.46)*[2]
Silicic acid (mmol m^{-3})	3.43 (1.48 – 7.42)	2.97 (0.49 – 5.96)	8.51 (8.07 – 9.30)*[2]
Phosphate (mmol m^{-3})	0.60 (0.50 – 0.76)	0.42 (0.09 – 0.56)	0.41 (0.36 – 0.50)
Total part. production (P_T: mg C m^{-2} d^{-1})	200 (69.9 – 385)	106 (72.4 – 132)	337 (266 – 435)*[2]
Total chl *a* biomass (B_T: mg chl *a* m^{-2})	25.6 (10.2 – 47.1)	16.7 (11.4 – 22.5)	25.5 (21.6 – 30.3)
Diatom biomass (mg C m^{-3})	38.2 (0.45 – 107)	9.50 (0.01 – 37.5)	47.2 (33.9 – 69.3)*[2]
Dinoflagellate biomass (mg C m^{-3})	2.99 (1.37 – 5.25)	1.39 (0.78 – 3.36)	4.02 (2.36 – 5.12)*[2]
Flagellate biomass (mg C m^{-3})	6.33 (0.99 – 16.8)	0.58 (0.20 – 0.79)	4.90 (1.96 – 8.01)*[2]
Ciliate + choanofla. biomass (mg C m^{-3})	17.3 (14.1 – 19.6)	10.2 (0.68 – 30.7)	10.6 (0.89 – 29.6)
Production of large cells (P_L:P_T ratio; %)	22.9 (13.4 – 42.0)	14.6 (11.1 – 20.4)	44.7 (38.9 – 52.0)*[1,2]
Biomass of large cells (B_L:B_T ratio; %)	27.7 (9.29 – 43.5)	23.6 (10.1 – 38.3)	49.9 (35.2 – 69.5)
f-ratio (calculated with P_L:P_T ratio)	0.21 (0.14 – 0.35)	0.15 (0.12 – 0.19)	0.37 (0.33 – 0.42)*[1,2]
Export ratio	(0.20 – 0.26)	0.51 (0.38 – 0.69)	0.19

Temperature and salinity were averaged over the euphotic zone depth (Z_{eu}). Z_{mix}: surface mixed layer depth. Nutrient concentrations were integrated over Z_{eu} and divided by Z_{eu}. Export ratios were measured only at stations in bold character. In superscript: * indicates a significant ($p < 0.05$) difference between station groups; 1, 2 and 3 identifies the groups for which the difference is significant.

Physical, chemical and biological characteristics for each group of stations are presented in Table 2. One-way ANOVAs revealed that the vertical stratification index and FWC were significantly lower in Group I than in the two other groups. In the euphotic zone, water temperature, P_L:P_T and *f*-ratio were significantly higher while salinity was

lower in Group III than in the two other groups. In addition, NH_4^+ and $Si(OH)_4$ concentrations, P_T, diatom, dinoflagellate and flagellate carbon biomass were significantly higher in Group III than in Group II.

Spearman rank order correlations between physical, chemical and biological variables are shown in Table 3. Significant positive correlations were observed between P_T or P_L and the vertical stratification index, the mean integrated $Si(OH)_4$ and NH_4^+ concentrations in the euphotic zone. B_T or B_L were significantly positively correlated with the mean integrated NH_4^+ concentration in the euphotic zone. Diatom carbon biomass at the Z_{CFM} was significantly positively correlated with the mean integrated $Si(OH)_4$ concentration in the euphotic zone.

Table 3. Spearman rank order correlations between biological variables and physical or chemical variables in Hudson Bay system during early fall 2005 (n = 12).

	Temperature (°C)	Salinity	Stratification index (kg m^{-3})	Nitrate (mmol m^{-3})	Ammonium (mmol m^{-3})	Silicic acid (mmol m^{-3})	Phosphate (mmol m^{-3})
Total part. production (P_T; mg C m^{-2} d^{-1})	0.39	-0.34	0.88*	0.18	0.90*	0.98*	-0.01
Production of large cells (P_L; mg C m^{-2} d^{-1})	0.48	-0.45	0.88*	0.09	0.93*	0.93*	-0.09
Total chl *a* biomass (B_T; mg chl *a* m^{-2})	0.37	-0.26	0.28	0.04	0.73*	0.37	0.01
Biomass of large cells (B_L; mg chl *a* m^{-2})	0.49	-0.39	0.40	0.08	0.90*	0.54	-0.11
Diatom biomass (mg C m^{-3})	0.13	-0.11	0.05	0.08	0.43	0.74*	0.22

In superscript: * identifies significant correlations at $p < 0.05$.

2.3.2 Sinking export of primary production and biomass

Daily loss rates of chl *a*, BioSi, TPC and FPC biomasses at 50 m were highly variable throughout the Hudson Bay system (Fig. 4a–d). Daily loss rates of total and ≥ 5 μm chl *a* biomass ranged from 0.24 to 2.80% d^{-1} and from 0.83 to 3.01% d^{-1}, respectively, and were maximum at station 14 in central Hudson Strait (Fig. 4a). BioSi and TPC daily loss rates ranged from 1.49 to 8.34% d^{-1} and from 0.83 to 2.66% d^{-1}, respectively, with maximum values at station 22 in central Hudson Bay (Fig. 4b, c). FPC daily loss rates ranged from 10.3 to 70.2% d^{-1} with the maximum value at station 27 in western Hudson Bay (Fig. 4d).

Export ratios and sinking fluxes and velocities of different organic constituents at 50 m are shown in Table 4. Export ratios ranged from 0.19 to 0.69. Total and ≥ 5 μm chl *a* sinking fluxes at 50 m ranged from 0.04 to 1.34 mg chl *a* m^{-2} d^{-1} and from 0.02 to 0.62 mg chl *a* m^{-2} d^{-1}, respectively. BioSi sinking flux ranged from 4.63 to 50.2 mg m^{-2} d^{-1}. POC and TPC sinking fluxes ranges from 50.0 to 76.8 mg C m^{-2} d^{-1} and from 50.0 to 95.3 mg C m^{-2} d^{-1}, respectively. FPC sinking flux ranged from 1.83 to 32.1 mg C m^{-2} d^{-1}. As Z_{mix} varied from 13 to 26 m (average of 21 m) at the stations where interceptor traps were deployed (Table 1), we assumed that the retention time within the mixed layer was comparable for all samples and had the same influence on sinking velocities. Consequently, we can spatially compare sinking velocities calculated throughout the Hudson Bay system. Total and ≥ 5 μm chl *a* sinking velocities at 50 m ranged from 0.12 to 1.42 m d^{-1} and from 0.42 to 1.51 m d^{-1}, respectively. BioSi and TPC sinking velocities ranged from 0.74 to

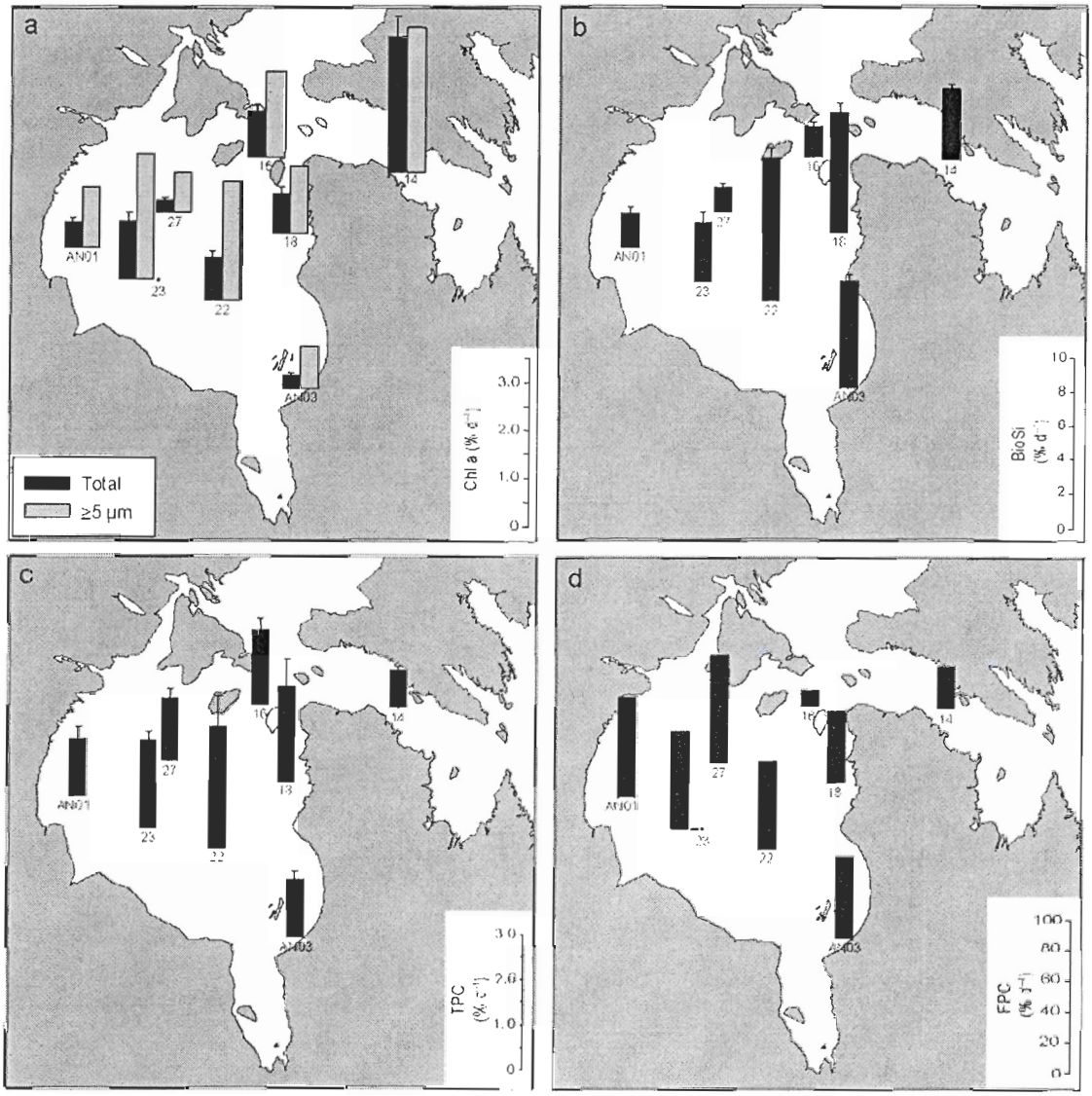

Fig. 4 Spatial variation in daily loss rates of (a) chlorophyll *a* (chl *a*) for total (≥ 0.7 μm) and large (≥ 5 μm) phytoplankton cells, (b) biogenic silica (BioSi), (c) total particulate carbon (TPC), and (d) fecal pellet carbon (FPC) measured at 50 m in the Hudson Bay system during early fall 2005. In (a), (b) and (c) error bars represent SD of daily loss rates calculated on duplicate samples.

Table 4. Export ratios, sinking fluxes and sinking velocities of total chlorophyll *a* (Tot chl *a*), chlorophyll *a* of large cells (Chl *a* ≥ 5 µm), biogenic silica (BioSi), particulate organic carbon (POC), total particulate carbon (TPC) and fecal pellet carbon (FPC) estimated with the traps deployed at 50 m in the Hudson Bay system during early fall 2005. Values are averages ± SD calculated on duplicate samples when available. The station groups were determined from physical variables (see Materials and Methods section). nd: no data

Station	Group	Export ratio	Sinking flux ($mg\ m^{-2}\ d^{-1}$)						Sinking velocities ($m\ d^{-1}$)				
			Tot chl *a*	Chl *a* ≥ 5 µm	BioSi	POC	TPC	FPC	Tot chl *a*	Chl *a* ≥ 5 µm	BioSi	TPC	FPC
14	I	0.20 ± 0.05	1.34 ± 0.07	0.62	50.2 ± 2.51	76.8	89.1 ± 1.85	7.82	1.42 ± 0.21	1.51	2.06 ± 0.12	0.42 ± 0.03	13.9
16	I	0.26 ± 0.03	0.30 ± 0.01	0.19	20.3 ± 0.90	60.7	63.8 ± 6.14	1.83	0.46 ± 0.07	0.89	0.91 ± 0.08	0.83 ± 0.12	5.15
18	II	0.38 ± 0.01	0.13 ± 0.002	0.06	41.2 ± 0.67	50.5	54.5 ± 12.9	16.2	0.42 ± 0.06	0.71	3.51 ± 0.23	1.05 ± 0.30	23.2
22	II	nd	0.19 ± 0.01	0.12	43.7 ± 2.35	71.3	95.3 ± 19.3	27.1	0.44 ± 0.07	1.24	4.17 ± 0.26	1.65 ± 0.35	28.8
23	II	0.69 ± 0.04	0.20 ± 0.02	0.04	7.09 ± 0.78	50.0	80.9 ± 2.34	2.94	0.60 ± 0.09	1.31	1.71 ± 0.28	0.97 ± 0.08	31.7
AN01	II	0.46 ± 0.01	0.12 ± 0.02	0.05	11.6 ± 1.76	51.8	50.0 ±7.53	4.20	0.26 ± 0.04	0.64	1.00 ± 0.16	0.62 ± 0.12	33.6
27	II	0.51 ± 0.02	0.04 ± 0.004	0.02	4.63 ± 0.48	51.5	66.5 ± 5.31	6.46	0.12 ± 0.02	0.42	0.74 ± 0.09	0.69 ± 0.09	35.1
AN03	III	0.19 ± 0.05	0.06 ± 0.002	0.10	41.0 ± 1.28	50.0	55.7 ± 3.95	32.1	0.13 ± 0.02	0.44	3.16 ± 0.18	0.48 ± 0.07	26.2

4.17 m d^{-1} and from 0.42 to 1.65 m d^{-1}, respectively. FPC sinking velocities ranged from 5.15 to 35.1 m d^{-1}. The spatial patterns of the sinking velocities at 50 m were comparable to those of daily loss rates (Fig. 4a–d). No significant correlation was observed between daily loss rates or sinking velocities and physical, chemical or biological variables.

2.4 Discussion

2.4.1 Primary production in the Hudson Bay system

The primary production rates measured in the Hudson Bay system during early fall 2005 (70–435 mg C m^{-2} d^{-1}, Fig 3a) were generally higher than values reported for the Canadian Beaufort Sea during the ice-free early fall (15–120 mg C m^{-2} d^{-1}, Brugel et al. 2009) and the central Arctic Ocean in partially ice-covered summer (50–150 mg C m^{-2} d^{-1}, Olli et al. 2007). Our Hudson Bay values (72–435 mg C m^{-2} d^{-1}) were similar to previous records reported by Harvey et al. (2006) in northern Hudson Bay in early August 2004 (54–344 mg C m^{-2} d^{-1}). During both studies, the primary production in Hudson Bay was generally dominated by small cells (0.7–5 μm). However, our values at the mouth of Foxe Basin (70 mg C m^{-2} d^{-1}) and in Hudson Strait (113–385 mg C m^{-2} d^{-1}) were lower than those reported by Harvey et al. (2006) for the same areas (i.e. 325 mg C m^{-2} d^{-1} in Foxe Basin, 954–3444 mg C m^{-2} d^{-1} in Hudson Strait). In these areas, the phytoplankton size-structure was also different between both studies. Primary production and chl *a* biomass were dominated by small cells during the present study (Fig. 3a, b) whereas they were

dominated by large cells (≥ 5 μm) during the study of Harvey et al. (2006). These discrepancies may be explained, in part, by difference in the sampling periods. Indeed, our study was carried out in early fall (23 September–16 October) when the photoperiod was shorter (11 h *versus* 16 h) and the surface mixed layer was deeper (22–72 m *versus* 6–14 m) than during the mid-summer study (2–15 August) of Harvey et al. (2006).

Assuming an algal growth season of 120 days in Arctic waters (Subba Rao & Platt 1984), the annual particulate primary production based on our measurements in early fall, would be *ca.* 46 g C m^{-2} for the Hudson Strait area, 40 g C m^{-2} for the southeastern Hudson Bay coastal waters and 14 g C m^{-2} for the rest of Hudson Bay. These are conservative estimates since they are based on measurements conducted during the late growth season and do not take into account the potential contribution of the phytoplankton spring bloom and sea-ice algae to the particulate primary production. Nevertheless, our estimate for southeastern Hudson Bay is close to the value of 35 g C m^{-2} y^{-1} proposed by Roff & Legendre (1986) for Hudson Bay coastal waters but somewhat lower than that of 50–70 g C m^{-2} y^{-1} proposed by Sakshaug (2004) for the entire Hudson Bay area. Overall, our results confirm that the Hudson Bay sustains a low annual production compared to other Arctic shelves, such as the Chukchi Sea (from 20 to > 400 g C m^{-2} y^{-1}), Baffin Bay (60–120 g C m^{-2} y^{-1}) and Barents Sea (from < 20 to 200 g C m^{-2} y^{-1}) (Sakshaug 2004).

2.4.2 Regional distribution of phytoplankton production and biomass

The three groups of stations characterized on their hydrography also showed differences in chemical and biological properties. Group I, which included stations 13 to 16 located in the Hudson Strait area, is characterized by a weak stratification (average of 0.83 kg m^{-3}; Table 2), related to the important wind and tidal mixing generally recorded in this area (Drinkwater & Jones 1987, Arbic et al. 2007). This region is also characterized by a gradient of decreasing salinity and increasing water temperature from the entrance of Hudson Strait to the mouth of Hudson Bay (Table 1), highlighting the seawater influx from the Baffin Bay estimated at 0.9 Sv (Drinkwater 1986, Straneo & Saucier 2008b) or conversely the freshwater transported by the outflow to the Labrador Sea estimated at 1–1.2 mSv (Drinkwater 1986, Saucier et al. 2004, Straneo & Saucier 2008a). This water inflow was associated with nutrient input and shaped a gradient of decreasing nutrient concentrations from the entrance of Hudson Strait to the mouth of Hudson Bay (Fig. 2a–d), as previously observed by Kuzyk et al. (2010). At stations 14 and 16, the abundance of nutrients in the shallow Z_{mix} has favored phytoplankton production (P_T of 385 and 233 mg C m^{-2} d^{-1}, respectively; Fig. 3a) and accumulation of phytoplankton in the euphotic zone (B_T of 47.1 and 32.7 mg chl *a* m^{-2}, respectively; Fig. 3b). However, at stations 13 and 15 where the surface mixed layer was deep ($Z_{mix} \geq 35$ m; Table 1), Z_{mix} was deeper than Z_{eu} (Z_{eu}:$Z_{mix} < 1$; Table 1) and P_T and B_T were low (< 115 mg C m^{-2} d^{-1} and < 13 mg chl *a* m^{-2}, respectively; Fig. 3a, b), indicating that phytoplankton production was likely limited by light availability at these stations. Therefore, on average, P_L and B_L were lower in Group I than in Group III comprising stations influenced by riverine input, as discussed below.

Grazing by herbivorous zooplankton could also have limited phytoplankton biomass accumulation at some stations in Group I. Unfortunately we do not have grazing rate measurements for this study. While the FPC biomass in the upper 50 m at stations 13 and 15 (31.7 and 20.5 mg C m^{-2}, respectively) was higher than at stations 14 and 16 (18.1 and 16.5 mg C m^{-2}, respectively; data not shown), we would remain cautious in drawing further interpretation from the FPC biomass as it may not be a reliable indicator of grazing rate.

Stations 19, AN03 and 21 of Group III are strongly influenced by freshwater from river discharge directly into Hudson Bay (e.g. Great Whale, Nastapoca and Innuksuac rivers) or *via* James Bay (e.g. through La Grande, Nottaway and Rupert rivers). The rivers and small tributaries discharging on the eastern side of Hudson Bay together collectively contribute 43% (i.e. 9.87×10^{-3} Sv) of the total freshwater discharge in Hudson Bay and Hudson Strait (Déry et al. 2005). This important freshwater inflow stratifies the water column in this area as reflected by the highest stratification index (average of 4.87 kg m^{-3}) observed for Group III (Table 2), and supplies new nutrients to coastal waters as shown by the decreasing gradient in surface $Si(OH)_4$ and NH_4^+ concentrations towards offshore waters in the southeastern Hudson Bay area (Fig. 2b, d). These three parameters positively influence P_T and P_L (Table 3). A similar gradient was observed in southwestern Hudson Bay particularly in the vicinity of the Churchill and Nelson river plumes. The riverine origin of $Si(OH)_4$ and NH_4^+ in Hudson Bay is clearly shown by strong negative correlations between euphotic zone concentrations of these two nutrients and salinity (r_s = -0.86 and -0.76, respectively, $p < 0.05$). These findings are in agreement with previous observations of

an important supply of $Si(OH)_4$ from the Great Whale and Churchill rivers to the Hudson Bay (Legendre et al. 1996, Kuzyk et al. 2008). High water temperature and enhanced riverine supply in $Si(OH)_4$ and NH_4^+ may have provided ideal conditions for diatom growth in the shallow waters of southeastern Hudson Bay; as reflected by the highest P_T (average of 337 mg C m^{-2} d^{-1}), P_L:P_T (average of 45%), B_T (average of 25.5 mg chl *a* m^{-2}) and B_L:B_T (average of 50%) of the three groups (Fig. 3a, b; Table 2).

In contrast, surface PO_4^{3-} and NO_3^- concentrations did not show gradients linked to riverine input. We rather observed a dilution effect on surface PO_4^{3-} concentrations in proximity to the Nelson River plume (Fig. 2a, c). The highest concentrations of PO_4^{3-} and NO_3^- in well-mixed marine waters of Group I stations (0.60 and 2.28 mmol m^{-3}, respectively; Table 2) indicate that these nutrients are mainly from marine origin in Hudson Bay, especially in the southeastern region as previously suggested (Legendre & Simard 1979, Hudon et al. 1996, Legendre et al. 1996, Kuzyk et al. 2010).

Group II (i.e. stations 17, 18, 22, 23, AN01 and 27) showed intermediate conditions (see Table 2) resulting from the mixing of water masses from different sources, i.e. seawater from Baffin Bay *via* Hudson Strait (Drinkwater 1986, Saucier et al. 2004, Straneo & Saucier 2008a) and the Arctic Ocean *via* Fury and Hecla Strait (Sadler 1982, Jones et al. 2003), freshwater from river runoff (Déry et al. 2005) and sea-ice melt (Hudon et al. 1996, Ingram & Prinsenberg 1998), and the redistribution of these water masses by the cyclonic

circulation in the Hudson Bay (Prinsenberg 1986c, Ingram & Prinsenberg 1998). These conditions were unfavorable for phytoplankton growth as reflected by the lowest P_T (106 mg C m^{-2} d^{-1}) and B_T (16.7 mg chl *a* m^{-3}) and the strong dominance of small cells at stations of this group (Figs. 2 and 3; Table 2).

These results show that the interactions between environmental factors and phytoplankton production and biomass were distinct in Hudson Strait and Hudson Bay, and corroborate our first hypothesis. Hudson Strait constitutes a well-mixed environment whose nutrient inputs, especially NO_3^- and PO_4^{3-}, are strongly influenced by seawater inflow from the Baffin Bay, whereas Hudson Bay is a well-stratified environment where vertical stability and nutrient input, especially $Si(OH)_4$ and NH_4^+, are closely linked to river runoff and entrainment. These observations are in agreement with those of Harvey et al. (1997, 2006) in eastern Hudson Bay and Hudson Strait. Our results also highlight that NH_4^+ may not only be a source of regenerated nutrients to nearshore and offshore waters but also a source of new nutrients to coastal waters, as shown previously in coastal environments (Mann & Lazier 1996). In this context, future changes in freshwater runoff (Gough & Wolfe 2001) are likely to affect phytoplankton dynamics in the coastal waters of Hudson Bay through their impact on nutrient inputs.

2.4.3 Coupling between primary producers and sinking export

In contrast with the spatial variability in phytoplankton biomass and production, the POC sinking flux was relatively constant throughout the Hudson Bay system (Table 4). Consequently, low export ratios (< 0.27) were observed at stations of high P_T and B_T (Group III and stations 14 and 16 from Group I) and, conversely, high export ratios were observed at stations of low P_T and B_T (Group II; average of 0.51) (Fig. 3a, b; Table 2). Hence, our results showed that at short time scales, high export ratios are not necessarily associated with high primary production rates. Moreover the export ratios estimated during our study were at times unexpectedly high (up to 0.69). Export ratios are typically of the order of 0.05 to 0.10 in regions of low production (Buesseler 1998, Sarmiento & Gruber 2006) and high export ratios, ranging from 0.25 to 0.70, are typically found in productive coastal systems (Harrison et al. 1993, Pommier et al. 2008, Reigstad et al. 2008).

To explain these counterintuitive results, we investigated the potential influence of protist community structure on organic material sinking export. Indeed, large cells, especially diatoms, constitute an efficient export pathway either as intact cells or after incorporation into fast sinking fecal pellets (e.g. Boyd et al. 2008, Wexels Riser et al. 2008, Buesseler & Boyd 2009). The *f*-ratio calculation proposed by Tremblay et al. (1997) is based on this underpinning principle. The highest diatom carbon biomass (107 mg C m^{-3}) and a moderate *f*-ratio (0.35) were observed in Hudson Strait (Group I: station 14), where the highest POC sinking flux was measured (77 mg C m^{-2} d^{-1}) (Fig. 3c; Tables 2 and 4).

Much lower diatom carbon biomass (average of 0.27 mg C m^{-3}) and *f*-ratios (average of 0.12) were observed at western Hudson Bay stations (Group II: stations AN01, 23 and 27) but only slightly lower POC sinking fluxes (i.e. 50–52 mg C m^{-2} d^{-1}) were measured (Fig. 3c; Tables 2 and 4). At these stations, the total protist carbon biomass was dominated by ciliates (mainly *Strombidium conicum*; see Results section), a group of protists usually associated with a high recycling efficiency of the euphotic zone primary production (Legendre & Le Fèvre 1995, Legendre & Rassoulzadegan 1995, Azam 1998). Despite the overwhelming contribution of heterotrophic ciliates to protist biomass, there was a high sinking export of the POC produced by the small phytoplankton cells (Fig. 3a, d; Table 4). Variations in phytoplankton size-structure and protist community composition observed between the three groups of stations (Fig. 3a–d; Table 2), did not clearly explain the narrow range of POC sinking fluxes measured throughout the Hudson Bay system (Table 4).

Similarly, Rivkin et al. (1996b) report, for the Gulf of St. Lawrence, fairly constant POC sinking fluxes during bloom and post-bloom conditions despite lower primary production and the dominance of a microbial food web during the later period. These authors concluded that neither food web structure nor primary production could be used to predict the magnitude of POC sinking export from the euphotic zone.

We cannot rule out the possibility of a spatio-temporal decoupling between primary production and export. Such decoupling may be amplified in the western Hudson Bay area

where modeling results evidence a cyclonic gyre with intensified currents during fall (Saucier et al. 2004). This gyre may have favored the accumulation and subsequent sedimentation of POC, which would explain the high export ratios observed in western Hudson Bay despite the low P_T and the potential grazing impact of the ciliates in this area. Overall, the results discussed in this section, do not support our second hypothesis that variations in the intensity and structure of phytoplankton production influence the magnitude of the POC sinking export and consequently export ratios in the Hudson Bay system.

2.4.4 Suspended organic material composition and sinking export

Daily loss rates of chl *a* and TPC were in the range of values reported in the Chukchi Sea by Lalande et al. (2007a) and in the northern Barents Sea by Reigstad et al. (2008) both in summer. FPC daily loss rates were in the range of values measured by Juul-Pedersen et al. (2006) in Disko Bay in summer. However the former regions are usually more productive environments than Hudson Bay (Sakshaug 2004). The magnitude of organic material daily loss rates mainly depend on its composition and sinking velocity. We observed the following trend for the daily loss rates: total chl *a* = chl *a* (≥ 5 μm) = TPC < SiBio < FPC (Fig. 4a–d). The discrepancies between variables are related to differences in sinking velocities linked to the size of the particles they are associated with and the preferential sinking or recycling of some variables. One could expect that BioSi would sink faster than chl *a* and TPC containing particles since it is associated with the

presence of diatoms (large cells) and also acts as a mineral ballast (e.g. Heiskanen & Keck 1996, Armstrong et al. 2009, Fischer et al. 2009). Moreover, BioSi is not degraded during zooplankton grazing (Conover et al. 1986, Ingalls et al. 2003) and, consequently, can be efficiently exported to depth incorporated into fecal pellets as previously observed in eastern Hudson Bay (Lapoussière et al. 2009, see Chapter I). Fecal pellets generally constitute larger particles compared to phytoplankton cells and, consequently, they are more readily exported to depth (Turner 2002) as denoted by FPC daily loss rates reaching 70% d^{-1} while daily loss rates of other components remained in an order of a few percents of the standing stock (Fig. 4a–d). Overall (except at station 16 where fecal pellet daily loss rate was 10% d^{-1}), fecal pellets constituted an efficient export pathway; yet, they were an important source of material to the seafloor only in eastern Hudson Bay (see Fig. 4d; Table 4). These spatial discrepancies can be explained by the higher suspended FPC biomass observed in eastern Hudson Bay (Stations 18, 22 and AN03; average of 26.9 mg C m^{-2}) compared to western Hudson Bay (Stations AN01, 23 and 27; average of 4.06 mg C m^{-2}) and Hudson Strait (Stations 14 and 16; average of 17.3 mg C m^{-2}) (data not shown). However, these discrepancies cannot be explained by a difference in fecal pellet origin since suspended FPC was dominated by cylindrical fecal pellets throughout the Hudson Bay system (average of 93 ± 4.4%), except at station AN01, where spherical fecal pellets dominated (82.7%; data not shown). These results are in accordance with the high abundance of appendicularians observed in this area compared to the rest of the system in late summer (Estrada 2010).

As no significant relationship was observed between daily loss rates and biological variables (P_T, P_L:P_T, B_T, B_L:B_T), we did not corroborate our second hypothesis on the influence of phytoplankton production, biomass or community structure on daily loss rates. Still, our results highlight that daily loss rates of organic material by sedimentation are closely linked to the composition of the material.

2.5 Conclusion

This first study on the coupling between primary production and sinking export in ice-free conditions in Hudson Bay system confirmed the overall low productivity and sinking export of the bay region. However, our results also highlight regional differences in physical and biological conditions and confirm that Hudson Strait and Hudson Bay are very different in terms of physical oceanographic conditions. Hudson Strait was characterized by an intense vertical mixing and influenced by seawater inflow from Baffin Bay, and Hudson Bay was well-stratified by the important river runoff particularly in the southeastern region. The different forcings in these two regions influence light and nutrient availability and, consequently, shape regional patterns in phytoplankton production and biomass. Our results did not reveal a tight coupling between the sinking export of organic material and the primary production, biomass or composition of phytoplankton communities. During our study, the highest export ratios were associated with low production rates dominated by small phytoplankton cells and a high biomass of microheterotophs. These counterintuitive results may be explained by a spatio-temporal decoupling between production and sinking

export and by the formation of a cyclonic gyre, intensified during fall, enhancing the POC sinking export. Our results also highlight that fecal pellets constitute an efficient export pathway in the Hudson Bay system although their contribution to the sinking export at depth can be highly variable. These interesting results were obtained for a short period during the growing season, thus providing a snapshot of primary production and sinking export processes during the fall. Further studies are needed to better understand the factors influencing the coupling between primary production and organic material sinking export during the remainder of the productive season. Future studies should also tackle the influence of physical processes such as strong currents or gyre formation but also the influence of the zooplankton community in the retention or the exportation of organic material to deep waters.

CHAPITRE III

ABUNDANCE OF FREE-LIVING *VERSUS* PARTICLE-ATTACHED BACTERIA AND THEIR ROLE IN THE RECYCLING AND EXPORT OF ORGANIC MATERIAL IN THE HUDSON BAY SYSTEM

RÉSUMÉ

L'abondance, la taille, le contenu en acides nucléiques et la vitesse de chute des bactéries libres et attachées aux particules ont été simultanément étudiées à l'aide d'une nouvelle approche combinant la méthode des colonnes à sédimentation avec la cytométrie de flux. L'échantillonnage a été effectué dans le système sub-arctique de la baie Hudson (i.e. baie d'Hudson, détroit d'Hudson et bassin de Foxe) à la fin des étés 2005 et 2006. Nous avons également estimé la biomasse, la production et la respiration des deux types de bactéries en utilisant des modèles existants. Les bactéries attachées représentaient seulement < 3% de l'abondance bactérienne totale. Leur abondance était étroitement corrélée au nombre de particules à coloniser. Les bactéries attachées étaient en moyenne deux fois plus grandes que les bactéries libres. Les bactéries avec un contenu important en acides nucléiques (HNA) contenaient 1,5 fois plus d'acides nucléiques lorsqu'elles étaient attachées aux particules que lorsqu'elles étaient libres. Nos résultats ont montré que les bactéries pouvaient sédimenter plus rapidement que la loi de Stoke le prédit lorsqu'elles colonisaient les particules. En effet, les vitesses de chute des bactéries attachées étaient comparables à celles de la biomasse chlorophyllienne et des protistes. Toutefois, au cours de notre étude, la contribution des bactéries attachées au carbone organique particulaire (COP) suspendu total était faible (i.e. < 1% du COP suspendu) et elles recyclaient potentiellement plus de COP que leur contribution en biomasse. De plus, les bactéries attachées dégradent généralement plus de matière organique que ce qu'elles peuvent utiliser. Par conséquent, les principaux acteurs dans la reminéralisation du COP étaient vraisemblablement les bactéries libres qui utilisent le matériel organique dissous qui s'échappe des particules.

ABSTRACT

The abundance, size, nucleic acid content and sinking velocity of free-living and particle-attached bacteria were studied simultaneously, using a new approach that combines the settling column method with flow cytometry. Sampling was carried out in the sub-arctic Hudson Bay system (i.e. Hudson Bay, Hudson Strait and Foxe Basin) in late summers 2005

and 2006. We also estimated the biomass, production and respiration of both types of bacteria using published models. Particle-attached bacteria represented only < 3% of total bacterial numbers and their abundance was closely linked to the amount of particles available for attachment. Particle-attached bacteria were, on average, twice larger than free-living bacteria. Bacteria with high nucleic acid (HNA) content contained 1.5 times more nucleic acids as attached to particles than as free-living. Our results show that bacteria can sink faster than predicted by Stoke's Law when they colonize particles, as estimated sinking velocities of particle-attached bacteria were comparable to those of chlorophyll a biomass and protist cells. Yet, during our study, the contribution of particle-attached bacteria to total suspended particulate organic carbon (POC) remained low (i.e. < 1% of suspended POC) while they potentially recycled more POC than their carbon biomass contribution. Moreover, particle-attached bacteria degrade usually more organic matter than they can take. Consequently, the main contributors to POC remineralization would be free-living bacteria using dissolved organic material leaking from particles.

3.1 Introduction

In marine systems, the study of pathways by which particulate organic matter (POM) is transferred within the food web, exported downward through the water column, and remineralized by microbes is crucial to understand the global carbon cycle and estimate the efficiency of the biological pump (e.g. de la Rocha & Passow 2007, Buesseler et al. 2008, Lutz et al. 2008). Microbes, and more specifically heterotrophic bacteria, have long been recognized as important contributors to marine food webs where they play a key role in the cycling of organic matter (Pomeroy 1974, Azam et al. 1983, Cho & Azam 1988). Heterotrophic bacteria can process between 10 and 50% of the carbon fixed by photosynthesis in marine systems (Azam et al. 1983, Anderson & Ducklow 2001, Robinson 2008) through ectoenzymatic hydrolysis, respiration and production of new bacterial biomass (Grossart & Ploug 2001, Grossart et al. 2007). Organic-rich sinking particles constitute substrate-rich microhabitats and, consequently can be considered as "hot spots" for bacterial colonization and growth as well as organic matter solubilization and remineralization (Alldredge et al. 1986, Turley & Mackie 1994, Simon et al. 2002, Aristegui et al. 2009).

Some studies have characterized the genetic, morphological and physiological characteristics of both free-living and particle-attached bacteria (e.g. Delong et al. 1993, Ghiglione et al. 2007, Grossart et al. 2007). It is now well-established that particle-attached bacteria are often larger than free-living bacteria probably owing to the more favorable nutritive conditions of the substrates compared to the surrounding waters (Alldredge et al.

1986, Cho & Azam 1988, Simon et al. 2002). However, differences between their metabolic activities are more controversial. Some studies have shown that particle-attached bacteria are metabolically more active on a per cell basis than free-living bacteria (Pedrós-Alió & Brock 1983, Fandino et al. 2001, Simon et al. 2002, Grossart et al. 2003a, 2007, Taylor et al. 2009), while the opposite has also been reported (Alldredge et al. 1986, Martinez et al. 1996). Motility, chemosensing and the ability of particle-attached bacteria to hydrolyze less degradable substrates have been proposed to explain the discrepancies between free-living and particle-attached bacteria (Grossart & Simon 1998, Kiørboe & Jackson 2001, Kiørboe et al. 2002). Free-living and particle-attached bacterial communities have often been reported to be phylogenetically distinct (Delong et al. 1993, Crump et al. 1998, Fandino et al. 2001, Grossart et al. 2005, 2006, Rink et al. 2007) although little difference between the two communities has also been reported (Hollibaugh et al. 2000, Riemann & Winding 2001, Ghiglione et al. 2007, 2009). Based on these observations, bacteria were divided into three functional types: (1) free-living, (2) colonizing particles, and (3) generalists which are able to grow in suspension as well as on particles (Grossart et al. 2005, 2006). According to Riemann & Winding (2001), free-living and particle-attached bacteria must be considered as interacting rather than independent communities. This last statement is supported by the attachment-detachment activity of bacteria to particles (Grossart et al. 2003b, Kiørboe et al. 2003), the leaking of hydrolyzate from particles and the release of progeny from particle-attached bacteria in the plume of sinking particles (Jacobsen & Azam 1984, Azam & Long 2001, Fandino et al. 2001, Stocker et al. 2008).

In pelagic oligo- and mesotrophic marine ecosystems, particle-attached bacteria generally constitute < 5% but can reach up to 10% of total bacterial numbers whereas in more eutrophic and notably in particle-rich environment such as estuarine systems, their contribution to total bacterial abundance may reach > 60% (Bell & Albright 1981, Bano et al. 1997, Crump et al. 1998, Garneau et al. 2009). Therefore, it appears pivotal to improve our knowledge of particle-attached bacteria, particularly in an estuarine environment like the Hudson Bay system which annually receives a large volume of riverine discharge corresponding to *ca.* one third of all Canadian rivers runoff taken together (Prinsenberg 1980, Déry et al. 2005). Kuzyk et al. (2009) estimated that 4.6×10^5 tons of suspended particulate organic carbon (POC) is transported by rivers into Hudson Bay each year. This is tremendous amount of carbon that is likely to be colonized and then remineralized by bacteria.

The role of bacteria in marine systems is typically associated with organic matter remineralization, and they are also responsible for some of the attenuation of the POC sinking export with depth through particle disaggregation, fragmentation and solubilization through a wide variety of enzymatic pathways (Karl et al. 1988, Cho & Azam 1990, Boyd & Trull 2007, Steinberg et al. 2008). The potential contribution of bacteria to carbon sinking export is usually overlooked owing to the extremely low sinking velocities predicted from Stoke's Law for their size range (Pedrós-Alió & Mas 1993). Nevertheless, a few studies have shown a significant sedimentation of bacteria measured with particle interceptor traps probably through their attachment to, and/or growth on sinking particles

(Ducklow et al. 1982, Pedrós-Alió & Mas 1993, Turley & Mackie 1994, Lapoussière et al. 2009, see Chapter I). Consequently, bacteria do not only attenuate the POC sinking export to depth but can also contribute to this export as they can sink to depth *via* attachment to particles. To our knowledge, there is no data addressing simultaneously this dual role of particle-attached bacteria in the recycling and export of POM. Here, a new protocol was developed coupling the settling column method of Bienfang (1981) with flow cytometry (Marie et al. 1997) to simultaneously determine the characteristics, abundance and sinking velocity of free-living and particle-attached bacteria.

The first objective of this study was to determine the abundance, size, nucleic acid content and sinking velocity of free-living and particle-attached bacteria and their relationships with environmental conditions and protist composition in the Hudson Bay system during summer. The second objective was to develop a carbon budget considering the potential contribution of particle-attached bacteria to the POC sinking export and carbon loss through respiration based on bacterial production and respiration, as estimated using existing models. We hypothesized that: (1) particle-attached bacteria dominate the total bacterial abundance in an estuarine system like the Hudson Bay system; (2) particle-attached bacteria have sinking velocities higher than predicted by Stoke's Law, and therefore can potentially contribute significantly to the POC sinking flux and, (3) particle-attached bacteria respire a larger fraction of the POC sinking flux than free-living bacteria.

3.2 Material and methods

3.2.1 Study area

The Hudson Bay system (i.e. Hudson Bay, Hudson Strait and Foxe Basin) is a large inland sea (1.23×10^6 km^2; Jones & Anderson 1994, Granskog et al. 2007) located in the Canadian sub-Arctic. This system is covered by sea ice from mid-October to early August (Markham 1986, Gagnon & Gough 2005b) and receives an important freshwater discharge (*ca.* 592 km^3 y^{-1}) from the large drainage basin which surrounds it (*ca.* 3.1×10^6 km^2) (Déry et al. 2005). River runoff together with precipitation and sea-ice melt contribute to the strong water column stratification in shallow Hudson Bay and Foxe Basin (average depths 120 m and < 100 m, respectively; Prinsenberg 1984, Jones & Anderson 1994, Granskog et al. 2007). In contrast, Hudson Strait, which connects Hudson Bay and Foxe Basin to the Labrador Sea, is deeper (average depth 400 m) and well-mixed by strong tidal currents (i.e. > 2–3 m s^{-1}) (Drinkwater 1988, Arbic et al. 2007).

3.2.2 Sampling

Sampling was carried out on board the CCGS *Pierre Radisson* during two oceanographic expeditions conducted within the framework of the time-series research program MERICA-nord (études des MERs Intérieures du CAnada, Hudson Bay northern component) in late summers 2005 (from 31 August to 10 September) and 2006 (from 30 August to 10 September) in the Hudson Bay system. A total of ten and nine stations were visited in 2005 and 2006, respectively (Fig. 1), with stations 1 and 6 visited only in 2005

and station 10 only in 2006. At each station, water samples were collected at depths of 50% of surface irradiance ($Z_{50\%}$) and of the chlorophyll fluorescence maximum (Z_{CFM}), using a rosette-CTD system (Seabird Electronics 911+) equipped with 12 Niskin bottles of 10 L. Optical depths were determined based on Secchi disk measurements (Holmes 1970). Z_{CFM} was determined with a fluorometer (Wetstar mini fluorometer model 9512008) coupled with the rosette-CTD system. At stations 7 in 2005 and 5 in 2006, the Z_{CFM} was observed at the $Z_{50\%}$.

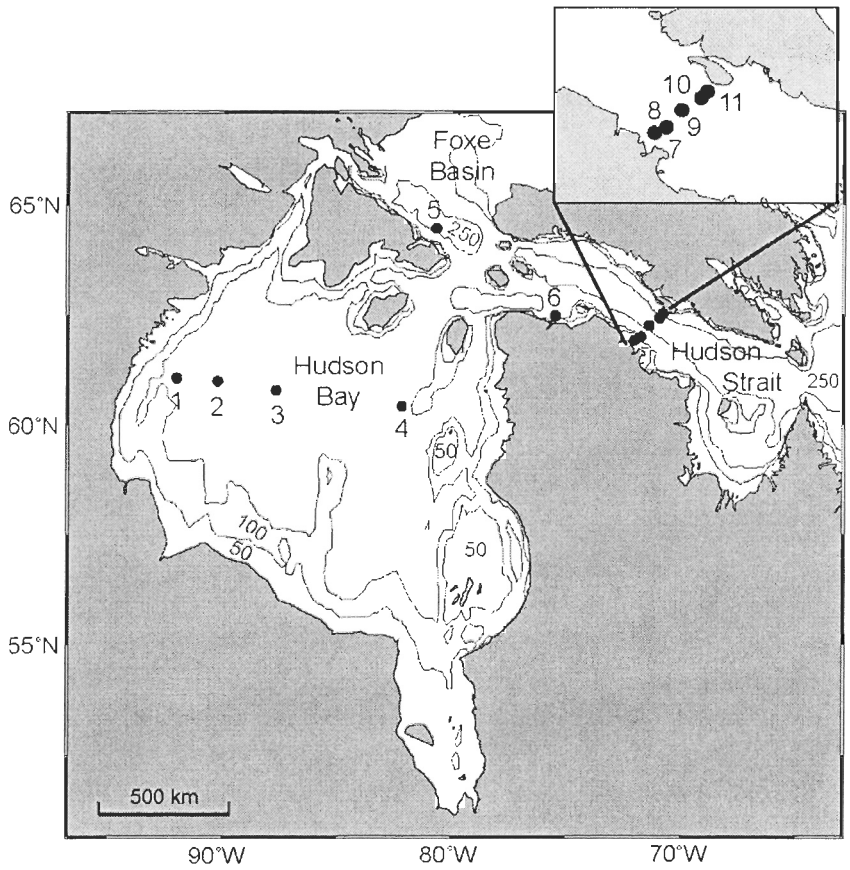

Fig. 1. Location of the sampling stations with isobaths (m) in the Hudson Bay system during late summers 2005 and 2006.

3.2.3 Sedimentation experiments

Sinking velocities of protists and bacteria were measured from water samples from $Z_{50\%}$ and Z_{CFM}, using settling columns (SetCol; Bienfang 1981). The SetCol technique is based on the principle that the column initially contains a uniformly mixed protist community and the sinking velocity is estimated from vertical changes in the distribution of a variable (e.g. protist cells) over a given time period. The SetCol consisted in a Plexiglas cylinder of 0.53 m in height equipped with ports for subsample removal at the top (0.43 L), middle (3.57 L) and bottom (0.40 L) sections of the column. At each station and for both sampled depths, a SetCol was filled with a gently mixed water sample and kept in a dark incubation room during 6 h at 4°C close to *in situ* water temperature (average 3.1°C during both sampling years). Incubation in the dark for 6 h should not affect the physiological control of settling (Waite et al. 1992). After the settling period, the various sections of the SetCol (top, middle and bottom) were collected and only the top and bottom sections were analyzed. A subsample kept under the same light and temperature conditions as during the SetCol incubation was processed at the beginning and at the end of each experiment in order to correct for any potential change in biomass due to processes other than sinking (e.g. cell growth) during the 6 h settling period. The difference between the biomass at T_0 and T_6 was usually within analytical variability. Sinking velocities were calculated according to Bienfang (1981).

3.2.4 Laboratory analysis

Water samples from $Z_{50\%}$ and Z_{CFM} were directly collected from the rosette, filtered through pre-combusted (at 450°C for 5 h) Whatman GF/F filters, and the filtrate was frozen at -80°C in acid-cleaned polycarbonate cryogenic vials until subsequent analyses of nitrate plus nitrite ($NO_3^-+NO_2^-$), nitrite (NO_2^-), phosphate (PO_4^{3-}) and silicic acid ($Si(OH)_4$) using a Technicon II Autoanalyzer (Mitchell et al. 2002). Samples from the same depths were kept in an isothermal container to analyze exopolymeric substances (EPS) and POC. Triplicate water samples were filtered onto 0.4 μm Nuclepore membrane filters and stained with Alcian blue for EPS determination. EPS were measured spectrophotometrically at 787 nm after a 2 h extraction in 80% H_2SO_4 (Passow & Alldredge 1995). EPS concentrations (expressed as μg gum xanthan equivalents L^{-1}) were converted into carbon equivalents according to Engel (2004). POC was determined on duplicate subsamples filtered onto pre-combusted (at 450°C for 5 h) Whatman GF/F filters and dried at 60°C for 24 h prior to analysis on a Elemental Americas Vario MICRO CHN analyzer.

The following analyses were conducted at the beginning and at the end of each sedimentation experiment and on the top and bottom SetCol sections for $Z_{50\%}$ and Z_{CFM}. Duplicate subsamples were filtered onto Whatman GF/F filters for fluorometric determination of chlorophyll *a* (chl *a*) after a 24 h extraction in 90% acetone at 4°C in the dark (acidification method; Parsons et al. 1984). Chl *a* was determined on board the ship using a TD-700 Turner designs fluorometer calibrated using chl *a* extract from *Anacystis nidulans* (Sigma). Subsamples (100 mL) were preserved with acidic Lugol's solution (1%

final concentration; Parsons et al. 1984) for the identification and enumeration of protist cells with an inverted microscope (Leica DM IRB) according to Lund et al. (1958). A minimum of 400 cells and three transects were counted for each sample and the abundance of each taxon was computed according to the equation of Horner (2002). Average cell sizes were obtained by measuring 30 individual cells from the most abundant taxa and average cell biovolumes were estimated using appropriate geometric equations (Hillebrand et al. 1999). For the least abundant taxa, average cell sizes were obtained from the literature (Tomas 1997, Bérard-Therriault et al. 1999). Protist carbon biomass was estimated using the conversion factors of Menden-Deuer & Lessard (2000), except for ciliates for which we used the specific conversion factor from Putt & Stoecker (1989). We distinguished 5 groups of protists: diatoms, flagellates, dinoflagellates, ciliates+choanoflagellates and *Dinobryon balticum* (Schütt) Lemmermann. Choanoflagellates are bacterivores and were, therefore, associated with ciliates to form a group of strictly heterotrophic protists. The chrysophyte *Dinobryon balticum* is shown separately from other flagellates because this species can form large colonies (McKenzie et al. 1995) which may have much higher sinking velocity compared to other flagellate species.

Bacterial abundance, size and nucleic acid content were determined by flow cytometry adapted from the protocol of Marie et al. (1997). Duplicate 4.95 mL subsamples were fixed with 50 µL of glutaraldehyde Grade I (1% final concentration; Sigma) in the dark at 4°C during 30 min, and then frozen at -80°C. Prior to analysis, subsamples were thawed at ambient temperature, with one of the duplicate kept for free-living bacteria

counts and the other for particle-attached bacteria counts. The recovery of particle-attached bacteria was performed by filtering a 5 mL sample through 5 μm Nuclepore membrane filter in order to retain large particles with attached bacteria. The filter was then washed with 1 mL of 0.2 μm filtered seawater. Logistic issues constrained us to filter samples after their frozen storage but this step is usually done before freezing (e.g. Garneau et al. 2006, Ghiglione et al. 2009). Further investigations will be done in summer 2010 to investigate the influence of the post-freezing filtration and estimate the bias. To detach bacteria previous studies recommended the use of sodium pyrophosphate and sonification (Alldredge et al. 1986, Grossart & Ploug 2001). We thus tested different concentrations of sodium pyrophosphate and sonification times to efficiently detach bacteria without disrupting them, and verified the efficiency of detachment using epifluorescence microscopy. Optimum conditions were the addition of 1 mL of sodium pyrophosphate (0.002 M, Sigma) to our sample and a sonification time of 15 s (sonifier model W350, Branson Sonic Power Co.). This sonification procedure, tested for each sample, resulted in an average loss of 8.9% ± 4.2% of the total bacterial abundance. Therefore bacterial numbers for particle-attached bacteria should be considered slight underestimates. For both free-living and particle-attached bacteria samples, 500 μL were pipetted and stained with 0.5 μL of SYBR-Green I (0.1% final concentration; Molecular Probes Inc; Marie et al. 1997) for 15 min in the dark at 80°C to optimize the staining (Marie et al. 1999). The staining was performed in TE buffer (10 mM Tris, 1 mM EDTA; Sigma) to dilute the sample and avoid coincidence of several particles in the laser beam, to minimize the error due to low-volume pipetting, and to maintain an optimum pH for the staining with SYBR-

Green I (Belzile et al. 2008). After cooling to ambient temperature, subsamples were analyzed with a FACSort flow cytometer (Becton & Dickinson, San Jose, CA) equipped with an air-cooled argon laser providing 15 mW and with a standard filter setup. Excitation wavelength was at 488 nm to be as close as possible to the optimum excitation wavelength of the SYBR-Green I in the visible region (495 nm; Marie et al. 1997). Each sample was run four times at a delivery rate of 8.21 $\mu L\ min^{-1}$ during 1 min for bacteria counts and discrimination according to their size and nucleic acid content. Coefficients of variation for replicate bacterial counts were 3.2% on average (range: 0.6—12%) and coefficients of variation for duplicate samples were 2.2% on average (range: 0.02—10%). Bacterial counts from flow cytometry were systematically compared with counts using epifluorescence microscopy after staining with DAPI (4,6-diamidino-2-phenylindole) (Velji & Albright 1993). The linear regression of bacterial counts obtained from the two methods was highly significant ($r^2 = 0.79$, $n = 63$) and the regression slope was not significantly different from one ($y = 0.87x + 0.03$, $p < 0001$).

Light scattering index (SSC: side angle light scatter) was used as a proxy for bacterial size (Troussellier et al. 1999) and the green fluorescence (FL1: 530 ± 15 nm), which is proportional to the nucleic acids–SYBR I complex, as a proxy for nucleic acid content (Marie et al. 1997). Cytograms SSC *versus* FL1 were used to define windows to discriminate bacterial cells with high (HNA) and low (LNA) nucleic acid content (Lebaron et al. 2001), as evidenced from their fluorescence intensities. The relative distance between the two groups on the cytograms was estimated as the ratio of FL1 HNA:FL1 LNA. Each

cytogram was visually inspected and the counting region was manually moved and shaped to fit the area of bacterial dot-plot. Data were computed with the CELLQUEST PRO software (Becton & Dickinson). Yellow-green fluorescent microspheres of 0.5 μm diameter (Polysciences Inc., Warrington, PA) were added to each sample as a reference to estimate the average size of each type of bacteria (i.e. HNA, LNA, free-living and particle-attached).

3.2.5 Bacterial biomass and respiration estimates

The average bacterial biovolume was calculated from the bacterial size estimated from average SSC proxy of each sample and considering each bacterium as a sphere. Different approaches can be found in the literature to estimate bacterial carbon biomass such as constant biomass models, constant biovolume to biomass models or allometric models and a wide range of relationships exist; some of them are summarized in Posch et al. (2001). Therefore, we compared results obtained with three different models specific to each type of bacteria (i.e. free-living *versus* particle-attached). For free-living bacteria, we used a constant conversion factor of 20 fg C $cell^{-1}$ and a biovolume to biomass ratio of 380 fg C μm^{-3} (Lee & Fuhrman 1987), and the following allometric model from Loferer-Krößbacher et al. (1998) and recommended by Posch et al. (2001):

$$BB = 218 \times V^{0.86}$$

where BB is the bacterial biomass (fg C $cell^{-1}$) and V is the volume of the bacterium (μm^{-3}). For particle-attached bacteria, we used a constant conversion factor of 50 fg C $cell^{-1}$ (Simon et al. 1990), a biovolume to biomass ratio of 120 fg C μm^{-3} (Fuhrman & Azam 1980), and

the same allometric model as above. To estimate bacterial production we used a specific growth rate of 0.204 d^{-1} as reported by Middelboe et al. (2002) for surface waters of the North Water and a specific mortality rate of 28% of bacterial production corresponding to the average values measured by Steward et al. (1996) in the upper 50 m of the Bering and Chukchi seas. Bacterial respiration rates were estimated from bacterial production using the following relationship for both types of bacteria (i.e. free-living and particle-attached) (Robinson 2008):

$$BR = 3.69 \times BP^{0.58}$$

where BR is the bacterial respiration rate (mg C m^{-3} d^{-1}) and BP the bacterial production rate (mg C m^{-3} d^{-1}).

3.2.6 Statistical analysis

The normality and homogeneity of variances were checked by Kolmogorov-Smirnov and Levene's tests, respectively (Sokal & Rohlf 1981). As most of our data were not normally distributed, we used rank-transformation before analysis. Three-way ANOVAs were performed using sampling year (2005 and 2006), type of bacteria (i.e. free-living and particle-attached) and sampling depth ($Z_{50\%}$ and Z_{CFM}) as factors (Conover & Iman 1981). The ANOVAs were followed by a post-hoc multiple comparison of means (Tukey's Honestly Significant Difference test for unequal sample size) (Legendre & Legendre 1998). Statistical differences between the three models used to estimate bacterial biomass were determined using a Friedman repeated measures analysis of variance on

ranks followed by pairwise multiple comparison procedures (Tukey test) (Sokal & Rohlf 1981). Statistical differences between two means were determined using two-tailed Student's *t*-tests. Correlations between variables were assessed using Spearman rank order correlation tests (Sokal & Rohlf 1981). For bacterial biomass, production and respiration, the mean of the values obtained using the three models was used to calculate correlations with other variables. Significant differences were established at 0.05 levels. Computations were carried out using the STATISTICA 7 software (StatSoft).

3.3 Results

3.3.1 Physical and biochemical conditions

Physical, chemical and biological variables at $Z_{50\%}$ and Z_{CFM} in 2005 and 2006 are shown in Table 1. For both depths, significantly lower NO_3^-, PO_4^{3-} and POC concentrations, and POC:chl *a* ratios were observed in 2005 compared to 2006 (ANOVAs, $p < 0.05$). EPS concentrations were significantly higher in 2005 compared to 2006 (ANOVA, $p < 0.05$). There were no significant differences between 2005 and 2006 for the other variables (ANOVAs, $p > 0.05$). During both years, average water temperature was significantly higher, while average salinity, NO_3^- concentration and chl *a* biomass were significantly lower at $Z_{50\%}$ than at Z_{CFM} (ANOVAs, $p < 0.05$). The average POC:chl *a* ratio was significantly higher at $Z_{50\%}$ than at Z_{CFM} in 2005, the average PO_4^{3-} and POC concentrations were significantly lower at $Z_{50\%}$ than at Z_{CFM} in 2005, and the average

$Si(OH)_4$ and EPS concentrations were significantly lower at $Z_{50\%}$ than at Z_{CFM} in 2006 (ANOVAs, $p < 0.05$). No significant differences between $Z_{50\%}$ and Z_{CFM} were observed for the other variables (ANOVAs, $p > 0.05$).

Table 1. Average and, in parentheses, range of physical, chemical and biological variables recorded at depths of 50% surface irradiance ($Z_{50\%}$) and chlorophyll fluorescence maximum (Z_{CFM}) in the Hudson Bay system during late summers 2005 and 2006.

	2005		2006	
	$Z_{50\%}$	Z_{CFM}	$Z_{50\%}$	Z_{CFM}
Depth (m)	6.68 (5.00 – 11.3)	35.9 (20.0 – 44.8)♣	7.26 (3.90 – 10.6)	41.2 (22.0 – 59.0)♣
Temperature (°C)	5.86 (2.13 – 11.0)♣	0.27 (-1.64 – 4.19)	5.11 (-0.23 – 8.67)♣	0.48 (-1.43 – 3.89)
Salinity	30.2 (26.7 – 32.8)	32.0 (29.5 – 32.9)♣	31.4 (29.4 – 32.8)	32.2 (30.4 – 33.5)♣
NO_3^- (μmol L^{-1})	0.24 (0.14 – 0.73)	1.24 (0.16 – 4.35)♣	1.02 (0.44 – 4.26)*	3.86 (0.42 – 11.5)♣*
PO_4^{3-} (μmol L^{-1})	0.45 (0.38 – 0.56)	0.67 (0.39 –1.11)♣	0.99 (0.45 – 1.77)*	1.11 (0.51 – 1.59)*
$Si(OH)_4$ (μmol L^{-1})	1.67 (0.27 – 3.13)	2.22 (0.68 – 5.60)	1.21 (0.25 – 4.10)	5.00 (0.37 –14.7)♣
Chl *a* (μg L^{-1})	0.74 (0.12 – 2.44)	2.21 (0.25 – 5.17)♣	0.89 (0.11 – 3.23)	1.89 (0.29 – 3.90)♣
POC (μg C L^{-1})	238 (141 – 347)	302 (191 – 485)♣	516 (386 – 628)*	548 (432 – 663)*
POC:chl *a* (g:g)	673 (142 – 1497)♣	269 (65.9 – 1172)	1400 (194 – 3415)*	513 (116 –1964)*
Protist (10^6 cells L^{-1})	0.30 (0.12 – 0.49)	1.01 (0.10 – 3.84)	0.41 (0.10 – 0.98)	0.49 (0.13 – 1.11)
Protist C (μg C L^{-1})	66.9 (27.6 – 144)	123 (30.8 – 405)	116 (16.0 – 351)	146 (14.8 – 543)
EPS (μg C L^{-1})	78.7 (45.0 – 123)*	77.7 (17.5 – 143)*	31.0 (6.85 – 67.2)	47.5 (26.1 – 73.4)♣

NO_3^-: nitrate; PO_4^{3-}: phosphate; $Si(OH)_4$: silicic acid; Chl *a*: chlorophyll *a*; POC: particulate organic carbon; EPS: exopolymeric substance.
*: indicates significantly higher value at same depth between 2005 and 2006; ♣: indicates significantly higher value between $Z_{50\%}$ and Z_{CFM} within the same year.

The relative abundance of different protist groups is presented in Fig. 2. For both sampling years, the protist community was mainly composed of diatoms (0.001–2.32×10^6 cells L^{-1}) and flagellates (0.05–0.64×10^6 cells L^{-1}), except at $Z_{50\%}$ stations 3 in

2005 and 4 in 2006 where diatom abundance was null. Dinoflagellates (0.007–0.06 × 10^6 cells L^{-1}) and ciliates+choanoflagellates (0–0.04 × 10^6 cells L^{-1}) were minor contributors to the total protist abundance. *Dinobryon balticum* were found in low abundance throughout the system except at station 5 where this species reached 1.11 × 10^6 cells L^{-1} in 2005 during the maximum protist abundance (3.84 × 10^6 cells L^{-1}). Diatom abundance was lower at $Z_{50\%}$ than at Z_{CFM} (average 0.14 × 10^6 *versus* 0.44 × 10^6 cells L^{-1}) in 2005 and ciliate+choanoflagellate abundance was lower in 2005 compared to 2006 for both sampling depths, with an average of 0.008 × 10^6 *versus* 0.017 × 10^6 cells L^{-1} at $Z_{50\%}$ and 0.005 × 10^6 *versus* 0.016 × 10^6 cells L^{-1} at Z_{CFM}, respectively (ANOVAs, $p < 0.05$).

3.3.2 Abundance of free-living and particle-attached bacteria

The abundance of free-living bacteria ranged from 0.63 × 10^9 to 2.32 × 10^9 cells L^{-1} (average 1.42 × 10^9 cells L^{-1}) in 2005 and from 0.82 × 10^9 to 2.18 × 10^9 cells L^{-1} (average 1.23 × 10^9 cells L^{-1}) in 2006 (Fig. 3). The abundance of particle-attached bacteria ranged from 0.24 × 10^6 to 27.0 × 10^6 cells L^{-1} (average 7.40 × 10^6 cells L^{-1}) in 2005 and from 1.50 × 10^6 to 32.9 × 10^6 cells L^{-1} (average 18.1 × 10^6 cells L^{-1}) in 2006 (Fig. 4). There was no significant difference in free-living bacteria abundance between sampling years; however, particle-attached bacteria were significantly less abundant in 2005 than in 2006

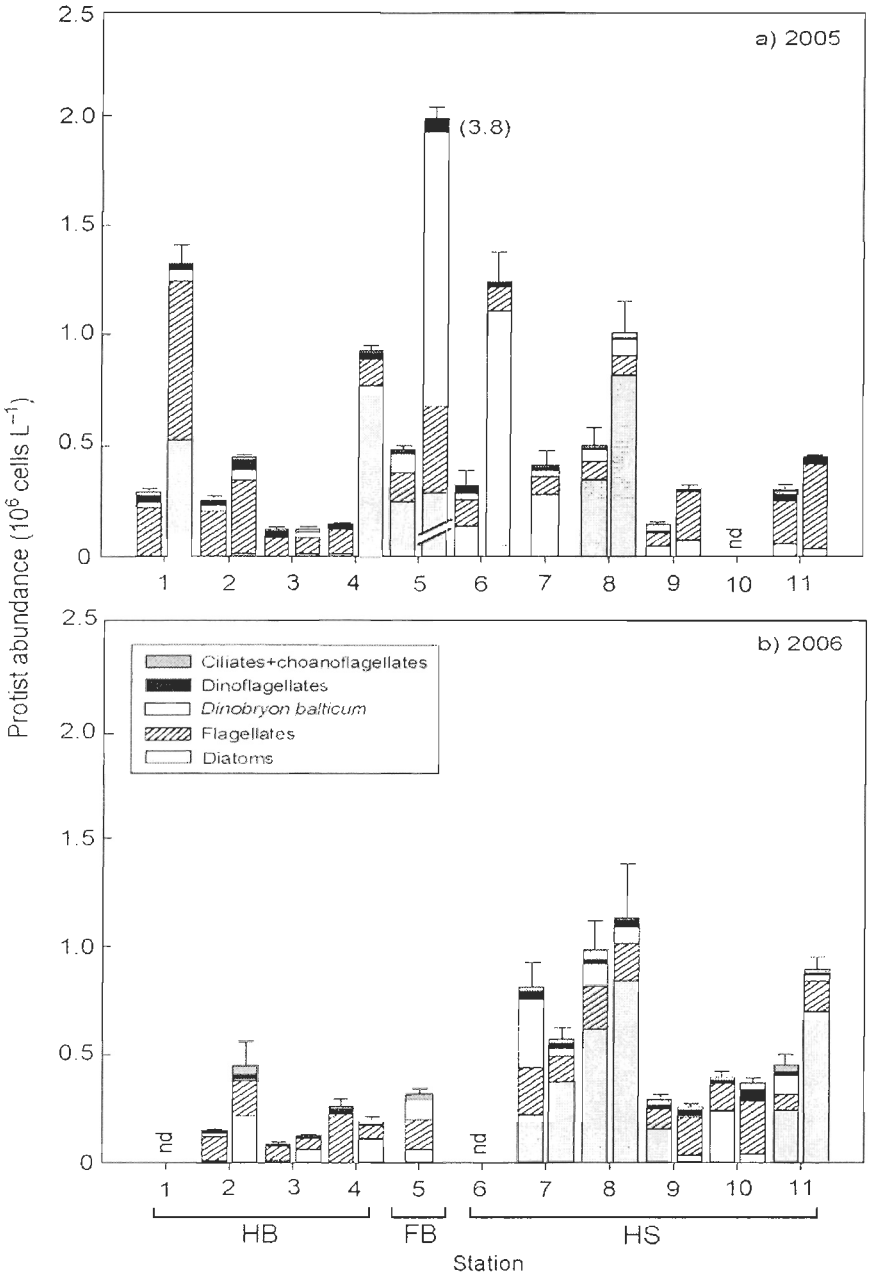

Fig. 2. Abundance of the different protist groups observed at 50% surface irradiance (left bar) and chlorophyll fluorescence maximum (right bar) in the Hudson Bay system during late summers (a) 2005 and (b) 2006. At station 5 in 2005, diatom abundance was 2.3×10^6 cells L^{-1} and total protist abundance was 3.8×10^6 cells L^{-1} at the chlorophyll fluorescence maximum. Error bars represent SD on the estimated total cell abundance. HB: Hudson Bay; FB: Foxe Basin; HS: Hudson Strait. nd: no data.

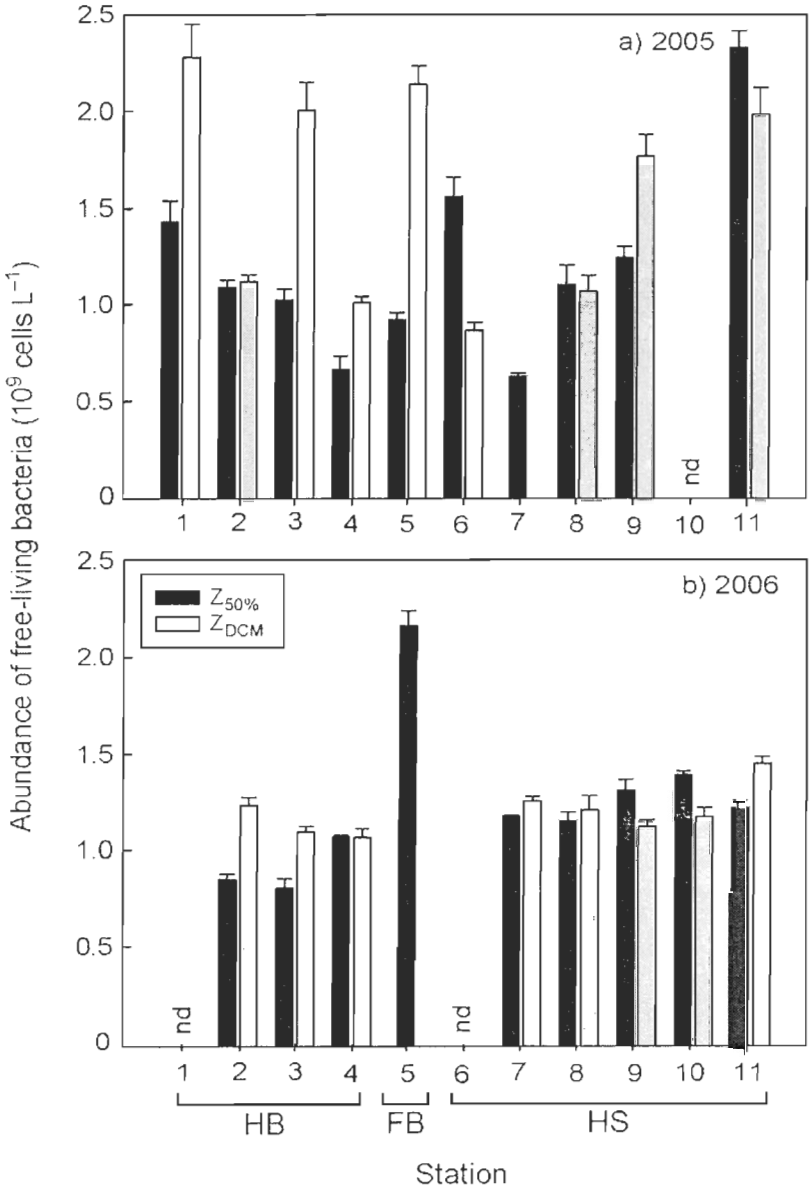

Fig. 3. Abundance of the free-living bacteria observed at depths of 50% surface irradiance ($Z_{50\%}$) and chlorophyll fluorescence maximum (Z_{CFM}) in the Hudson Bay system during late summers (a) 2005 and (b) 2006. At stations 7 in 2005 and 5 in 2006, Z_{CFM} was at the same depth as $Z_{50\%}$. Error bars represent SD calculated from duplicate samples or replicate counts when duplicates were not available. HB: Hudson Bay; FB: Foxe Basin; HS: Hudson Strait. nd: no data.

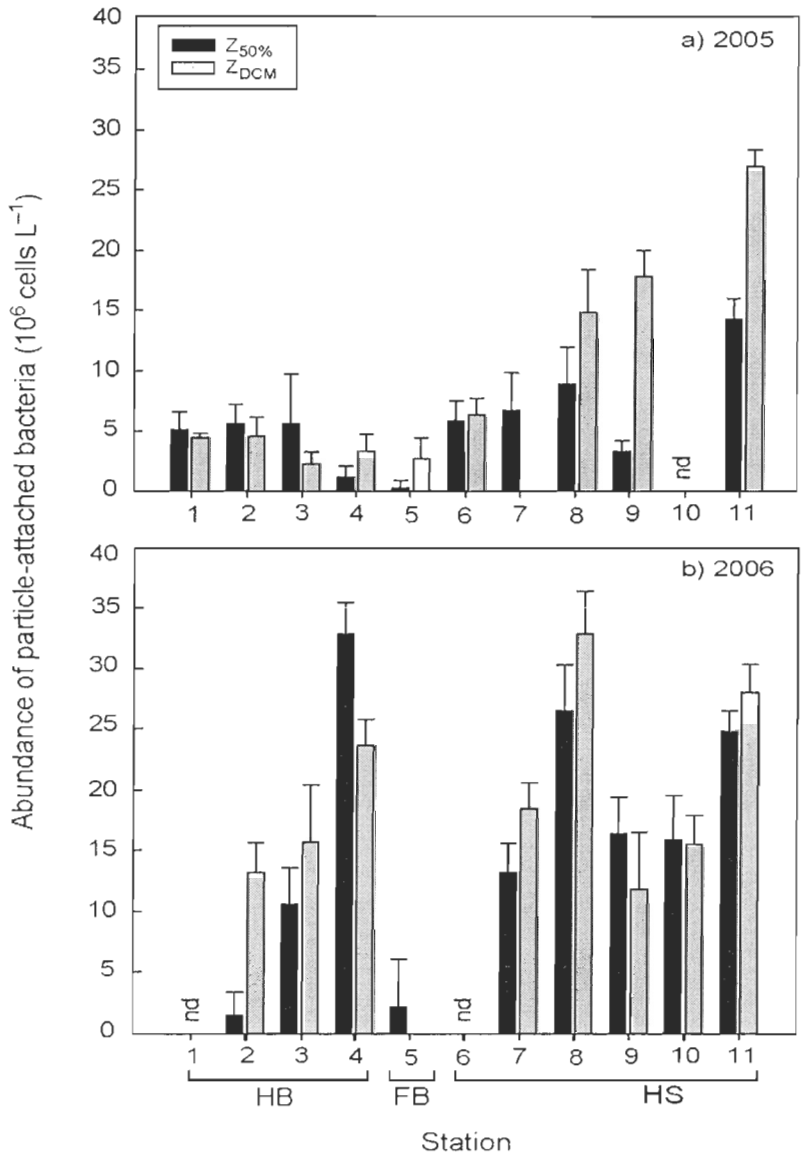

Fig. 4. Abundance of the particle-attached bacteria observed at depths of 50% surface irradiance ($Z_{50\%}$) and chlorophyll fluorescence maximum (Z_{CFM}) in the Hudson Bay system during late summers (a) 2005 and (b) 2006. At stations 7 in 2005 and 5 in 2006, Z_{CFM} was at the same depth as $Z_{50\%}$. Error bars represent SD calculated from duplicate samples or replicate counts when duplicates were not available. HB: Hudson Bay; FB: Foxe Basin; HS: Hudson Strait. nd: no data.

(ANOVAs, $p < 0.05$). There was no depth-related difference in free-living or particle-attached bacteria abundance during both years (ANOVAs, $p > 0.05$).

3.3.3 HNA and LNA bacteria

FL1 *versus* SSC plots (Fig. 5) clearly highlight the distinction between HNA and LNA bacteria during both years. Range and average SSC and FL1 values for HNA and LNA bacteria for free-living and particle-attached bacteria are shown in Table 2. HNA and LNA bacterial abundance, contribution of HNA bacteria to total bacterial abundance and FL1 HNA: FL1 LNA ratio for both bacterial forms are also shown in Table 2. As there was no significant difference between the $Z_{50\%}$ and the Z_{CFM} for all values for either bacterial form or year (ANOVAs, $p > 0.05$), it is average values from $Z_{50\%}$ and Z_{CFM} that are shown in Table 2. Regardless of sampling year, particle-attached HNA bacteria had significantly higher SSC than LNA bacteria (ANOVA, $p < 0.05$). In addition, particle-attached bacteria, either HNA or LNA had significantly higher SSC than free-living HNA and LNA bacteria (ANOVA, $p < 0.05$). Particle-attached HNA bacteria had significantly higher FL1 than free-living HNA bacteria, whereas particle-attached LNA bacteria had significantly lower FL1 than free-living LNA bacteria (ANOVAs, $p < 0.05$).

HNA and LNA free-living bacteria had significantly lower SSC in 2005 compared to 2006 (Fig. 5; Table 2) while their FL1 were not significantly different (ANOVAs, $p > 0.05$). For particle-attached bacteria, HNA bacteria had significantly higher SSC in

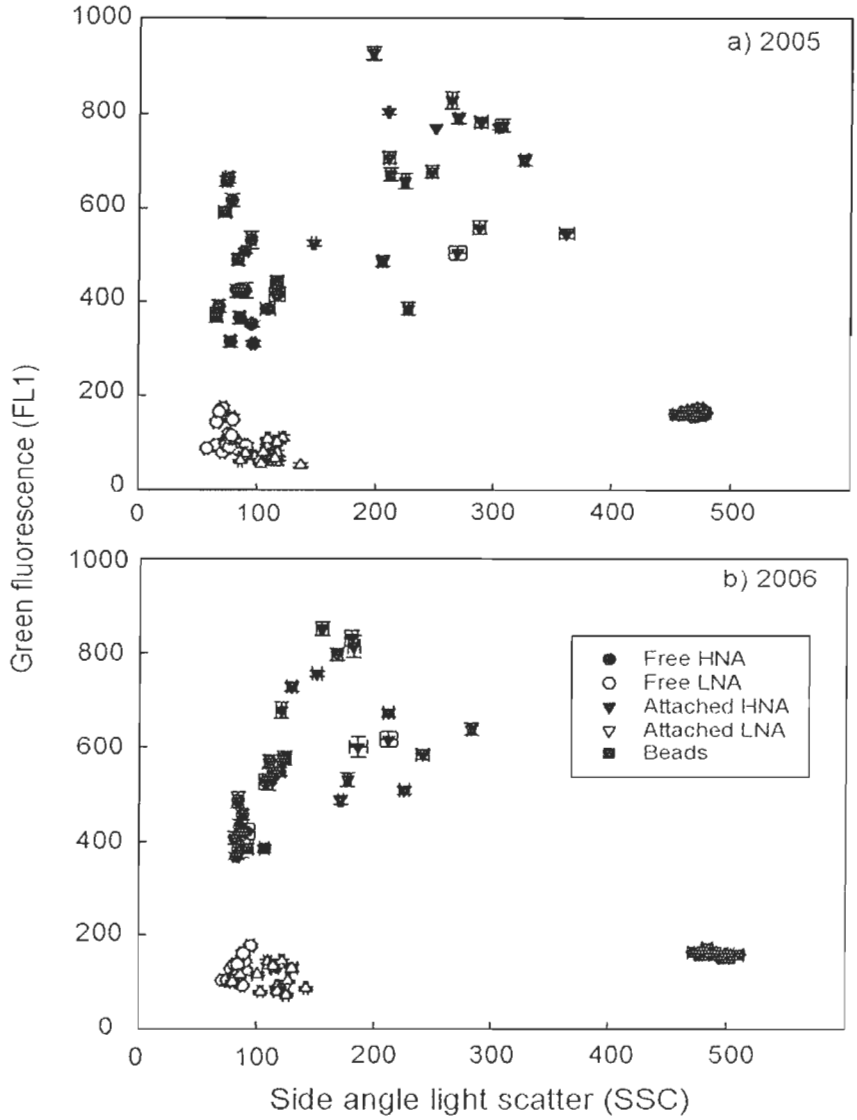

Fig. 5. Green fluorescence (FL1) *versus* side angle light scatter (SSC) for high nucleic acid (HNA) and low nucleic acid (LNA) bacteria for the free-living and particle-attached forms in the Hudson Bay system during late summers (a) 2005 and (b) 2006. Black squares represent fluorescent beads. Each data point represents the average FL1 and SSC measured for one sample. Error bars represent SD calculated from duplicate samples or replicate counts when duplicates were not available. Some SD are not visible because they are smaller than the size of the symbol.

2005 compared to 2006 but their FL1 were not significantly different (ANOVAs, $p > 0.05$). In contrast, there was no significant difference in the SSC of particle-attached LNA bacteria during both years but particle-attached LNA bacteria FL1 were significantly lower in 2005 than in 2006 (ANOVAs, $p < 0.05$).

Table 2. Average and, in parentheses, range of high nucleic acid (HNA) and low nucleic acid (LNA) bacterial size proxy (SSC), green fluorescence (FL1), abundance, contribution of HNA bacteria to total bacterial abundance and FL1 HNA to FL1 LNA ratio for free-living and particle-attached bacteria in the Hudson Bay system during late summers 2005 and 2006.

	2005		2006	
	Free-living	Particle-attached	Free-living	Particle-attached
HNA SSC	86.4 (64.9 – 116)	253 (147 – 361)*	98.6 (81.4 – 123)*	186 (120 – 283)
LNA SSC	74.5 (57.5 – 90.7)	110 (85.9 – 137)	83.6 (71.1 – 95.2)*	115 (80 – 142)
HNA FL1	455 (311 – 661)	675 (384 – 925)	468 (368 – 577)	673 (487 – 851)
LNA FL1	117 (82.0 – 174)	81.1 (54.9 – 112)	130 (93.6 – 178)	108 (73.6 – 146)*
HNA abundance (10^6 cells L^{-1})	928 (254 – 1590)	3.63 (0.85 – 13.9)	801 (442 – 1120)	12.1 (5.36 – 24.0)*
LNA abundance (10^6 cells L^{-1})	454 (92.0 – 850)	5.28 (1.22 – 13.8)	456 (267 – 1040)	9.35 (4.75 – 16.3)*
HNA (%)	66.6 (43.2 – 78.7)	39.2 (15.5 – 61.7)	64.2 (51.4 – 75.4)	56.0 (39.2 – 83.5)*
FL1 HNA:FL1 LNA	3.84 (3.28 – 4.96)	8.34 (4.71 – 13.5)*	3.63 (3.23 – 4.18)	6.43 (2.84 – 9.66)

Values from 50% surface irradiance and chlorophyll fluorescence maximum depths were averaged.
*: indicates significantly higher value at same depth between 2005 and 2006

Free-living HNA bacteria were significantly more abundant than free-living LNA bacteria during both sampling years but particle-attached HNA and LNA were equally abundant (ANOVAs, $p > 0.05$) (Table 2). There was no significant difference in the average abundance of free-living HNA and LNA bacteria during both years but the average abundance of particle-attached HNA and LNA bacteria was significantly lower in 2005 than in 2006 (ANOVAs, $p < 0.05$). HNA and LNA abundance was not significantly

different between the $Z_{50\%}$ and the Z_{CFM} whatever the type of bacteria was (ANOVAs, $p > 0.05$). The contribution of HNA bacteria to total abundance was significantly higher for free-living bacteria than for particle-attached bacteria in both years (ANOVAs, $p < 0.05$). The contribution of free-living HNA was similar in 2005 and 2006, but the attached HNA bacteria contributed more to total abundance in 2006 than in 2005 (ANOVAs, $p < 0.05$). The average FL1 HNA:FL1 LNA ratio was significantly lower for free-living bacteria than for particle-attached bacteria for both years (ANOVAs, $p < 0.05$).

3.3.4 Bacteria, chl *a* and protist cell sinking velocities

Table 3. Average and, in parentheses, range of sinking velocities (m d^{-1}) of free-living and particle-attached bacteria, chlorophyll *a* (chl *a*) biomass and different protist groups estimated at depths of 50% surface irradiance ($Z_{50\%}$) and chlorophyll fluorescence maximum (Z_{CFM}) in the Hudson Bay system during late summers 2005 and 2006.

	2005		2006	
	$Z_{50\%}$	Z_{CFM}	$Z_{50\%}$	Z_{CFM}
Free bacteria	0.02 (0.01 – 0.05)	0.01 (0.00 – 0.03)	0.01 (0.00 – 0.03)	0.01 (0.00 – 0.01)
Attached bacteria	0.14 (0.02 – 0.30)	0.23 (0.03 – 0.53)	0.20 (0.03 – 0.76)	0.15 (0.01 – 0.43)
Chl *a* biomass	0.25 (0.01 – 0.58)	0.12 (0.01 – 0.23)	0.26 (0.07 – 0.75)	0.15 (0.02 – 0.22)
Diatoms	0.38 (0.15 – 1.20)♣	0.17 (0.03 –0.35)	0.33 (0.01 – 1.06)♣	0.08 (0.01 – 0.22)
Dinoflagellates	0.22 (0.02 – 0.65)	0.16 (0.02 – 0.31)	0.17 (0.02 – 0.57)	0.10 (0.00 –0.25)
D. balticum	1.49 (0.13 – 6.02)♣	0.61 (0.12 – 1.49)	2.95 (0.11 – 8.26)♣	0.69 (0.21 – 2.11)
Flagellates	0.28 (0.05 – 0.73)	0.41 (0.01 – 1.07)	0.23 (0.03 – 0.59)	0.09 (0.01 – 0.19)
Ciliates+Choano.	0.63 (0.13 – 2.36)♣	0.33 (0.02 – 0.92)	0.89 (0.06 – 3.57)♣	0.24 (0.00 – 0.70)

♣: indicates significantly higher value between $Z_{50\%}$ and Z_{CFM} within a same year

The sinking velocities of free-living bacteria were significantly lower than those of particle-attached bacteria (ANOVA, $p < 0.05$) (Table 3). The sinking velocities of particle-attached bacteria were not significantly different than for the chl *a* biomass and abundances of diatoms, dinoflagellates and flagellates (ANOVAs, $p > 0.05$). *Dinobryon balticum* and ciliates+choanoflagellates had significantly higher sinking velocities than the other groups of protists and bacteria (ANOVAs, $p < 0.05$). There was no significant difference in the sinking velocities of bacteria, chl *a* biomass and different protist group abundance between 2005 and 2006 (ANOVAs, $p > 0.05$). The sinking velocities of diatoms, *D. balticum* and ciliates+choanoflagellates were significantly higher at the $Z_{50\%}$ than at the Z_{CFM} (ANOVAs, $p < 0.05$).

3.3.5 Biomass and respiration rate

Table 4 presents a summary of the bacterial carbon biomass, contribution to suspended POC and estimated bacterial production and respiration rates for free-living and particle-attached bacteria from the three models used. For free-living bacteria, the biomass estimate using the biovolume to biomass ratio model was significantly higher than the two other biomass estimates (Friedman repeated measures analysis of variance on ranks, $p < 0.05$). Consequently, for free-living bacteria, production and respiration rates estimated from the biovolume to biomass ratio model were significantly higher than the other estimates. For particle-attached bacteria, the biomass estimate using the allometric model was significantly higher than the two other biomass estimates (Friedman repeated measures analysis of variance on ranks, $p < 0.05$). Consequently, for attached bacteria, production

and respiration rates estimated from the allometric model biomass were significantly higher than the other estimates. The average biomass of free-living bacteria and their contribution to POC were significantly higher than for particle-attached bacteria during both years (ANOVAs, $p < 0.05$). Similarly, respiration rates of free-living bacteria were significantly higher than those of particle-attached bacteria in both years (ANOVAs, $p < 0.05$). There were no significant differences in free-living and particle-attached bacterial biomasses, contributions to POC and respiration rates between the $Z_{50\%}$ and the Z_{CFM} in either year (ANOVAs, $p > 0.05$).

Table 4. Average and, in parentheses, range of carbon biomass, production and respiration rates estimated using three different models, for free-living and particle-attached bacteria in the upper 50 m of the water column, in the Hudson Bay system during late summers 2005 and 2006. Bacterial contribution to total suspended particulate organic carbon (POC) was calculated using the mean of the three estimates for each type of bacteria.

	2005		2006	
	Free-living	Particle-attached	Free-living	Particle-attached
Biomass ($\mu g\ C\ L^{-1}$)				
Constant conversion factor	26.9 (12.6 – 43.3)	0.37 (0.01 – 1.33)	24.1 (14.1 – 41.7)	0.95 (0.54 – 1.44)*
Biovolume to biomass ratio	39.9 (13.6 – 112)	0.83 (0.02 – 4.57)	46.8 (18.6 – 86.5)	1.20 (0.30 – 2.84)*
Allometric model	32.4 (11.8 – 83.9)	1.50 (0.04 – 7.89)	36.7 (15.5 – 64.4)	2.34 (0.71 – 4.96)*
Average contribution to POC (%)	13.4 (4.57– 31.7)*	0.36 (0.01 – 1.59)	6.76 (4.07 – 13.2)	0.29 (0.10 – 0.66)
Production				
Constant conversion factor	3.96 (1.85 – 6.36)	0.05 (0.00 – 0.20)	3.54 (2.07 – 6.12)	0.14 (0.08 – 0.21)*
Biovolume to biomass ratio	5.86 (2.00 – 16.4)	0.12 (0.00 – 0.67)	6.87 (2.73 – 12.7)	0.18 (0.04 – 0.42)*
Allometric model	4.75 (1.73 – 12.3)	0.22 (0.01 – 1.16)	5.38 (2.27 – 9.45)	0.34 (0.10 – 0.73)*
Respiration rate ($\mu g\ C\ L^{-1}\ d^{-1}$)				
Constant conversion factor	8.06 (5.27 – 10.8)	0.64 (0.09 – 1.43)	7.63 (5.62 – 10.6)	1.17 (0.84 – 1.50)*
Biovolume to biomass ratio	9.92 (5.51 – 18.7)	0.95 (0.14 – 2.93)	11.0 (6.61 – 16.1)	1.29 (0.61 – 2.22)*
Allometric model	8.84 (5.06 – 15.8)	1.36 (0.20 – 4.02)	9.60 (5.94 – 13.6)	1.92 (0.99 – 3.07)*

Values from 50% surface irradiance and chlorophyll fluorescence maximum depths were averaged.
*: indicates significantly higher value at same depth between 2005 and 2006.

3.3.6 Influence of environmental and biological conditions on bacterial communities

Spearman rank correlation coefficients for relationships between biological and environmental variables and for relationships between free-living and particle-attached bacteria, and protist characteristics are presented in Tables 5 and 6, respectively. In contrast to free-living bacteria, the abundance and carbon biomass of particle-attached bacteria were positively correlated with NO_3^-, POC and chl *a* concentrations and their sinking velocity were positively correlated with diatom abundance and EPS concentration.

Table 5. Spearman rank correlation coefficients between environmental factors and free-living bacteria, particle-attached bacteria and protist characteristics. Significant correlations ($p < 0.05$) are presented in bold character.

	NO_3^-	$Si(OH)_4$	PO_4^{3-}	POC	POC:chl *a*	Protist C:POC	EPS
Free-living bacteria							
Abundance	0.16	-0.06	0.08	0.08	-0.26	0.11	0.23
SSC	0.31	0.23	0.26	0.33	-0.11	0.24	-0.03
FL1	0.25	-0.20	0.07	0.09	**-0.56**	**0.40**	0.28
Biomass	0.27	0.09	0.15	0.19	-0.30	0.25	0.19
SV	-0.12	-0.03	-0.28	-0.24	-0.13	**0.43**	0.14
Particle-attached bacteria							
Abundance	**0.41**	0.00	0.32	**0.50**	-0.22	0.12	-0.25
SSC	-0.01	0.18	-0.17	-0.31	-0.14	-0.20	0.34
FL1	0.13	-0.07	0.06	0.21	-0.06	0.15	0.00
Biomass	**0.53**	-0.03	0.31	**0.53**	-0.29	-0.13	-0.25
SV	0.01	-0.02	0.05	0.05	-0.32	0.20	**0.36**
Protists							
Total abundance	0.09	-0.10	0.00	**0.34**	**-0.68**	**0.72**	0.33
Chl *a* biomass	0.28	-0.11	0.15	**0.36**	**-0.92**	**0.55**	0.33
Diatom abund.	0.15	-0.14	0.09	0.30	**-0.72**	**0.69**	**0.39**

NO_3^-: nitrate; PO_4^{3-}: phosphate; $Si(OH)_4$: silicic acid; POC: particulate organic carbon; Chl *a*: chlorophyll *a* biomass; EPS: exopolymeric substance; SSC: side angle light scatter; FL1: green fluorescence; SV: sinking velocity.

Table 6. Spearman rank correlation coefficients between free-living bacteria, particle-attached bacteria and protist characteristics. Significant correlations ($p < 0.05$) are presented in bold character.

	Free-living bacteria					Particle-attached bacteria				
	Abund	SSC	FL1	Biomass	SV	Abund.	SSC	FL1	Biomass	SV
Free-living bacteria										
Abundance										
SSC	0.06									
FL1	0.23	0.14								
Biomass	**0.83**	**0.55**	0.24							
SV	-0.32	0.16	0.30	-0.14						
Particle-attached bacteria										
Abundance	0.15	**0.55**	**0.50**	**0.42**	0.08					
SSC	0.24	-0.19	-0.04	0.10	-0.13	-0.10				
FL1	**0.48**	0.33	**0.46**	**0.54**	-0.06	**0.56**	0.07			
Biomass	0.31	**0.37**	**0.34**	**0.45**	-0.18	**0.84**	0.26	**0.45**		
SV	0.28	0.06	0.25	0.30	0.06	0.04	0.07	0.08	0.09	
Protists										
Total abundance	0.22	0.20	**0.42**	0.31	0.21	0.26	-0.16	0.17	0.18	0.28
Chl *a* biomass	0.23	0.22	**0.53**	0.31	0.07	**0.36**	0.00	0.11	**0.42**	0.30
Diatom abund.	0.10	0.14	**0.51**	0.19	0.26	0.21	-0.18	0.09	0.16	**0.37**

SSC: side angle light scatter; FL1: green fluorescence; SV: sinking velocity.

3.4 Discussion

3.4.1 Abundance and biomass of free-living and particle-attached bacteria

The abundance of free-living bacteria in the upper 50 m of the water column of the Hudson Bay system in late summer ranged from 0.10×10^9 to 2.18×10^9 cells L^{-1} (Fig. 3) and is comparable to values reported for other polar seas such as the northern Baffin Bay in early summer ($0.42–1.38 \times 10^9$ cells L^{-1}), the Bering and Chukchi seas in late summer

(0.21–2.10 × 10^9 cells L^{-1}) and the Barents Sea in summer (0.41–4.10 × 10^9 cells L^{-1}) (see Table 7 and references therein). The contribution of particle-attached bacteria was < 3% of the total bacterial abundance and < 10% (often ≤ 5%) of the total suspended bacterial carbon biomass during both years in the Hudson Bay system (Figs. 3 and 4; Table 4). The abundances of particle-attached bacteria in Hudson Bay are in agreement with early findings that particle-attached bacteria often contributed < 5% of total bacteria abundance in many oligotrophic and mesotrophic marine environments (e.g. Alldredge et al. 1986, Cho & Azam 1988). However, the contribution of particle-attached bacteria to total bacterial abundance can be much higher in estuarine systems where percent abundances reaching up to 96% (see Table 7 and references therein) are typically associated with high particle loads from river runoff and decreases from river plume to offshore waters (Crump et al. 1998, Vallières et al. 2008). It is important to note that the studies reporting particle-attached bacterial abundance cited in Table 7 used filters of similar porosity (often 3 μm) than in this study to discriminate particle-attached bacteria from free-living bacteria, hence taking into account the contribution of small particles for bacterial attachment. Clearly, these results did not corroborate our first hypothesis that particle-attached bacteria dominate the total bacterial abundance in the Hudson Bay system. This aspect is discussed in more details in the next paragraph.

Table 7. Average and, in parentheses, range (when available) of free-living and particle-attached bacterial abundance, particle-attached bacterial contribution to total bacterial abundance and particulate organic carbon (POC) concentrations in the upper water column (i.e. < 50 m) of polar environments and estuaries. nd: no data.

Location	Period	Free bacteria (10^9 cells L^{-1})	Attached bacteria (10^9 cells L^{-1})	Attached bacteria (%)	POC ($\mu g\ L^{-1}$)	Reference
Polar environments						
Hudson Bay system	Aug-Sept	1.31 (0.10 – 2.18)	0.01 (0.002 – 0.03)	0.98 (0.03 – 2.95)	390 (141 – 663)	This study
Bering & Chukchi seas	Aug-Sept	(0.21 – 2.10)	nd	nd	nd	Steward et al. 1996
Northern Baffin Bay	June-July	0.76 (0.42 – 1.38)	nd	nd	299 (150 – 390)	Middelboe et al. 2002 Miller et al. 2002
Barents Sea	May-Aug	0.36	nd	nd	250	Reigstad et al. 2008 Sturluson et al. 2008
	June-July	(0.41 – 4.10)	nd	nd	nd	Howard-Jones et al. 2002
Laptev Sea	Sept	0.37 (0.13 – 0.82)	nd	nd	40 (10 – 100)	Kellogg & Deming 2009
Central Arctic Ocean	June-Sept	0.32 (0.19 – 0.67)	nd	nd	nd	Sherr et al. 2003
	Nov-May	0.18 (0.13 – 0.29)	nd	nd	nd	
Estuaries						
Columbia River	May	1.25 (0.61 – 2.42)	1.02 (<0.002 – 5.10)	< 0.16 – 75	nd	Crump et al. 1998
Fraser River	All year	6.89 (0.95 – 13.0)	1.17 (0.37 – 2.90)	69 (44 – 96)	1410 (1180 – 1750)	Bell & Albright 1981
St. Lawrence River	May-June	0.54 (0.27 – 1.06)	0.36 (0.11 – 0.75)	37 (26 – 45)	nd	Vincent et al. 1996
Mackenzie River	June-July	0.88 (0.57 – 1.38)	0.35 (0.16 – 0.76)	37 (22 – 63)	nd	Garneau et al. 2009
	July-Aug	0.67	nd	nd	50 – 400	Vallières et al. 2008
	Sept-Oct	0.52 (0.19 – 0.63)	nd	nd	nd	Garneau et al. 2006

3.4.2 Influence of environmental conditions or protist composition on bacterial communities

Estuarine studies referred to in Table 7 were mainly conducted in river plumes with a high particle load as opposed to most of the offshore stations visited during our study that were characterized by low suspended POC concentrations (average 390 μg C L^{-1}). For example, our results are much lower than those from the Fraser River estuary where particle-attached bacteria have been reported to contribute to up to 96% of total bacterial numbers and to 60% of the total suspended bacterial carbon biomass where an average suspended POC concentration of 1410 μg C L^{-1} was measured. The positive relationships observed between the abundance (or biomass) of particle-attached bacteria and POC or chl *a* concentrations during this study (Tables 5 and 6) are consistent with previous studies showing that the abundance (or biomass) of particle-attached bacteria is dependent on the number and/or size of particles available for attachment (Pedrós-Alió & Brock 1983, Cho & Azam 1988, Garneau et al. 2009). Yet, the abundance (or biomass) of particle-attached bacteria is also known to be related to the composition of the suspended material (Fandino et al. 2001, Wang & Yin 2009). This may not have been the case during our study as we did not observe any significant relationships between the POC:chl *a* ratio or protist contribution to suspended POC and the abundance or biomass of particle-attached bacteria (Table 5). Given our current coverage of the Hudson Bay system, we surmise that the low abundance of particles for bacterial colonization constrained the abundance and biomass of particle-attached bacteria in this pelagic system during late summer.

The abundance and biomass of particle-attached bacteria were also higher in waters where NO_3^- concentrations were high (Table 5). However the significant positive correlation observed between NO_3^- and POC concentrations ($r_s = 0.42$, $p < 0.05$; data not shown) suggests that NO_3^- was not directly used by particle-attached bacteria but that NO_3^- concentration would have influenced particle-attached bacteria indirectly through its effect on POC concentrations. Consequently, the lower suspended POC and NO_3^- concentrations observed in 2005 compared to 2006 may have explain the lower abundance of particle-attached bacteria observed in 2005 (Fig. 4; Table 1).

Another factor that might influence the attachment of bacteria to particles is the presence of EPS. According to the literature, EPS are mainly produced by diatoms (Passow & Alldredge 1994, Grossart 1999, Grossart et al. 2006), as suggested here by the significant positive correlation observed between EPS concentration and diatom abundance observed in this study (Table 5). EPS are rich in organic carbon and can represent an important food source for bacteria (Grossart 1999, Krembs & Engel 2001, Simon et al. 2002, Bar-Zeev et al. 2009). They also act as biological glue facilitating bacterial attachment to phytoplankton cells (Alldredge & Silver 1988, Riedel et al. 2006). Hence, EPS usually constitute "hot spots" for bacterial colonization (Alldredge et al. 1993, Passow & Alldredge 1994, Worm & Søndergaard 1998) and, therefore, could contribute to enhance sinking velocities of particle-attached bacteria (Kiørboe & Hansen 1993, Passow & Alldredge 1994). In contrast, EPS are positively buoyant and can increase the residence time of particles in the upper water column (Azetsu-Scott & Passow 2004). During our study, we did not observe

any significant relationship between EPS concentration and the abundance of particle-attached bacteria (Table 5), which suggests that EPS may not have constituted a preferred energy source for bacterial growth. However, the significant positive correlation between the sinking velocity of particle-attached bacteria and EPS concentration (Table 5) suggests that EPS produced by diatoms influenced the sinking velocity of bacteria, likely by favoring their attachment to diatoms.

Interestingly, we did not observe any significant difference in the abundance of free-living and particle-attached bacteria between the two sampling depths, even though values for nutrients and phytoplankton variables (e.g. POC, chl *a* and diatom cells) were lower at the $Z_{50\%}$ than at the Z_{CFM} (Figs. 2, 3 and 4; Table 1). Similar observations in the northwestern Mediterranean Sea (Scharek & Latasa 2007) were interpreted as the result of a balance between bacterial growth rates and grazing pressure. This emphasizes that a complex balance of top-down and bottom-up control on bacterial abundance may have come into play. On the one hand, dissolved organic carbon concentrations are usually high in the Hudson Bay system (Mundy et al. 2010), and consequently would likely not be limiting for bacterial growth. On the other hand, grazers such as flagellates, ciliates or choanoflagellates were abundant during this study (Fig. 2), indicating that top-down control of bacterial abundances may have dominated during our study.

3.4.3 Bacterial size and nucleic acid content in free-living and particle-attached communities

Particle-attached bacteria are usually larger than free-living bacteria (e.g. Alldredge et al. 1986, Cho & Azam 1988, Simon et al. 2002), as corroborated during our study (Fig. 5). Given their larger size, we expected a higher metabolic activity and, therefore, a higher proportion of HNA cells for particle-attached bacteria than for free-living bacteria (Servais et al. 1999, Morán et al. 2007, Ghiglione et al. 2009). Indeed, HNA bacteria are usually more active (e.g. Jochem et al. 2004, Longnecker et al. 2005, Scharek & Latasa 2007) and larger (Lebaron et al. 2001, Longnecker et al. 2006, Sherr et al. 2006, Morán et al. 2007) than LNA bacteria in natural communities. Here, we estimated that HNA bacteria were slightly larger (factor of 1.2) and contained *ca.* 4 times more nucleic acids than LNA bacteria in the free-living community. In contrast, particle-attached HNA bacteria were twice as large and contained *ca.* 7 times more nucleic acids than particle-attached LNA bacteria (Fig. 5; Table 2). According to Button & Robertson (1993), bacterial metabolic activity is associated with nucleic acid content but also with cell size. As HNA bacteria were always larger and contained more nucleic acids than LNA bacteria, we can then assume with confidence that HNA bacteria were more active than LNA bacteria during our study, particularly when they colonized particles. According to our results, the higher bacterial metabolic activity potentially associated with particle colonization was due to higher metabolic activity of HNA bacteria, rather than a higher percent contribution of HNA bacteria in the particle-attached community.

Our results are in accordance with those of Sherr et al. (2006) in the northeast Pacific Ocean and Belzile et al. (2008) in the Beaufort Sea and showed that only HNA bacteria responded positively to variations in phytoplankton biomass. This is evidenced by the positive significant correlations between HNA bacterial abundance and chl *a* biomass for both free-living and particle-attached communities ($r_s = 0.40$ and 0.35, respectively, $p < 0.05$) or with POC concentration for particle-attached HNA bacteria ($r_s = 0.49$, $p < 0.05$; data not shown). In addition to the higher FL1 HNA:FL1 LNA ratio for the particle-attached bacterial community compared to the free-living bacterial community (Table 2), these new observations support the assumption that HNA bacteria are the most dynamic members of the bacterial community in marine environments in general (Calvo-Diáz & Morán 2006, Morán et al. 2007) as well as in the Antarctic (Corzo et al. 2005) and now in the sub-Arctic areas, where they adapt their metabolic to substrate availability and, *per se* the presence of organic-rich particles. However, it is interesting to note that a recent paper from Bouvier et al. (2007) did not support the simple dichotomous view of HNA as active cells and LNA as inactive cells. According to their analyses of cytometric parameters obtained on bacterial samples from various aquatic systems, these two fractions are not fixed and interactions between them can occur. Our cytograms did not show any continuum between the clouds of the two fractions (Fig. 5) suggesting that the two fractions were well distinct during the time of our study. Similarly, exchanges between free-living and particle-attached bacterial communities can occur (Kiørboe et al. 2002, 2003). Such exchanges may have happened between free-living LNA and particle-attached LNA cells because the two

cells clouds formed a continuum, contrasting with the two distinct clouds of HNA cells (Fig. 5).

3.4.4 Bacteria and protist sinking velocities

The sinking velocities measured for chl *a* biomass and protist cells in the present study (Table 3) are within the range of values previously reported in the literature (Bienfang & Harrison 1984, Heiskanen & Keck 1996, Pommier et al. 2009) (Table 3). High sinking velocities recorded for the chrysophyte *Dinobryon balticum* and ciliates+choanoflagellates compared to other protist groups can be explained by the fact that *D. balticum* and the choanoflagellate *Parvicorbicula socialis* (Meunier) Deflandre, also observed in our samples, are known to form large and fast sinking colonies (McKenzie et al. 1995, 1997).

Using an average bacterial density of 1.08 g cm^{-3} (Pedrós-Alió & Mas 1993) and seawater density and viscosity calculated based on salinity and temperature measurements during our study (data not shown), and according to Stoke's Law, we estimated that sinking velocities of free-living bacteria should be 0.02–0.07 m d^{-1}. These values are not significantly different than the sinking velocities of free-living bacteria measured from our SetCol experiments (Two-tailed *t*-test, $p > 0.05$; Table 3). In contrast and as postulated, measured sinking velocities for particle-attached bacteria were significantly higher than those predicted from Stoke's Law and similar to those of protists to which they were

attached (Two-tailed *t*-tests, $p < 0.05$). The sinking velocities measured for particle-attached bacteria during SetCol experiments are in the range of values previously reported based on particle interceptor trap results (0.1–1.0 m d^{-1}, Ducklow et al. 1982), This shows the need for this type of experiments to measure the sinking velocities, especially for attached bacteria, and highlights the importance of attachment to protist cells for the vertical export of bacteria.

3.4.5 Bacterial turnover and potential contribution to POC sinking export

Our results reflect the small contribution of bacteria to the suspended material in the upper 50 m of the water column, as the total bacterial contribution to suspended POC in the Hudson Bay system was much smaller than the protist contribution and this is particularly the case for the contribution of particle-attached bacteria (< 1%; Table 4). However, despite their low contribution to suspended material, particle-attached bacteria contributed, on average, 13% of the total bacterial respiration rates (Table 4). Consequently, particle-attached bacteria recycled potentially more POC than their biomass contribution.

To estimate the turnover time needed for bacteria to remineralize the carbon associated with sinking particles, we used the fraction of protist carbon biomass that settled during the 6 h settling period and the respiration rates calculated for free-living and particle-attached bacteria. Assuming a constant respiration rate with time, we estimated that the turnover time due to particle-attached bacteria respiration would be 251 days whereas

for the free-living bacterial community, the turnover time would be 28 days. Our results corroborate previous findings showing that particle-attached bacteria carbon demand was very low compared to free-living bacteria (Karl et al. 1988, Simon et al. 1990, Smith et al. 1992, Ploug & Grossart 2000) despite the rapid vertical attenuation of POC sinking flux usually observed. This discrepancy has been called the "particle decomposition paradox" by Karl et al. (1988) and can be explained by the much faster hydrolysis of organic matter by particle-attached bacteria than their uptake of end products. Indeed, only a small fraction of the hydrolysates from particles is directly taken up by particle-attached bacteria, thus allowing for a large transfer of organic matter from sinking particles to the dissolved phase and consequently, supply of organic carbon to free-living bacteria (Cho & Azam 1988, Smith et al. 1992). Hence, our results do not support our third hypothesis, and rather suggest that only a small fraction of the suspended POC is respired by particle-attached bacteria, and that free-living bacteria are the main recyclers of the POM during its sedimentation.

3.5 Conclusions

This study, which combines for the first time the settling column method with flow cytometry, provided insights into the characteristics and processes associated with particle-attached bacteria. This study also complemented a previous study in which we report significant sinking fluxes of bacterial carbon, sometimes higher than protist carbon sinking fluxes, at 50 m suggesting an important contribution of bacteria to organic material sinking export (Lapoussière et al. 2009, see Chapter I). In agreement with previous studies, our

results showed higher bacterial metabolic activity and size associated with particle colonization. We also demonstrated the importance of particle attachment for the sinking export of bacteria, as the sinking velocities of bacteria attached to protist cells are significantly higher than those of free-living bacteria. Our results also showed that particle-attached bacteria had a minor contribution to total bacterial abundance (< 3%) and to the suspended POC in the offshore Hudson Bay waters (< 1%) but that their respiration could represent up to 13% of total bacterial respiration rates Consequently, our results suggest that the role of particle-attached bacteria was mainly as recyclers and not as contributors to suspended POC during our study. However, as particle-attached bacteria hydrolyze more organic matter than they can take up, the main contributors to organic matter recycling would be free-living bacteria using the dissolved phase leaking from sinking particles. Further investigations on organic material sinking export with particle interceptor trap and direct measurements of bacterial production and respiration on the collected material, would certainly improve our understanding of the microbial ecology of the sinking particles and aggregates, and its significance for POM cycle.

CONCLUSION GÉNÉRALE

Au cours des prochaines décennies, les changements climatiques, amplifiés aux hautes latitudes, entraineront une altération des conditions du milieu et, par conséquent, le cycle de la matière organique au sein des écosystèmes arctiques et sub-arctiques. Il apparaît donc essentiel de connaître l'intensité et le fonctionnement des différents processus intervenant dans la production, l'exportation et la reminéralisation de la matière organique. C'est dans cette optique que cette thèse présente les premières données sur la production et l'exportation du matériel organique particulaire au sein du SBH en période libre de glace.

Le premier chapitre de cette thèse a, tout d'abord, permis de quantifier l'intensité des flux verticaux de matériel organique particulaire ainsi que de déterminer la composition du matériel qui sédimente en période automnale dans le SBH. Malgré certaines limitations logistiques liées aux opérations sur le navire, nous avons pu mettre en évidence des patrons spatiaux d'exportation. Sur l'ensemble du SBH, les flux verticaux de COP étaient faibles comparativement aux valeurs observées dans d'autres mers arctiques et sub-arctiques. Cette étude montre que le SBH est un système complexe présentant des variations spatiales marquées des conditions hydrographiques (i.e. température et salinité de surface) et des patrons de sédimentation. Trois régions ont ainsi pu être distinguées : le détroit d'Hudson,

l'est de la baie d'Hudson et l'ouest de la baie d'Hudson. Le détroit d'Hudson était caractérisé par les flux verticaux de matériel particulaire les plus élevés et une forte contribution des diatomées intactes au COP exporté. Au contraire, l'ouest de la baie d'Hudson est apparu comme un environnement plus propice au recyclage du matériel organique particulaire, avec de faibles flux verticaux et un COP principalement exporté sous forme de détritus amorphes et de carbone bactérien. Enfin, l'est de la baie présentait des conditions intermédiaires avec une forte contribution des pelotes fécales au COP exporté, suggérant une forte pression de broutage par le zooplancton herbivore dans la couche de surface.

Les résultats du premier chapitre ont également permis d'estimer l'atténuation des flux verticaux avec la profondeur ainsi que l'intensité et la composition des apports de nourriture pour les communautés benthiques au sein de cette mer intérieure peu profonde qu'est la baie d'Hudson. Contrairement à la théorie de Martin et al. (1987), l'atténuation des flux avec la profondeur n'a pas toujours été observée. La principale explication à ce phénomène est l'advection latérale de matériel dans les pièges à particules. Malheureusement, le protocole utilisé au cours de notre étude ne m'a pas permis de quantifier cette advection potentielle. La faible atténuation des flux avec la profondeur sous-entend que le matériel qui atteint le fond de la baie d'Hudson est peu dégradé et ainsi disponible pour les communautés benthiques. De façon très préliminaire, j'ai ainsi pu mettre en évidence que les patrons de répartition spatiale des flux verticaux en termes

d'intensité et de composition coïncidaient avec les patrons d'abondance et de diversité des communautés benthiques.

Le second chapitre de cette thèse étudie pour la première fois, le couplage entre la production primaire et l'exportation du matériel organique particulaire hors de la zone euphotique au sein du SBH en période libre de glace. Cette étude a confirmé les observations réalisées au cours de précédentes études au sein du SBH. Le SBH apparaît comme une mer peu productive (Sakshaug 2004, Ferland 2010) et le détroit d'Hudson et la baie d'Hudson sont deux systèmes distincts avec des conditions océanographiques différentes (Harvey et al. 1997, 2006, Ferland 2010). En effet, le détroit d'Hudson est caractérisé par un important mélange vertical et l'influence d'une entrée d'eau salée provenant de la baie de Baffin. Au contraire, la baie d'Hudson est fortement stratifiée à cause des importants apports d'eau douce liés aux nombreuses rivières qui se jettent dans la baie. Les résultats ont permis de démontrer que ces différences de conditions environnementales créent des patrons régionaux de production et de biomasse phytoplanctonique au sein du SBH.

Les observations réalisées au cours de cette étude ont montré que le flux vertical de COP à 50 m variait peu sur l'ensemble du système malgré les variations spatiales observées pour la production et la biomasse phytoplanctonique. Ainsi nos résultats n'ont pas mis en évidence de relation entre l'exportation verticale de matériel organique et la production

primaire et/ou la biomasse importante des grandes cellules phytoplanctoniques. Dans le SBH à l'automne, les rapports d'exportation les plus élevés ont été observés dans les régions où la production primaire était faible et où la biomasse des hétérotrophes était importante. Ces résultats pourraient être liés à un découplage spatio-temporel entre les processus de production et d'exportation, tout particulièrement pour la région ouest de la baie où la formation d'une gyre cyclonique plus intense à l'automne favorise la sédimentation du matériel suspendu (Sibert 2010). Ce chapitre met donc l'accent sur la complexité des processus (physiques, chimiques et biologiques) influençant la relation entre la production primaire et son exportation sous la zone euphotique.

La forte contribution du carbone bactérien observée dans le cadre du premier chapitre sur l'ensemble du SBH et plus particulièrement à l'ouest de la baie, était quelque peu surprenante. En effet, la contribution des bactéries au flux vertical de matériel organique est souvent considérée comme négligeable étant donné leur faible vitesse de chute. Les bactéries sont généralement considérées comme d'importants acteurs de la reminéralisation de la matière organique au cours de sa sédimentation et non comme des contributeurs. Ces résultats m'ont donc poussé à approfondir le rôle des bactéries dans l'exportation verticale du matériel organique particulaire, ce qui a fait l'objet du troisième chapitre de cette thèse.

Le troisième chapitre de cette thèse visait à approfondir les connaissances sur le rôle des bactéries dans l'exportation et la reminéralisation de la matière organique, particulièrement lorsque celles-ci sont attachées à la surface des particules qui sédimentent. Au cours de cette étude, les bactéries attachées étaient peu abondantes comparativement aux bactéries libres mais étaient plus volumineuses et présentaient une activité métabolique plus élevée. Les résultats ont démontré que la colonisation des particules permet aux bactéries de sédimenter à des vitesses similaires à celles des protistes. Ce chapitre a également permis d'établir un budget de la contribution de la biomasse des bactéries attachées au COP suspendu et de la perte de COP liée à leur respiration. Ce budget a été établit à partir de trois estimations indépendantes de la biomasse bactérienne, sur la base de relations trouvées dans la littérature (i.e. biomasse constante, relation biovolume-biomasse, relation allométrique), suivi d'une estimation de la production et de la respiration bactérienne. Étant donné la faible biomasse des bactéries attachées pendant la période d'échantillonnage, leur contribution au COP total était faible comparativement à celles des bactéries libres et des protistes. De plus, la respiration des bactéries attachées était faible par rapport à celle des bactéries libres mais supérieure à leur contribution au COP suspendu. Ce budget suggère donc que les bactéries attachées recyclent potentiellement plus de matériel organique particulaire au cours de sa sédimentation que ce qu'elles y contribuent et que les principaux acteurs de la reminéralisation du matériel organique au cours de sa sédimentation sont les bactéries libres. En effet les bactéries libres peuvent bénéficier des substances dissoutes qui s'échappent des particules qui sédimentent suite à leur hydrolyse par les bactéries attachées. Ces résultats complètent et nuancent les résultats

du premier chapitre qui suggéraient que les bactéries attachées pouvaient avoir une contribution en carbone plus importance que les protistes ou les pelotes fécales d'herbivores au cours de l'exportation verticale du COP.

Cette thèse de doctorat met en évidence l'influence des processus physiques et chimiques sur les processus biologiques intervenant dans la production et l'exportation en profondeur de la matière organique. Les résultats ont montré la complexité des interactions entre les différentes composantes biologiques telles que le broutage du phytoplancton par le zooplancton ou la reminéralisation de la matière organique par les bactéries, et leur influence sur la composition et l'intensité des flux verticaux de matériel organique. Toutefois, ces résultats ne peuvent être extrapolés à l'ensemble de la saison productive car ils se limitent à une courte période (fin de l'été-début de l'automne) et ne comprennent ni la floraison printanière ni la période de production par les algues de glace. La libération des algues de glace lors de la fonte de la glace ainsi que la floraison printanière conduisent fréquemment, en milieu polaire, à d'importants épisodes d'exportation et, par conséquent, sont importants pour le maintien des communautés benthiques. Ces deux événements devraient donc être ciblés lors de prochaines expéditions au sein du SBH. Une étude conjointe de l'exportation verticale et des communautés benthiques permettrait également de mieux appréhender le fonctionnement du couplage pélago-benthique dans un système peu profond comme celui de la baie d'Hudson. Par ailleurs, au cours de cette étude nous avons uniquement évalué l'influence de la communauté zooplanctonique dans l'exportation de la matière organique par l'intermédiaire de l'analyse des pelotes fécales. Il apparaît

nécessaire de pousser plus loin cette étude en évaluant par exemple l'influence de l'abondance et de la composition de la communauté zooplanctonique sur l'exportation et/ou la rétention du matériel organique dans la zone euphotique. Enfin, il serait intéressant de poursuivre l'étude des processus microbiens intervenant au cours de l'exportation du matériel organique notamment en réalisant des mesures de production et de respiration bactériennes directement sur le matériel collecté à l'aide de pièges à particules et ainsi de mesurer *in situ* la dégradation du matériel qui sédimente.

Les travaux de cette thèse s'inscrivent dans l'effort de recherche international développé ces dernières années au travers de divers programmes de recherche (e.g. ArcticNet, NABOS, Arctic SOLAS, EPOCA Arctic Campaign) visant à approfondir les connaissances sur le fonctionnement des écosystèmes polaires et évaluer leur devenir face au réchauffement climatique d'ores et déjà observé. Cette thèse de doctorat a ainsi permis d'obtenir des données uniques sur le fonctionnement du cycle du carbone au sein du SBH avec une couverture spatiale sans précédent. Ces données sont essentielles à la calibration des modèles climatiques afin de prévoir au mieux l'évolution des écosystèmes pélagiques et benthiques du SBH face aux changements climatiques attendus.

RÉFÉRENCES

Aksnes DL, Wassmann P (1993) Modelling the significance of zooplankton grazing for export production. Limnol Oceanogr 38:978–985

Alldredge AL, Jackson GA (1995) Aggregation in marine systems. Deep-Sea Res II 42:1–7

Alldredge AL, Silver MW (1988) Characteristics, dynamics and significance of marine snow. Prog Oceanogr 20:41–82

Alldredge AL, Cole JJ, Caron DA (1986) Production of heterotrophic bacteria inhabiting macroscopic organic aggregates (marine snow) from surface waters. Limnol Oceanogr 31:68–78

Alldredge AL, Passow U, Logan BE (1993) The abundance and significance of a class of large transparent organic particles in the ocean. Deep-Sea Res 40:1131–1140

Anderson JT, Roff JC (1980) Seston ecology of the surface waters of Hudson Bay. Can J Fish Aquat Sci 37:2242–2253

Anderson TR, Ducklow HW (2001) Microbial loop carbon cycling in ocean environments studied using a simple steady-state model. Aquat Microb Ecol 26:37–49

Andreassen IJ, Wassmann P (1998) Vertical flux of phytoplankton and particulate biogenic matter in the marginal ice zone of the Barents Sea in May 1993. Mar Ecol Prog Ser 170:1–14

Arbic BK, St-Laurent P, Sutherland G, Garrett C (2007) On the resonance and influence of the tides in Ungava Bay and Hudson Strait. Geophys Res Lett 34, L17606, doi:10.1029/2007GL030845

Archer D (2005) Fate of fossil fuel CO_2 in geologic time. J Geophys Res 110, C09S05, doi:10.1029/2004JC002625

Aristegui J, Gasol JM, Duarte CM, Herndl GJ (2009) Microbial oceanography of the dark ocean's pelagic realm. Limnol Oceanogr 54:1501–1529

Armstrong RA, Lee C, Hedges JI, Honjo S, Wakeham SG (2002) A new mechanistic model for organic carbon fluxes in the ocean based on the quantitative association of POC with ballast minerals. Deep-Sea Res II 49:219–236

Armstrong RA, Peterson ML, Lee C, Wakeham SG (2009) Settling velocity spectra and the ballast ratio hypothesis. Deep-Sea Res II 56:1470–1478

Arrigo KR, van Dijken GL, Pabi S (2008) Impact of a shrinking Arctic ice cover on marine primary production. Geophys Res Lett 35, L19603, doi:10.1029/2008GL035028

Atkinson EG, Wacasey JW (1987) Sedimentation in Arctic Canada: particulate organic carbon flux to a shallow marine benthic community in Frobisher Bay. Polar Biol 8:3–7

Azam F (1998) Microbial control of oceanic carbon flux: The plot thickens. Science 280:694–696

Azam F, Long RA (2001) Sea snow microcosms. Nature 414:495–498

Azam F, Fenche T, Field JG, Gray JS, Meyer-Reil LA, Thingstad F (1983) The ecological role of water column microbes in the sea. Mar Ecol Prog Ser 10:57–63

Azetsu-Scott K, Passow U (2004) Ascending marine particles: Significance of transparent exopolymer particles (TEP) in the upper ocean. Limnol Oceanogr 49:741–748

Bano N, Nisa M-U, Khan N, Saleem M, Harrison PJ, Ahmed SI, Azam F (1997) Significance of bacteria in the flux of organic matter in the tidal creeks of the mangrove ecosystem of the Indus River delta, Pakistan. Mar Ecol Prog Ser 157:1–12

Bates NR, Moran SB, Hansell DA, Mathis JT (2006) An increasing CO_2 sink in the Arctic Ocean due to sea-ice loss. Geophys Res Lett 33, L23609, doi:10.1029/2006GL027028

Bar-Zeev E, Berman-Frank I, Stambler N, Dominguez EV, Zohary T, Capuzzo E, Meeder E, Suggett DJ, Iluz D, Dishon G, Berman T (2009) Transparent exopolymer particles (TEP) link phytoplankton and bacterial production in the Gulf of Aqaba. Aquat Microb Ecol 56:217–225

Behrenfeld MJ, O'Malley RT, Siegel DA, McClain CR, Sarmiento JL, Feldman GC, Milligan AJ, Falkowski PG, Letelier RM, Boss ES (2006) Climate-driven trends in contemporary ocean productivity. Nature 444:752–755

Bell CR, Albright LJ (1981) Attached and free-floating bacteria in the Fraser River Estuary, Bristish Columbia, Canada. Mar Ecol Prog Ser 6:317–327

Belzile C, Brugel S, Nozais C, Gratton Y, Demers S (2008) Variations of the abundance and nucleic acid content of heterotrophic bacteria in Beaufort Shelf waters during winter and spring. J Mar Syst 74: 946–956

Bérard-Therriault L, Poulin M, Bossé L (1999). Guide d'identification du phytoplancton marin de l'estuaire du Saint-Laurent, incluant également certains protozoaires. Publ Spéc Can Sci Halieut Aquat 128:1–387

Berelson WM (2001) The flux of particulate organic carbon into the ocean interior: A comparison of four U.S. JGOFS regional studies. Oceanography 14:59–67

Betzer PR, Showers WJ, Laws EA, Winn CD, DiTullio GR, Kroopnick PM (1984) Primary productivity and particle fluxes on a transect of the equator at 153°W in the Pacific Ocean. Deep-Sea Res 31:1–11

Bienfang PK (1981) Setcol, a technologically simple and reliable method for measuring phytoplankton sinking rates. Can J Fish Aquat Sci 38:1289–1294

Bienfang PK, Harrison PJ (1984) Co-variation of sinking rate and cell quota among nutrient replete marine phytoplankton. Mar Ecol Prog Ser 14:297–300

Bishop JKB (1989) Regional extremes in particulate matter composition and flux: effects on the chemistry of the ocean interior. In: Berger WH, Smetacek VS, Wefer G (eds) Productivity of the ocean: present and past. John Wiley & Sons, New York, p 117–138

Blazewicz-Paszkowycz M, Ligowski R (2002) Diatoms as food source indicator for some Antarctic Cumacea and Tanaidacea (Crustacea). Antarct Sci 14:11–15

Bopp L, Monfray P, Aumont O, Dufresne J-L, Le Treut H, Madec G, Terray L, Orr JC (2001) Potential impact of climate change on marine export production. Global Biogeochem Cycles 15:81–99

Bopp L, Aumont O, Cadule P, Alvain S, Gehlen M (2005) Response of diatoms distribution to global warming and potential implications: A global model study. Geophys Res Lett 32, L19606, doi:10.1029/2005GL023653

Bouvier T, del Giorgio PA, Gasol JM (2007) A comparative study of the cytometric characteristics of High and Low nucleic-acid bacterioplankton cells from different aquatic ecosystems. Environ Microb 9:2050–2066

Boyd PW, Newton P (1995) Evidence of the potential influence of planktonic community structure on the interannual variability of particulate organic carbon flux. Deep-Sea Res I 42:619–639

Boyd PW, Newton P (1999) Does planktonic community structure determine downward particulate organic carbon flux in different oceanic provinces? Deep-Sea Res I 46:63–91

Boyd PW, Trull TW (2007) Understanding the export of biogenic particles in oceanic waters: Is there consensus? Prog Oceanogr 72:276–312

Boyd PW, Sherry ND, Berges JA, Bishop JKB, Calvert SE, Charette MA, Giovannoni SJ, Goldblatt R, Harrison PJ, Moran SB, Roy S, Soon M, Strom S, Thibault D, Vergin KL, Whitney FA, Wong CS (1999) Transformations of biogenic particulates from the pelagic to the deep ocean realm. Deep-Sea Res II 46:2761–2792

Boyd PW, Gall MP, Silver MW, Coale SL, Bidigare RR, Bishop JKB (2008) Quantifying the surface–subsurface biogeochemical coupling during the VERTIGO ALOHA and K2 studies. Deep-Sea Res II 55:1578–1593

Brown L, Sanders R, Savidge G (2006) Relative mineralisation of C and Si from biogenic particulate matter in the upper water column during the North East Atlantic diatom bloom in spring 2001. J Mar Syst 63:79–90

Brugel S, Nozais C, Poulin M, Tremblay J-É, Miller LA, Simpson KG, Gratton Y, Demers S (2009) Phytoplankton biomass and production in the southeastern Beaufort Sea in autumn 2002 and 2003. Mar Ecol Prog Ser 377:63–77

Brzezinski MA (1985) The Si:C:N ratio of marine diatoms: interspecific variability and the effect of some environmental variables. J Phycol 21:347–357

Buesseler KO (1998) The decoupling of production and particulate export in the surface ocean. Global Biogeochem Cycles 12:297–310

Buesseler K (2008) Introduction to ''Understanding the ocean's biological pump: Results from VERTIGO''. Deep-Sea Res II 55:1519–1521

Buesseler K, Boyd P (2009) Shedding light on processes that control particle export and flux attenuation in the twilight zone of the open ocean. Limnol Oceanogr 54:1210–1232

Buesseler KO, Trull TW, Steinberg DK, Silver MW, Siegel DA, Saitoh S-I, Lamborg CH, Lam PJ, Karl DM, Jiao NZ, Honda MC, Elskens M, Dehairs F, Browng SL, Boyd PW, Bishop JKB, Bidigare RR (2008) VERTIGO (VERtical Transport In the Global Ocean): A study of particle sources and flux attenuation in the North Pacific. Deep-Sea Res II 55:1522–1539

Buesseler KO, Antia AN, Chen M, Fowler SW, Gardner WD, Gustafsson O, Harada K, Michaels AF, Rutgers van der Loeff M, Sarin M, Steinberg DK, Trull TW (2007) An assessment of the use of sediment traps for estimating upper ocean particle fluxes. J Mar Res 65:345–416

Bursa A (1961) Phytoplankton of the Calanus expedition in Hudson Bay, 1953 and 1954. J Fish Res Board Can 18:51–83

Bursa A (1968) Marine life in Hudson Bay. I. Marine plants. In: Beals CS (ed) Science, history and Hudson Bay. Department of energy, mines and resources, Ottawa, p 343–351

Button DK, Robertson BR (1993) Use of high-resolution flow cytometry to determine the activity and distribution of aquatic bacteria. In: Kemp PF, Sherr BF, Sherr EB, Cole JJ (eds) Handbook of methods in aquatic microbial ecology. Lewis, Boca Raton, p 163–173

Callaghan TV, Björn LO, Chernov Y, Chapin T, Christensen TR, Huntley B, Ims RA, Johansson M, Jolly D, Jonasson S, Matveyeva N, Panikov N, Oechel W, Shaver G, Schaphoff S, Sitch S (2004) Effects of changes in climate on landscape and regional processes and feedbacks to the climate system. Ambio 33:459–468

Calvo-Díaz A Morán XAG (2006) Seasonal dynamics of picoplankton in shelf waters of the southern Bay of Biscay. Aquat Microb Ecol 42:159–174

Caron G, Michel C, Gosselin M (2004) Seasonal contributions of phytoplankton and fecal pellets to the organic carbon sinking flux in the North Water (northern Baffin Bay). Mar Ecol Prog Ser 283:1–13

Casgrain P, Legendre P (2000) The R package for multivariate and spatial analysis version 4.0, http://www.bio.umontreal.ca/casgrain/en/labo/R/v4/

Cho BC, Azam F (1988) Major role of bacteria in biogeochemical fluxes in the ocean's interior. Nature 332:441–443

Cho BC, Azam F (1990) Biogeochemical significance of bacterial biomass in the ocean's euphotic zone. Mar Ecol Prog Ser 63:253–259

Comiso JC (2006a) Arctic warming signals from satellite observations. Weather 61:70–76

Comiso JC (2006b) Abrupt decline in the Arctic winter sea ice cover. Geophys Res Lett 33, L18504, doi:10.1029/2006GL027341

Comiso JC, Parkinson CL, Gersten R, Stock L (2008) Accelerated decline in the Arctic sea ice cover. Geophys Res Lett 35, L01703, doi:10.1029/2007GL031972

Conover RJ, Durvasula R, Roy S, Wang R (1986) Probable loss of chlorophyll-derived pigments during passage through the gut of zooplankton, and some of the consequences. Limnol Oceanogr 31:878–887

Conover WJ, Iman RL (1981) Rank transformation as a bridge between parametric and nonparametric statistics. Am Stat 35, 124–129

Corzo A, Rodríguez-Gálvez S, Lubian L, Sobrino C, Sangra P, Martínez A (2005) Antarctic marine bacterioplankton subpopulations discriminated by their apparent content of nucleic acids differ in their response to ecological factors. Polar Biol 29:27–39

Crump BC, Baross JA, Simenstad CA (1998) Dominance of particle-attached bacteria in the Columbia River estuary, USA. Aquat Microb Ecol 14:7–18

Cusson M, Archambault P, Aitken A (2007) Biodiversity of benthic assemblages on the Arctic continental shelf: historical data from Canada. Mar Ecol Prog Ser 331:291–304

Davidson VM (1931) Biological and oceanographic conditions in Hudson Bay. 5 The planktonic diatoms in Hudson Bay. Can Biol Fish 6:495–509

de la Rocha C, Passow U (2007) Factors influencing the sinking of POC and the efficiency of the biological carbon pump. Deep-Sea Res II 54:639–658

de la Rocha CL, Nowald N, Passow U (2008) Interactions between diatom aggregates, minerals, particulate organic carbon, and dissolved organic matter: Further implications for the ballast hypothesis. Global Biogeochem Cycles 22, GB4005, doi:10.1029/2007GB003156

Delong EF, Franks DG, Alldredge AL (1993) Phylogenetic diversity of aggregate-attached vs free-living marine bacterial assemblages. Limnol Oceanogr 38:924–934

Déry SJ, Stieglitz M, McKenna EC, Wood EF (2005) Characteristics and trends of river discharge into Hudson, James, and Ungava Bays, 1964–2000. J Climate 18:2540–2557

Dilling L, Alldredge AL (1993) Can chaetognath fecal pellets contribute significantly to carbon flux? Mar Ecol Prog Ser 92:51–58

Doney SC (2006) Plankton in a warmer world. Nature 444:695–696

Drinkwater KF (1986) Physical oceanography of Hudson Strait and Ungava Bay. In: Martini IP (ed) Canadian inland seas. Elsevier Oceanography Series, Amsterdam, p 237–264

Drinkwater KF (1988) On the mean and tidal currents in Hudson Strait. Atmos Ocean 26:252–266

Drinkwater KF, Jones EP (1987) Density stratification, nutrient and chlorophyll distribution in the Hudson Strait region during summer and their relation to tidal mixing. Cont Shelf Res 7:599–607

Ducklow HW, Kirchman DL, Rowe GT (1982) Production and vertical flux of attached bacteria in the Hudson River plume of the New York bight as studied with floating sediment trap. Appl Environ Microb 43:769–776

Ducklow HW, Erickson M, Kelly J, Montes-Hugo M, Ribic CA, Smith RC, Stammerjohn SE, Karl DM (2008) Particle export from the upper ocean over the continental shelf of the west Antarctic Peninsula: A long-term record, 1992–2007. Deep-Sea Res II 55:2118–2131

Dugdale RC, Goering JJ (1967) Uptake of new and regenerated forms of nitrogen in primary productivity. Limnol Oceanogr 12:196–206

Dunne JP, Armstrong A, Gnanadesikan A, Sarmiento JL (2005) Empirical and mechanistic models for the export ratio. Global Biogeochem Cycles 19, GB4026, doi:10.1029/2004GB002390

Dyrssen DW (2001) The biogeochemical cycling of carbon dioxide in the oceans, perturbations by man. Sci Total Environ 277:1–6

Ellingsen IH, Dalpadado P, Slagstad D, Loeng H (2008) Impact of climatic change on the biological production in the Barents Sea. Clim Chang 87:155–175

Else BGT, Yackel JJ, Papakyriakou TN (2008) Application of satellite remote sensing techniques for estimating air-sea CO_2 fluxes in Hudson Bay, Canada during the ice-free season. Remote Sens Environ 112:3550–3562

Emerson SR, Hedges JI (2008) Chemical oceanography and the marine carbon cycle. Cambridge University Press, Cambridge

Engel A (2004) Distribution of transparent exopolymer particles (TEP) in the northeast Atlantic Ocean and their potential significance for aggregation processes. Deep-Sea Res I 51:83–92

Eppley RW, Peterson BJ (1979) Particulate organic matter flux and planktonic new production in the deep ocean. Nature 282:677–680

Estrada R (2010) Structure des communautés mesozooplanctoniques en relation avec les conditions du milieu dans le système de la baie d'Hudson à la fin des étés 2003 à 2006. Thèse de maîtrise, UQAR, Rimouski

Falkowski PG, Raven JA (2007) Aquatic photosynthesis, 2nd edn. Princeton University Press, New Jersey

Falkowski PG, Barber RT, Smetacek V (1998) Biogeochemical controls and feedbacks on ocean primary production. Science 281:200–206

Fandino LB, Riemann L, Steward GF, Long RA, Azam F (2001) Variations in bacterial community structure during a dinoflagellate bloom analyzed by DGGE and 16S rDNA sequencing. Aquat Microb Ecol 23:119–130

Fasham MJR (2003) Ocean biogeochemistry: the role of the ocean carbon cycle in global change. Springer-Verlag, Berlin

Feely RA, Sabine CL, Lee K, Berelson W, Kleypas J, Fabry VJ, Frank J (2004) Impact of anthropogenic CO_2 on the $CaCO_3$ system in the oceans. Science 305:362–366

Feely RA, Sabine CL, Takahashi T, Wanninkhof R (2001) Uptake and storage of carbon dioxide in the ocean: the global CO_2 survey. Oceanography 14:18–32

Ferland J (2010) Répartition spatiale de la production et de la biomasse phytoplanctonique dans le système de la baie d'Hudson au cours des étés 2004, 2005 et 2006. Thèse de maîtrise, UQAR, Rimouski

Field CB, Behrenfeld MJ, Randerson JT, Fakowski P (1998) Primary production of the biosphere: integrating terrestrial and oceanic components. Science 281:237–240

Field DB, Baugartner TR, Charles CD, Ferreira-Bartrina V, Ohman MD (2006) Planktonic foraminifera of the California current reflect 20th-century warming. Science 311:63–66

Fischer G, Karakas G, Blaas M, Ratmeyer V, Nowald N, Schlitzer R, Helmke P, Davenport R, Donner B, Neuer S, Wefer G (2009) Mineral ballast and particle settling rates in the coastal upwelling system off NW Africa and the South Atlantic. Int J Earth Sci 98:281–298

Forest A, Sampei M, Hattori H, Makabe R, Sasaki H, Fukuchi M, Wassmann P, Fortier L (2007) Particulate organic carbon fluxes on the slope of the Mackenzie Shelf (Beaufort Sea): Physical and biological forcing of shelf-basin exchanges. J Mar Syst 68:39–54

François R, Honjo S, Krishfield R, Manganini S (2002) Factors controlling the flux of organic carbon to the bathypelagic zone of the ocean. Global Biogeochem Cycles 16, 1087, doi:10.1029/2001GB001722

Fuhrman JA, Azam F (1980) Bacterioplankton secondary production estimates for coastal waters of British Columbia, Antarctica and California. Appl Environ Microbiol 39:1085–1095

Gagnon AS, Gough WA (2005a) Climate change scenarios for the Hudson Bay region: an intermodel comparison. Clim Chang 69:269–297

Gagnon AS, Gough WA (2005b) Trends in the dates of ice freeze-up and breakup over Hudson Bay, Canada. Arctic 58:370–382

Gagnon AS, Gough WA (2006) East-west asymmetry in long-term trends of landfast ice thickness in the Hudson Bay region, Canada. Climate Res 32:177–186

Gardner WD (2000) Sediment traps sampling in surface water. In: Hanson RB, Ducklow HW, Field JG (eds) The changing ocean carbon cycle: a midterm synthesis of the JGOFS. Cambridge University Press, Cambridge, p 181–240

Garneau M-È, Vincent WF, Alonso-Saez L, Gratton Y, Lovejoy C (2006) Prokaryotic community structure and heterotrophic production in a river-influenced coastal arctic ecosystem. Aquat Microb Ecol 42:27–40

Garneau M-È, Vincent WF, Terrado R, Lovejoy C (2009) Importance of particle-associated bacterial heterotrophy in a coastal Arctic ecosystem. J Mar Syst 75:185–197

Gasol JM, Pinhassi J, Alonso-Saez L, Ducklow H, Herndl GJ, Koblizek M, Labrenz M, Luo Y, Morán XAG, Reinthaler T, Simon M (2008) Towards a better understanding of microbial carbon flux in the sea. Aquat Microb Ecol 53:21–38

Ghiglione JF, Conan P, Pujo-Pay M (2009) Diversity of total and active free-living vs. particle-attached bacteria in the euphotic zone of the NW Mediterranean Sea. FEMS Microbiol Lett 299:9–21

Ghiglione JF, Mevel G, Pujo-Pay M, Mousseau L, Lebaron P, Goutx M (2007) Diel and seasonal variations in abundance, activity, and community structure of particle-attached and free-living bacteria in NW Mediterranean Sea. Microb Ecol 54:217–231

González HE, Smetacek V (1994) The possible role of the cyclopoid copepod *Oithona* in retarding vertical flux of zooplankton faecal material. Mar Ecol Prog Ser 113:233–246

González HE, González SR, Brummer G-JA (1994) Short-term sedimentation pattern of zooplankton faeces and microplankton at a permanent station in the Bjørnafjorden (Norway) during April-May 1992. Mar Ecol Prog Ser 105:31–45

Gough WA, Wolfe E (2001) Climate change scenarios for Hudson Bay, Canada, from general circulation models. Arctic 54:142–148

Gough WA, Cornwell AR, Tsuji LJS (2004) Trends in seasonal sea ice duration in southwestern Hudson Bay. Arctic 57:299–305

Grainger EH (1982) Factors affecting phytoplankton stocks and primary productivity at the Belcher islands, Hudson Bay. Nat Can 109:787–791

Granskog MA, Macdonald RW, Mundy CJ, Barber DG (2007) Distribution, characteristics and potential impacts of chromophoric dissolved organic matter (CDOM) in Hudson Strait and Hudson Bay, Canada. Cont Shelf Res 27:2032–2050

Grasshoff K, Kremling K, Ehrhardt M (1999) Methods of seawater analysis, 3rd edn. Wiley-VCH, New York

Grebmeier JM, Barry JP (1991) The influence of oceanographic processes on pelagic-benthic coupling in polar regions: a benthic perspective. J Mar Syst 2:495–518

Grossart H-P (1999) Interactions between marine bacteria and axenic diatoms (*Cylindrotheca fusiformis, Nitzschia laevis,* and *Thalassiosira weissflogii*) incubated under various conditions in the lab. Aquat Microb Ecol 19:1–11

Grossart H-P, Ploug H (2001) Microbial degradation of organic carbon and nitrogen on diatom aggregates. Limnol Oceanogr 46:267–277

Grossart H-P, Simon M (1998) Limnetic macroscopic organic aggregates (lake snow): abundance, characteristics, and bacterial dynamics in Lake Constance. Limnol Oceanogr 38:532–546

Grossart H-P, Hietanen S, Ploug H (2003a) Microbial dynamics on diatom aggregates in Øresund, Denmark. Mar Ecol Prog Ser 249:69–78

Grossart H-P, Kiørboe T, Tang K, Ploug H (2003b) Bacterial colonization of particles: growth and interactions. Appl Environ Microb 69:3500–3509

Grossart H-P, Levold F, Allgaier M, Simon M, Brinkhoff T (2005) Marine diatom species harbour distinct bacterial communities. Environ Microbiol 7:860–873

Grossart H-P, Kiørboe T, Tang K, Allgaier M, Yam EM, Ploug H (2006) Interactions between marine snow and heterotrophic bacteria: aggregate formation and microbial dynamics. Aquat Microb Ecol 42:19–26

Grossart H-P, Tang K, Kiørboe T, Ploug H (2007) Comparison of cell-specific activity between free-living and attached bacteria using isolates and natural assemblages. FEMS Microbiol Ecol 266:194–200

Gruber N, Gloor M, Fletcher SEM, Doney SC, Dutkiewicz S, Follows MJ, Gerber M, Jacobson AR, Joos F, Lindsay K, Menemenlis D, Mouchet A, Muller SA, Sarmiento JL, Takahashi T (2009) Oceanic sources, sinks, and transport of atmospheric CO_2. Global Biogeochem Cycles 23, GB1005, doi:10.1029/2008GB003349

Hargrave BT, Walsh ID, Murray DW (2002) Seasonal and spatial patterns in mass and organic matter sedimentation in the North Water. Deep-Sea Res II 49:5227–5244

Harrison WG, Head EJH, Horne EPW, Irwin B, Li WKW, Longhurst AR, Paranjape MA, Platt T (1993) The western North Atlantic bloom experiment. Deep-Sea Res II 40:279–305

Harvey M, Therriault J-C, Simard N (1997) Late-summer distribution of phytoplankton in relation to water mass characteristics in Hudson Bay and Hudson Strait (Canada). Can J Fish Aquat Sci 54:1937–1952

Harvey M, Therriault J-C, Simard N (2001) Hydrodynamic control of late summer species composition and abundance of zooplankton in Hudson Bay and Hudson Strait (Canada). J Plankton Res 23:481–496

Harvey M, Starr M, Therriault J-C, Saucier F, Gosselin M (2006) MERICA-Nord Program: monitoring and research in the Hudson Bay complex. Atlantic Zone Monitoring Program Bulletin 5:27–32

Heiskanen A-S, Keck A (1996) Distribution and sinking rates of phytoplankton, detritus and particulate biogenic silica in the Laptev Sea and Lena River (Arctic Siberia). Mar Chem 53:229–245

Higgins ME, Cassano JJ (2009) Impacts of reduced sea ice on winter Arctic atmospheric circulation, precipitation, and temperature. J Geophys Res 114, 16, doi:10.1029/2009JD011884

Hillebrand H, Dürselen C-D, Kirschtel D, Pollingher U, Zohary T (1999) Biovolume calculation for pelagic and benthic microalgae. J Phycol 35:403–424

Holland MM, Serreze MC, Stroeve J (2010) The sea ice mass budget of the Arctic and its future change as simulated by coupled climate models. Clim Dynam 34:185–200

Hollibaugh T, Wong PS, Murrell MC (2000) Similarity of particle-associated and free-living bacterial communities in northern San Franscico Bay, California. Aquat Microb Ecol 21:102–114

Holmes RM, Aminot A, Kerouel R, Hooker BA, Peterson JB (1999) A simple and precise method for measuring ammonium in marine and freshwater ecosystems. Can J Fish Aquat Sci 56:1801–1808

Holmes RW (1970) The Secchi disk in turbid coastal waters. Limnol Oceanogr 15:688–694

Horner RA (2002) A taxonomic guide to some common marine phytoplankton. Biopress Limited, Bristol

Houghton RA (2003) The contemporary carbon cycle. In: Holland HD, Turekian KK (eds) Treatise on geochemistry. Elsevier Pergamon, Amsterdam, p 473–513

Houser C, Gough WA (2003) Variations in sea ice in the Hudson Strait: 1971–1999. Polar Geogr 27:1–14

Howard-Jones MH, Ballard VD, Allen AE, Frischer ME, Verity PG (2002) Distribution of bacterial biomass and activity in the marginal ice zone of the central Barents Sea during summer. J Mar Syst 38:77–91

Howell SEL, Duguay CR, Markus T (2009) Sea ice conditions and melt season duration variability within the Canadian Arctic Archipelago: 1979–2008. Geophys Res Lett 36, L10502, doi:10.1029/2009GL0376

Hudon C, Morin R, Bunch J, Harland R (1996) Carbon and nutrient output from the Great Whale River (Hudson Bay) and a comparison with other rivers around Québec. Can J Fish Aquat Sci 53:1513–1525

Ingalls AE, Lee C, Wakeham SG, Hedges JI (2003) The role of biominerals in the sinking flux and preservation of amino acids in the Southern Ocean along 170°W. Deep-Sea Res II 50:713–738

Ingram RG, Prinsenberg SJ (1998) Coastal oceanography of Hudson Bay and surrounding eastern Canadian Arctic waters coastal segments. In: Robinson AR, Brink KH (eds) The Sea, Volume 11. John Wiley, New York, p 835–861

IPCC (2007) Climate change 2007: The physical science basis. Contribution of Working Group I to the Fourth Assessment Report of the Intergovernmental Panel on Climate Change. Cambridge University Press, Cambridge and New York

Jacobsen TR, Azam F (1984) Role of bacteria in copepod fecal pellet decomposition: colonization, growth rates and mineralization. Bull Mar Sci 35:495–502

Jochem FJ, Lavrentyev PJ, First MR (2004) Growth and grazing rates of bacteria groups with different apparent DNA content in the Gulf of Mexico. Mar Biol 145:1213–1225

Johannessen OM, Shalina EV, Miles MW (1999) Satellite evidence for an Arctic sea ice cover in transformation. Science 286:1937–1939

Johannessen OM, Miles MW, Bjørgo E (1995) The Arctic's shrinking sea ice. Nature 376:126–127

Johnsen G, Sakshaug E, Vernet M (1992) Pigment composition, spectral characterization and photosynthetic parameters in *Chrysochromulina polylepis*. Mar Ecol Prog Ser 83:241–249

Joly S, Senneville S, Caya D, Saucier FJ (2010) Sensitivity of Hudson Bay sea ice and ocean climate to atmospheric temperature forcing. Clim Dyn, doi:10.1007/s00382-009-0731-4

Jones EP, Anderson LG (1994) Northern Hudson Bay and Foxe Basin: water masses, circulation and productivity. Atmos Ocean 32:361–374

Jones EP, Swift JH, Anderson LG, Lipizer M, Civitarese G, Falkner KK, Kattner G, McLaughlin F (2003) Tracing Pacific water in the North Atlantic Ocean. J Geophys Res 108, 3116, doi: 10.1029/2001JC001141

Juul-Pedersen T, Nielsen TG, Michel C, Møller EF, Tiselius P, Thor P, Olesen M, Selander E, Gooding S (2006) Sedimentation following the spring bloom in Disko Bay, West Greenland, with special emphasis on the role of copepods. Mar Ecol Prog Ser 314:239–255

Juul-Pedersen T, Michel C, Gosselin M (2008) Influence of the Mackenzie River plume on the sinking export of particulate material on the shelf. J Mar Syst 74:810–824

Kahl LA, Vardi A, Schofield O (2008) Effects of phytoplankton physiology on export flux. Mar Ecol Prog Ser 354:3–19

Karl DM, Knauer GA, Martin JH (1988) Downward flux of particulate organic matter in the ocean: A particle decomposition paradox. Nature 332:438–441

Karl DM, Hebel DV, Christian JR, Dore JE, Letelier RM, Tupas LM, Winn CD (1996) Seasonal and interannual variability in primary production and particle flux at station ALOHA. Deep-Sea Res II 43:539–568

Kellogg CTE, Deming JW (2009) Comparison of free-living, suspended particle, and aggregate-associated bacterial and archaeal communities in the Laptev Sea. Aquat Microb Ecol 57:1–18

Kendall M, Stuart A (1977) The advanced theory of statistics, Vol. 1. Charles Griffin and Company Limited, London and High Wycombe

Kiørboe T, Hansen JLS (1993) Phytoplankton aggregate formation: observations of patterns and mechanisms of cell sticking and the significance of exopolymeric material. J Plankton Res 15:993–1018

Kiørboe T, Jackson JA (2001) Marine snow, organic solute plumes, and optimal chemosensory behaviour of bacteria. Limnol Oceanogr 46:1309–1318

Kiørboe T, Grossart H-P, Ploug H, Tang K (2002) Mechanisms and rates of bacterial colonization of sinking aggregates. Appl Environ Microb 68:3996–4006

Kiørboe T, Tang K, Grossart H-P, Ploug H (2003) Dynamics of microbial communities on marine snow aggregates: colonization, growth, detachment, and grazing mortality of attached bacteria. Appl Environ Microb 69:3036–3047

Knap A, Michaels A, Close A, Ducklow H, Dickson A (1996) Protocols for the Joint Global Ocean Flux Study (JGOFS) core measurements. JGOFS Report Nr. 19, Reprint of the Intergovernmental Oceanographic Commission. Manuals and Guides No. 29, UNESCO, Bergen

Köberle C, Gerdes R (2003) Mechanisms determining the variability of Arctic sea ice conditions and export. J Climate 16:2843–2858

Krembs C, Engel A (2001) Abundance and variability of microorganisms and transparent exopolymer particles across the ice-water interface of melting first-year sea ice in the Laptev Sea (Arctic). Mar Biol 138:173–185

Kuzyk ZA, Goñi MA, Stern GA, Macdonald RW (2008) Sources, pathways and sinks of particulate organic matter in Hudson Bay: Evidence from lignin distributions. Mar Chem 112:215–229

Kuzyk ZA, Macdonald RW, Johannessen OM, Gobeil C, Stern GA (2009) Towards a sediment and organic carbon budget for Hudson Bay. Mar Geol 264:190–208

Kuzyk ZA, Macdonald RW, Tremblay JÉ, Stern GA (2010) Elemental and stable isotopic constraints on river influence and patterns of nitrogen cycling and biological productivity in Hudson Bay. Cont Shelf Res 30:163–176

Kwok R (2007) Near zero replenishment of the Arctic multiyear sea ice cover at the end of 2005 summer. Geophys Res Lett 34, L05501, doi:10.1029/2006GL028737

Lalande C, Grebmeier JM, Wassmann P, Cooper LW, Flint MV, Sergeeva VM (2007a) Export fluxes of biogenic matter in the presence and absence of seasonal sea ice cover in the Chukchi Sea. Cont Shelf Res 27:2051–2065

Lalande C, Moran SB, Wassmann P, Grebmeier JM, Cooper LW (2007b) ^{234}Th derived particulate organic carbon fluxes in the northern Barents Sea with comparison to drifting sediment trap fluxes. J Mar Syst 73:103–113

Lalande C, Bélanger S, Fortier L (2009) Impact of a decreasing sea ice cover on the vertical export of particulate organic carbon in the northern Laptev Sea, Siberian Arctic Ocean. Geophys Res Lett 36, L21604, doi:10.1029/2009GL040570

Lapoussière A, Michel C, Gosselin M, Poulin M (2009) Spatial variability in organic material sinking export in the Hudson Bay system, Canada, during fall. Cont Shelf Res 29:1276–1288

Laws EA, Falkowski PG, Smith Jr WO, Ducklow H, McCarty JJ (2000) Temperature effects on export production in the open ocean. Global Biogeochem Cycles 14:1231–1246

Lebaron P, Servais P, Agogue H, Courties C, Joux F (2001) Does the high nucleic acid content of individual bacterial cells allow us to discriminate between active cells and inactive cells in aquatic systems? Appl Environ Microb 67:1775–1782

Lee C, Peterson ML, Wakeham SG, Armstrong RA, Cochran JK, Miquel JC, Fowler SW, Hirschberg D, Beck A, Xue JH (2009) Particulate organic matter and ballast fluxes measured using time-series and settling velocity sediment traps in the northwestern Mediterranean Sea. Deep-Sea Res II 56:1420–1436

Lee S, Fuhrman JA (1987) Relationship between biovolume and biomass of naturally derived marine bacterioplankton. Appl Environ Microb 53:1298–1303

Legendre L, Le Fèvre J (1991) From individual plankton cells to pelagic marine ecosystems and to global biogeochemical cycles. In: Demers S (ed) Particle analysis in oceanography. Springer-Verlag, Berlin, p 261–300

Legendre L, Le Fèvre J (1995) Microbial food webs and the export of biogenic carbon in oceans. Aquat Microb Ecol 9:69–77

Legendre P, Legendre L (1998) Numerical Ecology, 2nd edn. Elsevier Science BV, Amsterdam

Legendre L, Rassoulzadegan F (1995) Plankton and nutrient dynamics in marine waters. Ophelia 41:153–172

Legendre L, Simard Y (1979) Océanographie biologique estivale et phytoplancton dans le sud-est de la baie d'Hudson. Mar Biol 52:11–22

Legendre L, Demers S, Yentsch CM, Yentsch CS (1983) The ^{14}C method: patterns of dark CO_2 fixation and DCMU correction to replace the dark bottle. Limnol Oceanogr 28:996–1003

Legendre L, Robineau B, Gosselin M, Michel C, Ingram RG, Fortier L, Therriault J-C, Demers S, Monti D (1996) Impact of freshwater on a subarctic coastal ecosystem under seasonal sea ice (southeastern Hudson Bay, Canada). II. Production and export of microalgae. J Mar Syst 7:233–250

Lepore K, Moran SB (2007) Seasonal changes in thorium scavenging and particle aggregation in the western Arctic Ocean. Deep-Sea Res II 54:919–938

Loferer-Krößbacher M, Klima J, Psenner R (1998) Determination of bacterial cell dry mass by transmission electron microscopy and densitometric image analysis. Appl Environ Microbiol 64:688–694

Longnecker K, Sherr BF, Sherr EB (2005) Activity and phylogenetic diversity of bacterial cells with high and low nucleic acid content and electron transport system activity in an upwelling ecosystem. Appl Environ Microb 71:7737–7749

Longnecker K, Sherr BF, Sherr EB (2006) Variation in cell-specific rates of leucine and thymidine incorporation by marine bacteria with high and with low nucleic acid content off the Oregon coast. Aquat Microb Ecol 43:113–125

Lorenzen CJ (1968) Carbon:chlorophyll relationships in an upwelling area. Limnol Oceanogr 13:202–204

Lund JWG, Kipling C, Le Cren ED (1958) The inverted microscope method of estimating algal number and the statistical basis of estimations by counting. Hydrobiologia 11:143–170

Lutz MJ, Caldeira K, Dunbar RB, Behrenfeld MJ (2008) Seasonal rhythms of net primary production and particulate organic carbon flux to depth describe the efficiency of biological pump in the global ocean. J Geophys Res 112, C10011, doi:10.1029/2006JC003706

Maier-Reimer E, Mikolajewicz U, Winguth A (1996) Future ocean uptake of CO_2: Interaction between ocean circulation and biology. Clim Dynam 12:711–721

Maiti K, Benitez-Nelson CR, Lomas MW, Krause JW (2009) Biogeochemical responses to late-winter storms in the Sargasso Sea, III- Estimates of export production using ^{234}Th:^{238}U disequilibria and sediment traps. Deep-Sea Res I 56:875–891

Mann KH, Lazier JRN (1996) Dynamics of marine ecosystems: biological-physical interaction in the ocean, 2nd edn. Blackwell Science, Cambridge

Marie D, Partensky F, Jacquet S, Vaulot D (1997) Enumeration and cell cycle of natural populations of marine picoplankton by flow cytometry using the nucleic acid stain SYBR Green I. Appl Environ Microb 63:186–193

Marie D, Brussaard CPD, Thyrhaug R, Bratbak G, Vaulot D (1999) Enumeration of marine viruses in culture and natural samples by flow cytometry. Appl Environ Microb 65:45–52

Markham VWE (1986) The ice cover. In: Martini IP (ed) Canadian inland seas. Elsevier Oceanography Series, Amsterdam p 101–116

Markus T, Stroeve JC, Miller J (2009) Recent changes in Arctic Sea ice melt onset, freezeup, and melt season length. J Geophys Res 114, C12024, doi:10.1029/2009JC005436

Martin JH, Knauer GA, Karl DM, Broenkow WW (1987) VERTEX: carbon cycling in the northeastern Pacific. Deep-Sea Res 34:267–285

Martinez J, Smith DC, Steward GF, Azam F (1996) Variability in ectohydrolytic enzyme activities of pelagic marine bacteria and its significance for substrate processing in the sea. Aquat Microb Ecol 10:223–230

McClelland JW, Déry SJ, Peterson BJ, Holmes RM, Wood EF (2006) A pan-Arctic evaluation of changes in river discharge during the latter half of the 20th century. Geophys Res Lett 33, L06715, doi:10.1029/2006GL025753

McKenzie CH, Deibel D, Paranjape MA, Thompson RJ (1995) The marine mixotroph *Dinobryon balticum* (Chrysophyceae): phagotrophy and survival in a cold ocean. J Phycol 31:19–24

McKenzie CH, Deibel D, Thompson RJ, MacDonald BA, Penney RW (1997) Distribution and abundance of choanoflagellates (Acanthoecidae) in the coastal cold ocean of Newfoundland, Canada. Mar Biol 129:407–416

Menden-Deuer S, Lessard EJ (2000) Carbon to volume relationships for dinoflagellates, diatoms, and other protist plankton. Limnol Oceanogr 45:569–579

Michaels AF, Silver MW (1988) Primary production, sinking fluxes and the microbial food web. Deep-Sea Res 35:473–490

Michel C, Legendre L, Therriault JC, Demers S, Vandevelde T (1993) Springtime coupling between ice algal and phytoplankton assemblages in southeastern Hudson Bay, Canadian Arctic. Polar Biol 13:441–449

Michel C, Gosselin M, Nozais C (2002) Preferential sinking export of biogenic silica during the spring and summer in the North Water polynya (northern Baffin Bay): temperature or biological control? J Geophys Res 107, 3064, doi:10.1029/2000JC000408

Middelboe M, Nielsen TG, Bjornsen PK (2002) Viral and bacterial production in the North Water: in situ measurements, batch-culture experiments and characterization and distribution of a virus-host system. Deep-Sea Res II 49:5063–5079

Middelburg JJ, Meysman FJR (2007) Burial at sea. Science 316:1294–1295

Miller LA, Yager PL, Erickson KA, Amiel D, Bâcle J, Cochran JK, Garneau M-È, Gosselin M, Hirschberg DJ, Klein B, LeBlanc B, Miller WL (2002) Carbon distributions and fluxes in the North Water, 1998 and 1999. Deep-Sea Res II 49:5151–5170

Mingelbier M, Klein B, Claereboudt MR, Legendre L (1994) Measurement of daily primary production using 24 h incubations with the ^{14}C method: a caveat. Mar Ecol Prog Ser 113:301–309

Mitchell MR, Harrison G, Pauley K, Gagné A, Maillet G, Strain P (2002) Atlantic zonal monitoring program sampling protocol. Can Tech Rep Hydrogr Ocean Sci n°223

Moran SB, Kelly RP, Hagstrom K, Smith JN, Grebmeier JM, Cooper LW, Cota F, Walsh JJ, Bates NR, Hansell DA, Maslowski W, Nelson RP, Mulsow S (2005) Seasonal changes in POC export flux in the Chukchi Sea and implications for water column-benthic coupling in Arctic shelves. Deep-Sea Res II 52:3427–3451

Morán XAG, Bode A, Suarez LA, Nogueira E (2007) Assessing the relevance of nucleic acid content as an indicator of marine bacterial activity. Aquat Microb Ecol 46:141–152

Moritz RE, Bitz CM, Steig EJ (2002) Dynamics of recent climate change in the Arctic. Polar Sci 297:1497–1502

Mundy CJ, Gosselin M, Starr M, Michel C (2010) Riverine export and the effects of circulation on dissolved organic carbon in the Hudson Bay system, Canada. Limnol Oceanogr 55:315-323

Murata A, Takizawa T (2003) Summertime CO_2 sinks in shelf and slope waters of the western Arctic Ocean. Cont Shelf Res 23:753–776

Noji TT, Estep KW, MacIntyre F, Norrbin F (1991) Image analysis of fecal material grazed upon by three species of copepods. Evidence for coprohexy, coprophagy and coprochaly. J Mar Biol Assoc UK 71:465–480

NSIDC (2010) (National snow and ice data center) Accessed 15 February, http://nsidc.org/

Olesen M, Lundsgaard C (1995) Seasonal sedimentation of autochthonous material from the euphotic zone of a coastal system. Estuar Coast Shelf Sci 41:475–490

Olli K, Riser CW, Wassmann P, Rat'kova T, Arashkevich E, Pasternak A (2002) Seasonal variation in vertical flux of biogenic matter in the marginal ice zone and the central Barents Sea. J Mar Syst 38:189–204

Olli K, Wassmann P, Reigstad M, Ratkova TN, Arashkevich E, Pasternak A, Matrai PA, Knulst J, Tranvik L, Klais R, Jacobsne A (2007) The fate of production in the central Arctic Ocean: top-down regulation by zooplankton expatriates? Prog Oceanogr 72:84–113

Orr JC, Fabry VJ, Aumont O, Bopp L, Doney SC, Feely RA, Gnanadesikan A, Gruber N, Ishida A, Joos F, Key RM, Lindsay K, Maier-Reimer E, Matear R, Monfray P, Mouchet A, Najjar RG, Plattner G-K, Rodgers KB, Sabine CL, Sarmiento JL, Schlitzer R, Slater RD, Totterdell IJ, Weirig M-F, Yamanaka Y, Yool A (2005) Anthropogenic ocean acidification over the twenty-first century and its impact on calcifying organisms. Nature 437:681–686

Overpeck J, Hughen K, Hardy D, Bradley R, Case R, Douglas M, Finney B, Gajewski K, Jacoby G, Jennings A, Lamoureux S, Lasca A, MacDonald G, Moore J, Retelle M, Smith S, Wolfe A, Zielinski G (1997) Arctic environmental change of the last four centuries. Science 278:1251–1256

Pabi S, van Dijken GL, Arrigo KR (2008) Primary production in the Arctic Ocean, 1998–2006. J Geophys Res, 113, C08005, doi:10.1029/2007JC004578

Parkinson CL, Cavalieri DJ, Gloersen P, Zwally HJ, Comiso JC (1999) Arctic sea ice extents, areas and trends, 1978–1996. J Geophys Res 104:20837–20856

Parsons TR, Maita Y, Lalli CM (1984) A manual of chemical and biological methods for seawater analysis. Pergamon Press, Toronto

Passow U, Alldredge AL (1994) Distribution, size and bacterial colonization of transparent exopolymer particles (TEP) in the ocean. Mar Ecol Prog Ser 113:185–198

Passow U, Alldredge AL (1995) A dye-binding assay for the spectrophotometric measurement of transparent exopolymer particles (TEP). Limnol Oceanogr 40:1326–1335

Passow U, de la Rocha CL (2006) The accumulation of mineral ballast on organic aggregates. Global Biogeochem Cycles, 20, GB1013, doi:10.1029/2005GB002579

Pasternak A, Wexels Riser C, Arashkevich E, Rat'kova T, Wassmann P (2002) *Calanus* spp. grazing affects egg production and vertical carbon flux (the marginal ice zone and open Barents Sea). J Mar Syst 38:147–164

Pedrós-Alió C, Brock TD (1983) The importance of attachment to particles for planktonic bacteria. Arch Hydrobiol 98:354–379

Pedrós-Alió C, Mas J (1993) Bacterial sinking losses. In: Kemp PF, Sherr BF, Sherr EB, Cole JJ (eds), Handbook of methods in aquatic microbial ecology. CRC Press, Boca Raton, Lewis, p 677–684

Pedrós-Alió C, Mas J, Gasol JM, Guerrero R (1989) Sinking speeds of free-living phototrophic bacteria determined with covered and uncovered traps. J Plankton Res 11:887–905

Peterson BJ, Holmes RM, McClelland JW, Vörösmarty CJ, Lammers RB, Shiklomanov AI, Shiklomanov IA, Rahmstorf S (2002) Increasing river discharge to the Arctic Ocean. Science 298:2171–2174

Peterson BJ, McClelland JW, Curry R, Holmes RM, Walsh JE, Aagaard K (2006) Trajectory shifts in the Arctic and Subarctic freshwater cycle. Science 313:1061–1066

Piepenburg D (2005) Recent research on Arctic benthos: common notions need to be revised. Polar Biol 28:733–755

Pilskaln CH, Honjo S (1987) The fecal pellet fraction of biogeochemical particle fluxes to the deep sea. Global Biogeochem Cycles 1:31–48

Ploug H, Grossart H-P (2000) Bacterial growth and grazing on diatom aggregates: respiratory carbon turnover as a function of aggregate size and sinking velocity. Limnol Oceanogr 45:1467–1475

Pomeroy LR (1974) The ocean's food web, a changing paradigm. Bioscience 24:499–504

Pommier J, Michel C, Gosselin M (2008) Particulate organic carbon export in the upper twilight zone of the northwest Atlantic Ocean during the decline of the spring bloom. Mar Ecol Prog Ser 356:81–92

Pommier J, Gosselin M, Michel C (2009) Size-fractionated phytoplankton production and biomass during the decline of the northwest Atlantic spring bloom. J Plankton Res 31:429–446

Posch T, Loferer-Krößbacher M, Gao G, Alfreider A, Pernthaler J, Psenner R (2001) Precision of bacterioplankton biomass determination: a comparison of two fluorescent dyes, and of allometric and linear volume-tocarbon conversion factors. Aquat Microb Ecol 25:55–63

Poulsen L, Kiørboe T (2005) Coprophagy and coprorhexy in the copepods *Acartia tonsa* and *Temora longicornis*: clearance rates and feeding behaviour. Mar Ecol Prog Ser 299:217–227

Prinsenberg SJ (1980) Man-made changes in freshwater input rates of Hudson and James Bays. Can J Fish Aquat Sci 37:1101–1110

Prinsenberg SJ (1984) Freshwater contents and heat budgets of James Bay and Hudson Bay. Cont Shelf Res 3:191–200

Prinsenberg SJ (1986a) Salinity and temperature distribution in Hudson Bay and James Bay. In: Martini IP (ed) Canadian inland seas. Elsevier Oceanography Series, Amsterdam, p 163–184

Prinsenberg SJ (1986b) On the physical oceanography of Foxe Basin. In: Martini IP (ed) Canadian inland seas. Elsevier Oceanography Series, Amsterdam, p 217–236

Prinsenberg SJ (1986c) The circulation pattern and structure of Hudson Bay. In: Martini IP (ed) Canadian inland seas. Elsevier Oceanography Series, Amsterdam, p 187–204

Putt M, Stoecker DK (1989) An experimentally determined carbon:volume ratio for marine oligotrichous ciliates from estuarine and coastal waters. Limnol Oceanogr 34:1097–1103

Ragueneau O, Tréguer P (1994) Determination of biogenic silica in coastal waters: applicability and limits of the alkaline digestion method. Mar Chem 45:43–51

Reigstad M, Wassmann P (2007) Does *Phaeocystis* spp. contribute significantly to vertical export of organic carbon? Biogeochemistry 83:217–234

Reigstad M, Wexels Riser C, Wassmann P, Rat'kova T (2008) Vertical export of particulate organic carbon: Attenuation, composition and loss rates in the northern Barents Sea. Deep-Sea Res II 55:2308–2319

Renaud PE, Morata N, Carroll ML, Denisenko SG, Reigstad, M (2008) Pelagic-benthic coupling in the western Barents Sea: Processes and time scales. Deep-Sea Res II 55:2372–2380

Rich J, Gosselin M, Sherr E, Sherr B, Kirchman DL (1997) High bacterial production, uptake and concentrations of dissolved organic matter in the Central Arctic Ocean. Deep-Sea Res II 44:1645–1663

Richardson AJ, Schoeman DS (2004) Climate impact on plankton ecosystems in the Northeast Atlantic. Science 305:1609–1612

Richardson TL, Jackson GA (2007) Small phytoplankton and carbon export from the surface ocean. Science 315:838–840

Riebesell U (2004) Effects of CO_2 enrichment on marine phytoplankton. J Oceanogr 60:719–729

Riebesell U, Zondervan I, Rost B, Tortell PD, Zeebe RZ, Morel FMM (2000) Reduced calcification of marine plankton in response to increased atmospheric CO_2. Nature 407:364–367

Riedel A, Michel C, Gosselin M (2006) Seasonal study of sea-ice exopolymeric substances on the Mackenzie shelf: implications for transport of sea-ice bacteria and algae. Aquat Microb Ecol 45:195–206

Riemann L, Winding A (2001) Community dynamics of free-living and particle-associated bacterial assemblages during a freshwater phytoplankton bloom. Microb Ecol 42:274–285

Rink B, Seeberger S, Martens T, Duerselen C-D, Simon M, Brinkhoff T (2007) Effects of phytoplankton bloom in a coastal ecosystem on the composition of bacterial communities. Aquat Microb Ecol 48:47–60

Rivkin RB, Legendre L (2001) Biogenic carbon cycling in the upper ocean: effects of microbial respiration. Science 291:2398–2400

Rivkin RB, Anderson MR, Lajzerowicz C (1996a) Microbial processes in cold oceans. I. Relationship between temperature and bacterial growth rate. Aquat Microb Ecol 10:243–254

Rivkin RB, Legendre L, Deibel D, Tremblay J-É, Klein B, Crocker K, Roy S, Silverberg N, Lovejoy C, Mesplé F, Romero N, Anderson MR, Matthews P, Savenkoff C, Vézina AF, Therriault J-C, Wesson J, Bérubé C, Ingram RG (1996b). Vertical flux of biogenic carbon in the ocean: is there food web control? Science 272:1163–1166

Robinson C (2008) Heterotrophic bacterial respiration. In: Kirchman DL (ed) Microbial ecology of the oceans, 2nd edn. John Wiley & Sons, New-York, p 299–334

Rochet M, Grainger EH (1988) Community structure of zooplankton in eastern Hudson Bay. Can J Zool 66:1626–1630

Roff JC, Legendre L (1986) Physico-chemical and biological oceanography of Hudson Bay. In: Martini IP (ed) Canadian inland seas. Elsevier Oceanography Series, Amsterdam, p 265–291

Rouse WR (1991) Impacts of Hudson Bay on the terrestrial climate of the Hudson Bay lowlands. Arctic Alpine Res 23:24–30

Rysgaard S, Nielsen TG, Hansen BW (1999) Seasonal variation in nutriments, pelagic primary production and grazing in high-Arctic coastal marine ecosystem, Young Sound, northeast Greenland. Mar Ecol Prog Ser 179:13–25

Sadler HE (1982) Water flow into Foxe Basin through Fury and Hecla Strait. Nat Can 109:701–707

Sakshaug E (2004) Primary and secondary production in the Arctic Seas. In: Stein R, Macdonald RW (eds) The organic carbon cycle in the Arctic Ocean. Springer, Berlin, p 57–82

Sarmiento JL, Gruber N (2006) Ocean biogeochemical dynamics. Princeton University Press, New Jersey

Sarmiento JL, Le Quéré C (1996) Oceanic carbon dioxide uptake in a model of century-scale global warming. Science 274:1346–1350

Sarmiento JL, Murnane R, Le Quéré C (1995) Air-sea CO_2 transfer and the carbon budget of the North Atlantic. Philos Trans R Soc Lond (B Biol Sci) 348:211–219

Sarmiento JL, Slater R, Barber R, Doney SC, Hirst AC, Kleypas J, Matear R, Mikolajewicz U, Monfray P, Soldatov V, Spall SA, Stouffer R (2004) Response of ocean ecosystems to climate warming. Global Biogeochem Cycles 18, GB3003, doi:10.1029/2003GB002134

Saucier FJ, Senneville S, Prinsenberg S, Roy F, Smith G, Gachon P, Caya D, Laprise R. (2004) Modelling the sea ice-ocean seasonal cycle in Hudson Bay, Foxe Basin and Hudson Strait, Canada. Clim Dynam 23:303–326

Scharek R, Latasa M (2007) Growth, grazing and carbon flux of high and low nucleic acid bacteria differ in surface and deep chlorophyll maximum layers in the NW Mediterranean Sea. Aquat Microb Ecol 46:153–161

Schlitzer R (2010) Ocean Data View. Accessed 15 February, http://odv.awi.de

Serreze MC (2010) Understanding recent climate change. Conserv Biol 24:10–17

Serreze MC, Holland MM, Stroeve J (2007) Perspectives on the Arctic's shrinking sea-ice cover. Science 315:1533–1536

Servais P, Courties C, Lebaron P, Troussellier M (1999) Coupling bacterial activity measurements with cell sorting by flow cytometry. Microb Ecol 38:180–189

Sherr EB, Sherr BF, Wheeler PA, Thompson K (2003) Temporal and spatial variation in stocks of autotrophic and heterotrophic microbes in the upper water column of the central Arctic Ocean. Deep-Sea Res I 50:557–571

Sherr EB, Sherr BF, Longnecker K (2006) Distribution of bacterial abundance and cell-specific nucleic acid content in the Northeast Pacific Ocean. Deep-Sea Res II 53:713–725

Sibert V (2010) Modélisation de la variabilité saisonnière et de la sensibilité au climat des productions glacielle et pélagique de la baie d'Hudson. Thèse de doctorat, UQAR, Rimouski

Simon M, Alldredge AL, Azam F (1990) Bacterial carbon dynamics on marine snow. Mar Ecol Prog Ser 65:205–211

Simon M, Grossart H-P, Schweitzer B, Ploug H (2002) Microbial ecology of organic aggregates in aquatic ecosystems. Aquat Microb Ecol 28:175–211

Singarayer JS, Bamber JL, Valdes PJ (2006) Twenty-first century climate impacts from a declining Arctic sea ice cover. J Climate 19:1109–1125

Smith DC, Simon M, Alldredge AL, Azam F (1992) Intense hydrolytic enzyme activity on marine aggregates and implications for rapid particle dissolution. Nature 359:139–142

Sokal RR, Rohlf FJ (1981) Biometry: the principles and practice of statistics in biological research, 2nd edn. WH Freeman, San Francisco

Steinberg DK, Van Mooy BAS, Buesseler KO, Boyd PW, Kobari T, Karl DM (2008) Bacterial vs. zooplankton control of sinking particle flux in the ocean's twilight zone. Limnol Oceanogr 53:1327–1338

Steward GF, Smith DC, Azam F (1996) Abundance and production of bacteria and viruses in the Bering and Chukchi Seas. Mar Ecol Prog Ser 131:287–300

Stirling I, Lunn NJ, Lacozza J (1999) Long-term trends in the population ecology of polar bears in western Hudson Bay in relation to climatic change. Arctic 52:294–306

Stocker R, Seymour JR, Samadani A, Hunt DE, Polz MF (2008) Rapid chemotactic response enables marine bacteria to exploit ephemeral microscale nutrient patches. Proc Natl Acad Sci 105:4209–4214

Stoll HM, Arevalos A, Burke A, Ziveri P, Mortyn G, Shimizu N, Unger D (2007) Seasonal cycles in biogenic production and export in Northern Bay of Bengal sediment traps. Deep-Sea Res II 54:558–580

Straneo F, Saucier F (2008a) The outflow from Hudson Strait and its contribution to the Labrador current. Deep-Sea Res I 55:926–946

Straneo F, Saucier F (2008b) The Arctic-Subarctic exchange through Hudson Strait. In: Dickson RR, Meincke J, Rhines P (eds) Arctic-subarctic ocean fluxes: defining the role of the northern seas in climate. Springer-Verlag, New-York, p 249–261

Stroeve J, Holland MM, Meier W, Scambos T, Serreze M (2007) Arctic sea ice decline: faster than forecast. Geophys Res Lett 34, L09501, doi:10.1029/2007GL029703

Sturluson M, Nielsen TG, Wassmann P (2008) Bacterial abundance, biomass and production during spring blooms in the northern Barents Sea. Deep-Sea Res II 55:2186–2198

Subba Rao DV, Platt T (1984) Primary production of Arctic waters. Polar Biol 3:191–201

Suess EA (1980) Particulate organic carbon flux in the ocean-surface productivity and oxygen utilization. Nature 288:260–263

Takahashi T (1989) The carbon dioxide puzzle. Oceanus 32:22–29

Taylor GT, Thunell R, Varela R, Benitez-Nelson C, Scranton MI (2009) Hydrolytic ectoenzyme activity associated with suspended and sinking organic particles within the anoxic Cariaco Basin. Deep-Sea Res I 56:1266–1283

Tian RC, Vézina AF, Starr M, Saucier F (2001) Seasonal dynamics of coastal ecosystems and export production at high latitudes: a modeling study. Limnol Oceanogr 46:1845–1859

Tomas CR (1997) Identifying marine phytoplankton. Academic Press, San Diego

Tortell PD, DiTullio GR, Sigman DM, Morel FMM (2002) CO_2 effects on taxonomic composition and nutrient utilization in an Equatorial Pacific phytoplankton assemblage. Mar Ecol Prog Ser 236:37–43

Tremblay C, Runge JA, Legendre L (1989) Grazing and sedimentation of ice algae during and immediately after a bloom at the ice-water interface. Mar Ecol Prog Ser 56:291–300

Tremblay J-É, Klein B, Legendre L (1997) Estimation of *f*-ratio in oceans based on phytoplankton size structure. Limnol Oceanogr 42:595–601

Tremblay J-É, Michel C, Hobson KA, Gosselin M, Price NM (2006) Bloom dynamics in early opening waters of the Arctic Ocean. Limnol Oceanogr 51:900–912

Tritton DJ (1988) Physical fluid dynamics, 2nd edn. Clarendon Press, Oxford

Troussellier M, Courties C, Lebaron P, Servais P (1999) Flow cytometric discrimination of bacterial populations in sea-water based on SYTO 13 staining of nucleic acids. FEMS Microbiol Ecol 29:319–330

Turley CM, Mackie PJ (1994) Biogeochemical significance of attached and free-living bacteria and the flux of particles in the NE Atlantic Ocean. Mar Ecol Prog Ser 115:191–203

Turner JT (2002) Zooplankton fecal pellets, marine snow and sinking phytoplankton blooms. Aquat Microb Ecol 27:57–102

Vallières C, Retamal L, Ramlal P, Osburn CL, Vincent WF (2008) Bacterial production and microbial food web structure in a large arctic river and the coastal Arctic Ocean. J Mar Syst 74:756–773

Velji MI, Albright LJ (1993) Improved sample preparation for enumeration of aggregated aquatic substrate bacteria. In: Kemp PF, Sherr BF, Sherr EB, Cole JJ (eds) Handbook of methods in aquatic microbial ecology. Lewis, Boca Raton, p 139–142

Vincent WF, Dodson JJ, Bertrand N, Frenette J-J (1996) Photosynthetic and bacterial production gradients in a larval fish nursery: The St. Lawrence River transition zone. Mar Ecol Prog Ser 139:227–238

Vinnikov KY, Robock A, Stouffer RJ, Walsh JD, Parkinson CL, Cavalieri DJ, Mitchell JFB, Garrett D, Zakharov VF (1999) Global warming and northern hemisphere sea ice extent. Sci Total Environ 286:1934–1939

Volk T, Hoffert MI (1985) Ocean carbon pumps: analysis of relative strengths and efficiencies in ocean driven CO_2 changes. In: Sundquist ET, Broecker WS (eds) The carbon cycle and atmospheric CO_2: natural variations archean to present. AGU Monograph 32, American Geophysical Union, Washington DC, p 99–110

Waite AM, Nodder SD (2001) The effect of in situ iron addition on the sinking rates and export flux of Southern Ocean diatoms. Deep-Sea Res II 48:2635–2654

Waite AN, Thompson PA, Harrison PJ (1992) Does energy control the sinking rates of marine diatoms? Limnol Oceanogr 37:468–477

Wang J, Yin X (2009) Growth of marine bacteria and ammonium regeneration from substrates in different C:N ratios. Acta Oceanol Sin 28:59–64

Wang J, Mysak LA, Ingram RG (1994) Interannual variability of sea-ice cover in Hudson Bay, Baffin Bay and the Labrador Sea. Atmos Ocean 32:421–447

Wassmann P (1990) Relationship between primary production and export production in the boreal coastal zone of the North Atlantic. Limnol Oceanogr 35:464–471

Wassmann P (1998) Retention versus export food chains: processes controlling sinking loss from marine pelagic systems. Hydrobiologia 363:29–57

Watterson IG (2003) Effects of a dynamic ocean on simulated climate sensitivity to greenhouse gases. Clim Dynam 21:197–209

Wexels Riser C, Wassmann P, Olli K, Pasternak A, Arashkevich E (2002) Seasonal variation in production, retention and export of zooplankton fecal pellets in the marginal ice zone and central Barents Sea. J Mar Syst 38:175–188

Wexel Riser C, Reigstad M, Wassmann P, Arashkevich E, Falk-Petersen S (2007) Export or retention? Copepod abundance, faecal pellet production and vertical flux in the marginal ice zone through snap shots from the northern Barents Sea. Polar Biol 30:719–730

Wexels Riser C, Wassmann P, Reigstad M, Seuthe L (2008) Vertical flux regulation by zooplankton in the northern Barents Sea during Arctic spring. Deep-Sea Res II 55:2320–2329

Wilson SE, Steinberg DK, Buesseler KO (2008) Changes in fecal pellet characteristics with depth as indicators of zooplankton repackaging of particles in the mesopelagic zone of the subtropical and subarctic North Pacific Ocean. Deep-Sea Res II 55:1636–1647

Wohlers J, Engel A, Zollner E, Breithaupt P, Jurgens K, Hoppe HG, Sommer U, Riebesell U (2009) Changes in biogenic carbon flow in response to sea surface warming. Proc Natl Acad Sci USA 106:7067–7072

Worm J, Søndergaard M (1998) Alcian blue-stained particles in a eutrophic lake. J Plankton Res 20:179–186

Yamamoto-Kawai M, McLaughlin FA, Carmack E, Nishino S, Shimada K (2009) Aragonite undersaturation in the Arctic Ocean: effects of ocean acidification and sea ice melt. Science 326:1098–1100